
University of Technology, Sydney

Faculty of Engineering and IT

School of Computing and Communications

# Modelling and Development of Wireless Inertial Measurement Units

**By**

**Yu, Zhengyu**

**Supervisor: Zenon Chaczko**

**Course Code: C03017**

**February 2014**

Submitted in fulfilment of the requirements for the degree of Master of Engineering Research

# CERTIFICATE OF AUTHORSHIP/ORIGINALITY

I certify that the work in this thesis has not previously been submitted for a degree nor has it been submitted as part of requirements for a degree except as fully acknowledged within the text.

I also certify that the thesis has been written by me. Any help that I have received in my research work and the preparation of the thesis itself has been acknowledged. In addition, I certify that all information sources and literature used are indicated in the thesis.

Signature of Candidate

_____

# ACKNOWLEDGMENTS

Firstly, I would like to express my sincere gratitude to my supervisor, Dr Zenon Chaczko, who has supported me in this work for the past 4 years. Zenon, you have been more than a supervisor to me during that time. In particular, you have been with me every step of the way throughout this research and have supported me during every stressful moment that I experienced. I greatly appreciate your clear guidance and feedback.

Secondly, I would like to thank my parents; You have been taking care of me for the whole life. Every time when I am stressful, you help me to deal with the pressure. During my study life, you encourage me a lot to achieve a higher academic result. I love you.
Also, I would like to thank my dear friends, Jiajia Shi and Andy Wei, for sharing their knowledge and lab equipment. Accept my best wish for your research projects and academic publications.

I am very thankful to UTS staff, who has supported my research work for the past 4 years. To Dr Xiaoying Kong, Prof Robin Braun, and A/Prof Sandrasegaran Kumbesan, thank you so much for delivering research seminars and presentations in the past two years. I have learned the most up-to-date technology, concepts and research information in these presentations.

Last but not least, I would like to thank to my family and friends, who have always been there for me, providing support and encouraging me. I could not have got this far today without your help.

# TABLE OF CONTENTS

# LIST OF TABLES

# LIST OF FIGURES

# ABSTRACT

This thesis presents the design and test of a wireless sensor mounted inertial navigation system. The innovative, low-cost and effective inertial measurement unit is based on three- axis accelerometer with USB and the serial direct interface. The accelerometer has connectors on both side of the module for control and communication. Wireless sensor, Bluetooth, has been mounted on the inertial navigation system to facilitate communications. By using this solution, it is possible to monitor and update the data of the accelerometers wirelessly and synchronously. The collected wireless data are analysed and compared with the data from other sources, such as USB cable, to determine errors in the system. The work discusses issues related to the accelerometer system technology, demonstrate application and process experiment. Particular consideration is given to the development of wireless technology and to a new micro-electro-mechanical accelerometer system test facility.

The main contributions of this thesis are as follows:

• Development of a wireless inertial measurement unit
• Development of an error model
• Implementation of this inertial measurement unit into a gyro-free inertial navigation system

# Chapter 1

# Introduction

An inertial measurement unit (IMU) provides self-contained high frequency information for vehicle positioning systems. When external position signals are unavailable, the IMU can provide continuous vehicle positioning information. An IMU contains accelerometers and gyros. Accelerometers provide acceleration information, and gyros measure the rotation rate of a moving vehicle. An inertial navigation system (INS) can be built with three accelerometers, three gyros and associated positioning computing algorithms. The INS computes the vehicle positioning information using acceleration. By integration of the acceleration, the velocity of a vehicle is obtained, and the vehicle position is then computed by integration of the velocity. The vehicle accelerations and accelerometer measurements are in different moving coordinate systems. During this real time integration process, gyro measurements continuously provide vehicle orientation information to transfer the acceleration in different moving coordinate systems. Inertial sensors have been applied in bridges, dynamometers, and aircraft since the early 1920s, but high accuracy inertial measurement units have been expensive until recently. In the previous 20 years, INSs have been used in air vehicles, land vehicles, ocean vessels, and robots. In recent years, the reduction in the cost of inertial sensors has made INS positioning applications available to many other areas such as autonomous systems in agriculture, mining, robotics, transport, health care, pedestrian navigation, and smart phone applications. Wireless technologies and wireless sensor networks have now also emerged. Remote monitoring systems using wireless sensors have become a new research and development direction, and these

wireless applications include robot positioning in disaster field discovery, healthcare monitoring systems, and so on. Consequently, there is a new need to develop wireless inertial sensors and understand the impacts of wireless IMUs for these positioning applications. The positioning mechanism using inertial sensors are based on the acceleration and velocity integration process. Any errors in acceleration will be integrated and amplified after integration. This thesis develops a wireless IMU which allows the IMU to communicate with a computer remotely and synchronously. An error model is developed for the wireless IMU to improve the accuracy of the system. The approach for modelling wireless inertial sensor errors is demonstrated in this work. The design and modelling approach are validated using dynamic positioning experiments in a gyro-free INS system.

## 1.1 Thesis Scope

Micro-electro-mechanical systems (MEMS) accelerometers are widely used in a variety of areas such as inertial navigation, automotive, and industry applications. There are many advantages to MEMS accelerometers such as low cost, low power and small size. The integrated MEMS accelerometer system combines MEMS with Bluetooth for wireless communications and monitoring. This system is able to sense a physical measurement, process it locally, and communicate it wirelessly. Such a system could be fully implemented in the areas of surveying, automotive, mining and environment detection applications for military, commercial and scientific use. This wireless accelerometers system has a low power consumption: 30ma at 3.3V for the inputs and signal outputs. The unit g, as used in this report, stands for the standard free-fall acceleration, or g=9.806650m/. The maximum measurement range of the accelerometer is 6g. This thesis aims to test and improve the performance of the wireless accelerometer system. A rotation test is

implemented. The unit under test is placed on a precision three axis test platform, and a series of constant rate tests and multi-position tests are then operated to identify the major sources of error of the wireless MEMS accelerometers system. An error model is developed as a black box which is calibrated remotely. A wireless gyro-free INS has been implemented with improved error modelling to develop the accuracy of the system.

## 1.2 Hypothesis

The inertial navigation system has several serial interfaces, such as RS232. In previous researches, these interfaces have been utilised for data logging and data processing; however, cable transmission limits the range and multi-task of real-time monitoring and communications. In addition, the system is difficult to implement on some small vehicles or robots when it is connected to the computer via cables, and the cost and power consumption will increase sharply. To achieve the purpose of real-time data processing, wireless communication and remote monitoring, a wireless sensor is integrated with the system. Bluetooth is the wireless sensor that is used in the thesis. It is a reliable wireless technology that should not introduce any data error during the data transmission. Theoretically, the data from wireless communication should be the same as the data from cable communication. However, inertial measurement unit is a high magnetic sensitive unit, any magnetic fields can interfere the accuracy of the output. Therefore, there is no error during the wireless communication, but the errors occur prior to the transmission. The IMU is interfered by Bluetooth and generates inaccurate data, and these data will be transferred to the computer wirelessly. The error modelling that is designed in my thesis is to minimise or correct these errors by this designed error modelling.

## 1.3 Thesis Contributions

This thesis presents the development process of a wireless inertial measurement unit (IMU). A wireless communication configuration is designed for this unit. Low cost micro-electro-mechanical-systems (MEMS) accelerometers are used in the hardware prototyping.

1. Development of a wireless IMU

A wireless IMU has been developed. This system enables IMU to communicate with computers when it is operating. Different from cable communications, wireless IMU minimises the size and weight of the system. Moreover, it is able to update the data from the sensor remotely and synchronously.

2. Development of an error model

Wireless measurement errors are modelled as a black box and calibrated at the remote processor end. A multi-position testing approach is designed in wireless IMU error modelling to estimate and reduce the errors. The approach for modelling the wireless inertial sensor errors and calibration is demonstrated in this thesis.

3. Implementation of this IMU into a gyro-free INS

A low cost gyro-free INS is prototyped using this wireless IMU. Gyro-free INS experiments present the improved accuracy level by using the error modelling. The design and modelling approach are validated using dynamic positioning experiments in this thesis.

## 1.4 Thesis Structure

This thesis presents the design and implementation of a wireless inertial measurement unit. The unit is configured using Bluetooth communication. The wireless acceleration measurements are modelled and calibrated using a 6-position testing approach. The unit is prototyped to a low cost wireless gyro-free INS. The INS experiments show that the accuracy of this wireless inertial measurement unit has been improved by using the modelling and calibration approach.

**Chapter 1** introduced the thesis, and included the thesis objective, thesis contributions, thesis structure and publication.

**Chapter 2** provided the necessary background and literature relating to inertial navigation systems as addressed in this thesis. The literature review in this chapter was divided into three sections:

- Inertial Measurement Unit Techniques Review
- Accelerometer Error Model Review
- Accelerometer Calibration and Alignment Techniques

**Chapter 3** presented a new design for wireless accelerometer communication. A functional block diagram was designed for the prototype of the system. Low cost accelerometers were provided to minimise the cost, power consumption and size of the system. An integrated IMEM accelerometer system with Bluetooth communication was implemented to achieve real-time data processing and remote monitoring. Hardware configurations and specifications were presented in this chapter. Three traditional accelerometers (X, Y, Z) were built in three orthogonal axes. A Bluetooth adaptor wirelessly and continuously transferred the raw acceleration measurements and communication configuration messages to a

remote processor. The remote processor collected these acceleration readings and formatted the data for later computing.

**Chapter 4** presented the major contribution of this thesis 'wireless accelerometer error modelling'. The error models were separated into two sections: linear error modelling and nonlinear error modelling for an inertial sensor in both cable mode and wireless mode. After the rotation was conducted with the various equations, errors were detected for both cable and wireless modes. The results were evaluated to validate the error coefficients in this chapter.

**Chapter 5** implemented IMU into a gyro-free wireless INS. The error modelling results of both measurement and estimation of positions were validated and plotted, which proved that the error modelling had achieved the result that was expected.

**Chapter 6** provided a summary of chapters and the conclusion of this thesis. Suggestions for future development have been made.

# Chapter 2

# Literature Review

This chapter presents a literature review of inertial navigation systems and their background, relevant to this thesis. Various inertial sensor error models have been reviewed, and details of the calibration and alignment of the accelerometer are also provided.

## 2.1 Inertial Measurement Unit Techniques Review

### 2.1.1 Inertial navigation systems

An inertial navigation system (INS) utilises accelerometers and gyroscopes to produce an estimate of velocity, position and attitude (Grewal 2007). An inertial measurement unit (IMU) has a cluster of sensors:

1) Generally, three accelerometers and three gyroscopes are mounted on a common platform to produce and measure acceleration and orientation (Grewal 2007).
2) A navigation computer is implemented to receive and process the data acceleration in order to integrate the net acceleration to calculate vehicle's position (Grewal 2007).

Inertial navigation processes the measurements provided by the gyroscopes and accelerometers to determine the position of the body within the inertial reference frame. Unlike other navigation systems, such as the Global Positioning System (GPS), the INS is entirely self-contained within the vehicle; it does not depend on the signals transferred from external sources, although it does depend on the accuracy of the initial value at the

beginning of navigation (Grewal 2007). There are two types of INS: gimballed INS and strapdown INS (Grewal 2007).

A gimballed system is a frame with a rotation bearing which is used to isolate the inside body frame from external rotations (Grewal 2007). To make the bearing perfectly frictionless, the frame needs to be perfectly balanced. The advantage of the gimbal system is that it achieves high system accuracy because the isolation of the inertial platform from the rotations of the vehicle can be utilised to eliminate a number of sensor error sources; however it is too expensive for commercial use (Grewal 2007).

The strapdown INS is different from the gimballed INS because the inertial sensors are strapped down to the frame of the vehicle without exploiting the gimbals for rotational isolation (Grewal 2007). The full six-degree-of-freedom equation of motion must be integrated by a system computer (Grewal 2007).

### 2.1.2 MEMS accelerometer technology

Titterton (2004c) mentions that to measure the specific force acting along the sensitive axis, the implementation of silicon to make the accurate micro components of an accelerometer is widely established (Titterton 2004). Currently, the development of the accelerometer is to construct the sensor entirely from silicon without a hermetically sealed case. Only five components are contained in a precision sensor which is made by precision micro-engineering and design (Titterton 2004).

A micro-electro-mechanical systems instrument is currently classified as two classes, which reflects the body movement where acceleration acting upon the case of the instrument is sensed:

- A mechanical sensor uses silicon components when the movement of a proof mass provided by a flexure or hinge in the presence of an acceleration (Titterton 2004).
- A change in frequency of a vibrating body due to the change of tension in the body caused by mechanical loading occurs when the body is subjected to applied acceleration (Titterton 2004).

Generally, the current development of these two classified classes in inertial sensor technology has been concerned as:

- The type of pendulous MEMS accelerometer, which is capable of generating the measurement of acceleration as accurately as 25 micro-g for inertial and 1 milli-g for sub-inertial (Titterton 2004).
- The instrument of vibrating beam or resonant sensors, which is capable of having a higher precision which achieves 1 micro-g (Titterton 2004).

#### *2.1.2.1 Translational motion measurement*

Titterton (2004c) explains that Newton's second law of motion holds that the translational acceleration of a body is dependent on the forces which act upon it. F stands for a force acting on a body, and m stands for a body of mass (Titterton 2004). The acceleration of the body due to the force with respect to inertial space is given by the equation below:

$$F = ma \tag{2.1}$$

It is not practical to use the measurement of the total force acting on the body to measure vehicle acceleration (Titterton 2004). It is possible, however, to estimate the force acting on a small mass or body inside the vehicle when that mass or body is constrained to move with the vehicle. An accelerometer is the simplest form of such a body. It contains a proof mass connecting with a spring to the device case; as the device case moves along the

acceleration's sensitive axis, the proof mass will resist the movement changes owing to its inertia (Titterton 2004). The proof mass is replaced with respect to the body. When the condition is steady state, the spring tension will balance the force acting upon the mass, the net spring extension is equal to the measurement of the acting force, which provides the acceleration (Titterton 2004).

The net force (F) acting on a mass (m) in space may be represented by the equation:

$$F = ma = mf + mg \tag{2.2}$$

In this case, $f$ stands for acceleration, which is produced by a force other than the gravitational field. $m$ stands for mass. In the equation, $F = a = f + g$, the net force per unit mass can be represent as acceleration (a). The unit (g) represents the gravitational acceleration (Titterton 2004).

In a gravitational field, the case of an accelerometer which is falling freely is taken. There will be no net spring extension when the case and the proof mass fall together; therefore, the net instrument output will be zero (Titterton 2004). In this case, the instrument acceleration with respect to an inertial fixed set of axes, $a = g$ and the specific force will be zero in terms of the equations (Titterton 2004). On the other hand, in the case that the instrument is held stationary,$a = 0$ , the force acting to stop falling will be measured by the accelerometer (Titterton 2004). Thus, to offset the effect of gravity, the equation, $mf = -mg$, is the specific force. The inertial acceleration measurement has been calculated in terms of the knowledge of the gravitational field (Titterton 2004).

Inertial navigation systems have been commonly used by mechanical instruments for the measurement of a specific force in spring systems and mass accelerometers (Titterton 2004). The full independent navigation measurement of specific force normally uses three single- axis accelerometers as well as multi-axis instruments. It is very common but not

essential to setup up these three accelerometers with their three sensitive axes mutually orthogonal (Titterton 2004).

#### *2.1.2.2 Typical sensor model*

The following calibration parameters present a sensor linear model of a typical low cost MEMS sensor (Vectornav 2011).

Bias of sensor X-axis ($B_x$)

Bias of sensor Y-axis ($B_y$)

Bias of sensor Z-axis ($B_z$)

Scale factor of sensor X-axis to X-axis inputs($S_x$)

Scale factor of sensor Y-axis to Y-axis inputs($S_y$)

Scale factor of sensor Z-axis to Z-axis inputs($S_z$)

Misalignment of sensor X-axis to Y-axis inputs($M_{xy}$)

Misalignment of sensor X-axis to Z-axis inputs($M_{xz}$)

Misalignment of sensor Y-axis to Z-axis inputs($M_{yz}$)

Misalignment of sensor Z-axis to X-axis inputs($M_{zx}$)

Misalignment of sensor Z-axis to Y-axis inputs($M_{zy}$)

The results of each of the linear calibration parameters are achieved using different tests. A number of detailed test processes are presented for determining the required calibration device with each parameter of the calibration (Vectornav 2011).

#### *2.1.2.3 Sensor Model Equations*

The linear sensor model has shown for each calibration of sensors is below (Vectornav 2011):

$$A = \begin{bmatrix} x \\ y \\ z \end{bmatrix}_1 = \begin{bmatrix} 1 & M_{xy} & M_{xz} \\ M_{yx} & 1 & M_{yz} \\ M_{zx} & Mzy & 1 \end{bmatrix} * \begin{bmatrix} \frac{1}{S_x} & 0 & 0 \\ 0 & \frac{1}{S_y} & 0 \\ 0 & 0 & \frac{1}{S_z} \end{bmatrix} \left( B_d + \begin{bmatrix} B_x \\ B_y \\ B_z \end{bmatrix} - \begin{bmatrix} V_x \\ V_y \\ V_z \end{bmatrix} \right) \tag{2.3}$$

The detailed algorithm has been given as (Vectornav 2011):

$$\begin{aligned} A_x &= \frac{B_d + B_x - V_x}{S_x} + \frac{M_{xy}\left(B_d + B_y - V_y\right)}{S_y} + \frac{M_{xz}(B_d + B_z - V_z)}{S_z} \\ A_y &= \frac{M_{yx}(B_d + B_x - V_x)}{S_x} + \frac{B_d + B_y - V_y}{S_y} + \frac{M_{yz}(B_d + B_z - V_z)}{S_z} \\ A_z &= \frac{M_{zx}(B_d + B_x - V_x)}{S_x} + \frac{M_{zy}\left(B_d + B_y - V_y\right)}{S_y} + \frac{B_d + B_z - V_z}{S_z} \end{aligned} \tag{2.4}$$

### 2.1.3 Implementation of inertial sensors

#### *2.1.3.1 Accelerometer for mobile robot positioning*

As mentioned by Liu and Pang (1999) in their research, bias offset drift accumulates with the measurement of distance due to the integration of the acceleration signal output with the time. Periodic recalibration can be used to fix the problem with external measurements of attitude, velocity and position, which is for comparing with corresponding inertial measurement. An estimated system error can be provided by a Kalman filter (Liu and Pang 1999). In the experiments, the real bias drift of the accelerometer was 2.5 mg, whereas the error of the accumulated distance was 1 cm. A low cost micro machined accelerometer, ADXL 202 produced by analog devices, was been used in these experiments (Liu and Pang 1999). The range of the measurement is 2g. Both static acceleration and dynamic

acceleration can be measured. The system bandwidth is from 0.01 Hz to 5000Hz. A 50 Hz bandwidth and 200 Hz sampling rate were implemented in the experiment (Liu and Pang 1999). It should be noted that when the higher bandwidth was used, a higher level of white noise occurred. A robot arm was used in the experiments. 23 data sets with different velocity and acceleration were generated (Liu and Pang 1999) and were separated into three different sets: low acceleration, moderately high acceleration and high acceleration. The final results showed that the error of integrated distance was 1.55cm when the acceleration was 10 m/s². The higher the acceleration used, the lower were the random biases produced (Liu and Pang 1999).

#### *2.1.3.2 Inertial navigation systems for mobile robots*

Barshan and Durant-Whyte (1995) developed an error model of a low-cost inertial navigation system which was presented with an extended Kalman filter for estimating the acceleration, distance and orientation of mobile robots. Generally, IMU should be mounted on other navigation sensors to provide a precise vehicle location. Basically, accelerometers generate data of acceleration, whereas gyroscopes generate data of angular rate (Barshan and Durrant-Whyte 1995). These data must be integrated to calculate the measurement of velocity, distance and orientation. Over a long period, a small error in the data could cause a big difference in distance. One method to deal with this issue is to add a navigation sensor which is able to correct the inertial sensor accumulated errors (Barshan and Durrant-Whyte 1995). Through a detailed understanding of system drift errors, another method of overcoming errors is to use a priori information of the errors of the inertial sensors in an extended Kalman filter to provide the rate of the location prior to generating the data from INS sensing (Barshan and Durrant-Whyte 1995).

## 2.1.4 Bluetooth technology

### *2.1.4.1 Introduction*

Bluetooth is an open wireless technology standard for data transmission over short distances using short wavelength radio transmissions from fixed and mobile equipment, as a result of which, it is able to build personal area networks (PANS) with high security performance. It was originally designed as a wireless communication in place of RS-232 data cables. The advantage of Bluetooth is that it is able to connect several pieces of equipment synchronically. A radio technology called 'frequency-hopping spread spectrum' has been used in Bluetooth. This radio technology is able to exchange chunks of data up to 79 bands in the range of 2400-2483.5MHz which is in the globally unlicensed ISM (Industrial, Scientific and Medical) 2.4 GHz short range radio frequency band (Wikipedia 2011).

Bluetooth provides a secure way to transmit data between mobile phones, laptops, printers and faxes, and GPS receivers. Up to seven devices can communicate with the Bluetooth master equipment. The Bluetooth equipment is also able to switch roles from slave to master at any time (Wikipedia 2011). Bluetooth is a wireless communication technology with low consumption of power and a short effective range; as such, no visual line of sight is needed between Bluetooth devices due to the implementation of radio broadcast communications. The range of communications varies according to conditions, such as material coverage, antenna configuration and propagation conditions (Wikipedia 2011).

### *2.1.4.2 List of applications*

Bluetooth technology has the following applications (Wikipedia 2011):

- Wireless communications and controls between mobile phones
- Wireless networks between computers with small bandwidth.
- Wireless input and output devices such as keyboard, mouse and printer

- Replacement of RS-232 serial cable communications between equipment's, pieces of equipment such as computers, GPS receivers and bar code scanners.
- Low bandwidth
- Wireless bridge within two Ethernet networks.
- Internet access, as a wireless modem.
- Transmission of health sensors between medical devices.
- Real-time navigation systems. Bluetooth is used to identify and track the position of devices with 'Nodes' and 'tags' in real-time.

## 2.2 Accelerometer Error Model Review

In this thesis, a low cost wireless IMU has been developed. An IMU has many error sources, thus this section reviews the error models of accelerometers.

### 2.2.1 Accelerometer sensor errors

Every type of accelerometer contains errors which affect the accuracy of the measurement of the specific acting force. This type of accelerometer is able to produce very high performance with low biases, good linearity and with a dynamic range from $10^4$ to $10^5$. Following is a list of the major source of error discovered in mechanical accelerometers, as noted by Titterton (2004b):

#### *2.2.1.1 Fixed bias*

This error is a bias or a displacement from zero according to the measurement of the acting force which is represented when the corresponding acceleration is zero (Titterton 2004). The error arises due to the residual spring torques. The bias error is not dependent on any motion to which the accelerometer can be subjected. This error is normally represented in

units from milli-g to micro-g, with the result depending on the precision of the instrument (Titterton 2004).

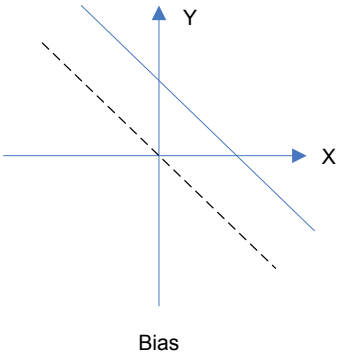


Figure 2-1: Errors of Bias

#### *2.2.1.2 Scale-factor errors*

Scale factor errors are the errors of a ratio change between the output sensors and the input acceleration measurement. Error arises due to the effects of the temperature and the non-ideal performance of the device. Usually, the scale factor is represented as a percentage of the full scale quantity measurement or as a ratio, such as, parts per million (PPM). The nonlinearity scale-factor depends on the systematic deviations from the least-squares straight line, which refers to the implemented acceleration and the output signal (Titterton 2004).

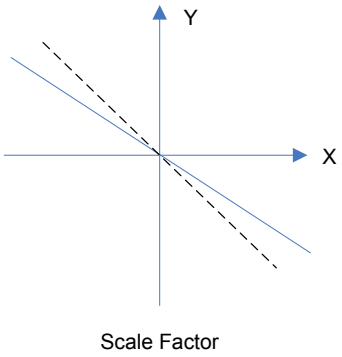


Figure 2-2: Errors of Scale Factor

#### *2.2.1.3 Cross-coupling errors*

Errors from accelerometer sensitivity to the accelerations system applied input axis and normal are resulted by the erroneous accelerometer outputs. This type of error is due to manufacturing imperfections which produce rise to the non-orthogonality of the sensor axes. The error of cross-coupling is usually presented as a percentage of the implemented acceleration (Titterton 2004).

#### *2.2.1.4 Vibro-pendulous errors*

Because of angular displacement of the pendulum which produces rise to a rectified output in the case of vibratory motion, dynamic cross-coupling in pendulous accelerometers arises. Vibro-pendulous error can occur in most pendulous accelerometers referring to the phasing between the displacement of the pendulum and the vibration. The maximum magnitude of the error is applied when the vibration is applied in a plane normal to the pivot axis at $\pi/4$ to the sensitive axis and when the pendulum movement is in phase with the vibration. The unit of $g/g^2$ can result in the error (Titterton 2004).

Errors arise in the case of gyroscopic sensors, such as, temperature dependent errors, repeatability errors and in-run errors. After system calibration, the residual errors caused by

the unpredictable error devices always represent the accuracy of the inertial system's performance (Titterton 2004).

#### *2.2.1.5 Accelerometer Error Model*

Titterton identified the error model of an accelerometer (Titterton 2004). Considering the error factors, the common accelerometer error model is described as follow:

In terms of the acceleration acting along the sensitive axis ($a_x$) and the applied accelerations acting along the pendulum, such as, hinge axes, $a_y$and $a_z$, the measurement given by the sensor ($\tilde{a}_x$) can be represented by the equation (Titterton 2004):

$$\tilde{a}_x = (1 + S_x)a_x + M_y a_y + M_z a_z + B_f + B_v a_x a_y + n_x \quad (2.5)$$

In this case, $S_x$ stands for the error of scale-factor, and is usually presented in polynomial form to contain non-linear effects. $M_y, M_z$stand for errors of the cross axis coupling factor. $B_f$ expresses the bias of the measurement, $B_v$ stands for the error coefficient of vibro-pendulous, and $n_x$ presents the random bias (Titterton 2004).

**Table 2-1: Typical performance of the accelerometer error factors**

| | |
|---|---|
| Input range | Up to $\pm$ 100g |
| Scale-factor stability | ~0.1% |
| Scale-factor non-linearity | ~0.05% of full scale |
| Fixed bias | 0.0001g-0.01g |
| Bias repeatability | 0.001g-0.03g |
| Bias temperature coefficient | ~0.001g/°C |
| Hysteresis | <0.002g |
| Threshold | ~0.00001g |
| Bandwidth | Up to 400Hz |

The very high accuracy accelerometers are applied to improve these figures significantly. A very low bias, a few micro-g, can be achieved with the high accuracy sensors, whereas a bias

of a few milli-g can be achieved with the experience of high acceleration in a dynamic platform. In theory, if the relationship between the input and output is known and invertible, errors of input data can be removed from the output results. In this case, errors of the dead-zone and quantisation have such problems. The cumulative effects of both errors of the dead zone and quantisation depend on zero-mean input noise; however, equal cumulative effects do not occur in all digitisation methods. Errors of cumulative quantisation for sensors with frequency outputs are bounded by ½ LSB, however, the variance of cumulative errors, such as A/D conversion errors from independent sample-to-sample can grow linearly with time (Titterton 2004).

### 2.2.2 A new approach to the integration of accelerometer data

Trujillo (1982) has found a new approach to the integration of accelerometer data and presented a dynamic programming formulation to correct the integration of accelerometer data. Distance and velocity results present significant drift due to noise and device errors. Mathematical methods, such as filtering and curve fitting with polynomials, can be used to correct the data sets. The mathematical methods can be designed using a set of measured accelerometer data $a_i^* \ (i = 1, N)$ with another expected data $(a_i)$ and integrated data set $V_N$ as a is the terminal velocity, and $h$ stands for time increment. The algorithm can be expressed as:

$$E = h \sum_{i=1}^{N} (a_i^* - a_i)^2 + \lambda V_N^2 \qquad (2.6)$$

$\lambda$ is a correction of original record (Trujillo 1982).

### 2.2.3 Error reduction for an inertial-sensor-based dynamic parallel kinematic machine positioning system

Gao et al. (2003) developed an inertial sensor error reduction method to improve the performance of inertial measurement. This method is designed to reduce system errors such as bias error, integration error and modelling error. The errors in the inertial sensor system can be categorised into several types, such as inertial sensor errors, misalignment error and process errors (Gao, Webb et al. 2003).

- Inertial sensor errors: include bias, cross-axis coupling and scale factor.
- Misalignment error: a gravity acceleration is calculated as a type of acceleration due to the angle of misalignment along the sensitive axis.
- Process errors: include errors of integration.

The dynamic environment in which the inertial system operates also affects system errors such as environmental noise, machine vibration and device electronic noise (Feng, Wen et al.). However, errors of bias, cross-axis coupling and scale factor can be measured by testing and observation. The errors of bias and scale factor are temperature dependent whereas the errors of noise and vibration are environment dependent. Fang conducted important research to improve the accuracy of an autonomous underwater vehicle (AUV). The accuracy of sensors is the main problem for an aided inertial navigation system. A Displaced Phase Centre Antenna (DPCA) technique was tested on an AUV Synthetic Aperture Sonar (SAS) test platform to enhance the performance of the aided inertial navigation system by micro navigation (Feng, Wen et al.). Oceanographic data was collected by the AUV researchers with a flexible, large-area and low-cost solution. AUVs were mounted with an aided inertial navigation system which was integrated by IMU and a Doppler-velocity-log (DVL). Sensor data was fused into the navigation system by Kalman filters. A displaced phase centre antenna (DPCA), also called a redundant phase centre (RPC), was used to improve the accuracy of the estimated motion (Feng, Wen et al.).

### 2.2.4 System errors development

Guobin et al. (2010) developed a system that did not use high-grade gyros and accelerometers to estimate errors. A systemic rotation auto compensation technique was introduced to improve the precision performance of a strapdown inertial navigation system. The system error equation was analysed by an eight-position dual-axis rotation-dwell scheme (Guobin, Jiangning et al. 2010) which effectively attenuated the error from constant bias of the inertial sensors failed to attenuate the errors from scale factor instability, misalignment and random noise. The output of low frequency was shifted to sinusoidal following the implementation of this technique (Guobin, Jiangning et al. 2010).

$$\varepsilon^{b} = C_{p}^{b}\varepsilon^{p} = \begin{bmatrix} \cos\gamma(t) & \sin\gamma(t) & 0 \\ -\sin\gamma(t) & \cos\gamma(t) & 0 \\ 0 & 0 & 1 \end{bmatrix} \begin{bmatrix} \varepsilon_x^p \\ \varepsilon_y^p \\ \varepsilon_z^p \end{bmatrix} = \begin{bmatrix} \varepsilon_x^p \cos\gamma(t) + \varepsilon_y^p \sin\gamma(t) \\ -\varepsilon_x^p \sin\gamma(t) + \varepsilon_y^p \cos\gamma(t) \\ \varepsilon_z^p \end{bmatrix} \quad (2.7)$$

Lupton and Sukkarieh (2008) mentioned that the projections of the two gyros' biases on the craft's body frame have sinusoidal forms, thus when integrated the bias will approach zero. An inertial measurement unit is implemented to remove any scale bias and ambiguity from 6DoF monocular SLAM (Simultaneous Localisation and Mapping). The solution shows that the scale bias is completely removed by the use of a square root information filter and the true scale of the map is observable over time with an IMU (Lupton and Sukkarieh 2008). An IMU provides useful information about the movement and the rotation of the platform. It is mounted for navigation and SLAM because it does not need an external infrastructure; however, low cost IMU obtains bias errors of the measurement which should be removed from the integration using an IMU integrated with the camera is capable of observing true

camera accelerations and this will reduce the bias errors of the map scale (Lupton and Sukkarieh 2008).

### 2.2.5 Real-time navigation accuracy

Bryson and Sukkarieh (2007) determined that the goal of the bearing-only inertial SLAM is to implement a real-time monitoring and communication system which provides real-time navigation accuracy to be used for the robot wireless monitoring system while building an accurate feature map.

An Un-aided inertial navigation system could be used in a number of places; however, the high cost, weight and power requirement of the necessary unit is prohibitive for most projects, and therefore, a low-cost INS can be used instead (Bryson and Sukkarieh 2007).

High performance space-oriented strapdown inertial navigation system (SINS) algorithms were introduced by Liduan et al. (2008). These algorithms contain a two-speed updating approach. One is the integration with a digital computer rather than the conventional method; the other is the improvement of the robustness of the inertial navigation system in high dynamic space environments (Liduan, Ping et al. 2008). High-grade simulations validate the performance of the system. True trajectories of space vehicles and error models of inertial sensors generate the inertial measurements data for the simulations. Recently, INS has been widely used for space vehicles with a GPS integrated system (Liduan et al. 2008). Nevertheless, a modern algorithm of a space-oriented strapdown INS has so far not been developed for public use; thus, two-speed updating algorithms have been developed for this purpose. The algorithm selects the Earth Centered Inertial (ECI) frame as strapdown INS navigation frame rather than the local geographic frame for most Single INS space flight applications (Liduan, Ping et al. 2008).

### 2.2.6 High reliability improvement

Qu et al. (2009) designed a micromechanical gyroscope and accelerometer as a mini and low-cost strapdown inertial navigation system for civilians. The system is based on a high calculation of SINS. A digital signal processor and complex programmable logic device are the main hardware of signal acquisition and data communication (Qu, Fu et al. 2009).

Inertial units have different devices from conventional gyroscopes and accelerometers, such as the optical gyroscope piezoelectric gyroscope, resonant beam accelerometer, hemispheric resonator gyroscope, microwave resonator accelerometer and micromechanical gyroscope (Qu, Fu et al. 2009). The micromechanical gyroscope is a kind of oscillation gyroscope, which contains no circumrotating part. Micro-manufacture technology is utilised to integrate a mini sensor, signal process and control circuit. Micromechanical gyroscope is a micro electro-mechanical system, which has several advantages, such as, small size, low cost, light weight and high reliability. However, it is still necessary to improve the precision of the system is necessary (Qu, Fu et al. 2009).

### 2.2.7 Navigation instrument errors

Gang et al. (2010) developed navigation instrument errors. To improve the accuracy of inertial navigation, the separation and compensation method of inertial measurement units were implemented in the system. The first step was to refine the navigation instrument error from the overall errors; the second step was to refine the coefficient deviation from navigation instrument error. In terms of the implementation of strap-down inertial navigation based on a ballistic missile, the dynamic separation method of INS instrument error was introduced. The Kalman filter was designed for error separation (Gang, Yong & Minghai 2010).

## 2.3 Accelerometer Calibration and Alignment Techniques

### 2.3.1 Inertial Navigation System Calibration

#### *2.3.1.1 Calibration*

Generally, the common method for estimating the bias errors of the inertial sensors is to obtain the output measurement from each sensor when the inertial platform is stationary. Calibration of the IMU is processed by these bias values. The measurement of these sensors is the bias of the sensor when the platform is stationary. The accelerometer bias can be determined by the alignment of the inertial unit.

Because the gravity can be determined, the anomalies in these values are resolved as bias during the alignment stage (Lueck & Wolk 2002).The equation of bias on the x-accelerometer is represented as:

$$b_{fx} = f_x - f_{xT} \tag{2.8}$$

In this case,$f_x$ stands for measurement of acceleration and $f_{xT}$ stands for the expected acceleration which is given during the alignment stage. The same operation is conducted to determine the remaining accelerometers (Lueck & Wolk 2002).

#### *2.3.1.2 Accelerometer Calibrator*

Lueck and Wolk (2002) developed a quick method for calibrating accelerometers. The device and implementation of high performance accelerometers were introduced and the consideration of the errors was established. With linear equipment, it is easy to calibrate the outputs of the devices by the careful alignment of their sensitive axis according to the direction of gravity. The alignment accuracies within a few degrees are usually 0.1% and better. The method is presented without any alignment with gravity. The method of developing the sensor's performance is to remove structural errors from the sensor output. The difference between a sensor's output and the output of its measurement is defined as a

structural error, which occurs consistently when a new measurement has been taken. Errors can be calculated and removed digitally in real-time by using the actual output of measurements during calibrations. Calibration is used to improve the accuracy of the sensors. It is performed by means of reading the accelerometer's output at equally spaced angular positions around a closed horizontal axis. Algorithms are generated for 3 angle (0, 120 and 240 degrees) and 4 angle (0, 90, 180 and 270 degrees) calibrations. It is not necessary to know the actual alignment of the sensitive axis of the accelerometers with respect to the angles of calibration (Lueck & Wolk 2002).

Four angles calibration:

The equation for position 1 is:

$$N_1 = ag\sin(\theta) + b \tag{2.9}$$

$a$ stands for the sensitivity of the accelerometer. $b$ stands for the offset and bias of the accelerometer. $\theta$ stands for the unknown angle between the local vertical gravity and the accelerometer axis. Both $a$ and $b$ can be determined during the calibration, therefore the output $N$ can be presented in terms of $g$ of acceleration (Lueck & Wolk 2002).

The equation for positions 2, 3 and 4 are expressed as:

$$N_2 = ag\sin\left(\theta + \frac{\pi}{2}\right) + b \tag{2.10}$$

$$N_3 = ag\sin(\theta + \pi) + b \tag{2.11}$$

$$N_4 = ag\sin\left(\theta - \frac{\pi}{2}\right) + b \tag{2.12}$$

From symmetry and trigonometry the equations can be solved without knowing $\theta$:

$$\sin(\theta + \pi) = -\sin\theta \tag{2.13}$$

$$\sin(\theta + \tfrac{\pi}{2}) = -\sin(\theta - \tfrac{\pi}{2}) = \cos(\theta) \tag{2.14}$$

Therefore,

$$b = \tfrac{1}{4}\{N_1 + N_2 + N_3 + N_4\} \tag{2.15}$$

$$ag = \tfrac{1}{2}\sqrt{(N_1 - N_3)^2 + (N_2 - N_4)^2} \tag{2.16}$$

Three angles calibration:

Three angles, equally reading 120 degrees can be used to calibrate the accelerometers (Lueck & Wolk 2002).

The three equations are:

$$N_1 = ag\sin(\theta) + b \tag{2.17}$$

$$N_2 = ag\sin\left(\theta + \tfrac{2\pi}{3}\right) + b = ag\cos(\theta + \tfrac{\pi}{6}) + b \tag{2.18}$$

$$N_3 = ag\sin\left(\theta - \tfrac{2\pi}{3}\right) + b = ag\cos(\theta - \tfrac{\pi}{6}) + b \tag{2.19}$$

The solution is

$$b = \tfrac{1}{3}\{N_1 + N_2 + N_3\} \tag{2.20}$$

$$ag = \tfrac{2}{3}\sqrt{{N_1}^2 + {N_2}^2 + {N_3}^2 - (N_1N_2 + N_1N_3 + N_2N_3)} \tag{2.21}$$

The accelerometer output can be modelled when it is considered to be linear. The following expression is applied (Olivares, Olivares et al. 2009):

$$\tilde{a}_{aa} = a_{aa}s_{aa} - b_{aa} \tag{2.22}$$

$a$=x, y, z stands for the axis of sensitivity.

$s_a$stands for the scale factor.

$b_a$stands for offset.

$\tilde{a}_a$stands for the acceleration output.

$a_a$stands for the output of raw data.

Two sets of data of the calibration line should be used to determine the scale factor and offset. Because the accelerometers are sensitive to accelerations, these should be g and –g respectively when the sensitive axes are placed parallel to both positive and negative gravity (Olivares, Olivares et al. 2009). Thus, two sets of data are generated for each sensitive axis by placing the two perpendicular sides of the device to the gravity axis, a 180° rotation is done along each of the x, y, and z, accelerometer axes. A diagram represents the position of each axis and the three outputs of each axis are recorded in each position. Errors of bias are computed following the alignment technique (Olivares, Olivares et al. 2009).

#### *2.3.1.3 Calibration of accelerometer triad of IMU with drifting Z-accelerometer bias*

Hung et al. (1989) developed a method which has been enhanced to multi-position test the accelerometer's calibration of an IMU. This method is used for bias drift of the Z-accelerometer (Hung, Thacher et al. 1989). Twelve parameters of the triad are determined during calibration which contains three biases, three scale factors, three dis-symmetry constants, and three triad non-orthogonality uncertainties. Initially, the coordinates of the three axes are shown as x, y, and z and a twelve position measurement and test has been constructed for calibration (Hung, Thacher et al. 1989). A set of twelve measurement equations are used to determine twelve constant parameters. During the course of the twelve position test, the z-accelerometer is temperature dependent and is therefore not stable. In this case, the three non-orthogonality uncertainties should not be negligible. A

method called 'deterministic correlation identification' is introduced as an error compensation method (Hung, Thacher et al. 1989).

#### *2.3.1.4 High-efficiency low-cost accelerometer-aided gyroscope calibration*

Olivares et al. (2009) found that a calibration system is design for an IMU containing a tri-axial accelerometer and a biaxial gyroscope. Since the MEMS accelerometers offer more accuracy and better performance than MEMS gyroscopes, the calibration system for the gyroscope is designed to use bicycle wheel as a turntable with the accelerometer data. Currently, errors such as misalignment, bias and noise are the most remarkable errors from the sensor output, and these errors can be reduced during the calibrations, the tri-axial accelerometers, ADXL330, with a range of ±3g are used in the calibrations (Olivares, Olivares et al. 2009). The sample rate was 50Hz. Because of the sensitivity of gravity acceleration, accelerometers should be placed parallel to gravity in both positive and negative directions. A 180° rotation is used for three accelerometer axes. Two sets of data are provided for each axis. Considering the model of accelerometer output could be linear, the corrections of bias are implemented to be no more than 0.76% of full scale (Olivares, Olivares et al. 2009).

#### *2.3.1.5 Numerical calibration for 3-axis accelerometers and magnetometers*

Camps et al. (2009) noted that the inertial unit contains magnetometers, accelerometers and gyro-meters. The calibration of these sensors therefore depends on several situations, such as the local magnetic field, the sensor attitude and the real parameters of bias and scale factor. The Levenberg-Marquardt Algorithm (LMA) is implemented to minimise the estimation for one-dimensional function (Camps, Harasse et al. 2009).

#### *2.3.1.6 Accelerometer calibration and dynamic bias and gravity estimation: analysis, design, and experimental evaluation*

Batista et al. (2009) presented a calibration of an accelerometer and a dynamic filtering method for reducing bias. Currently, a new generation of MEMS accelerometer is being

widely used; however, large bias, scale factor and other nonlinearities have been discovered during the implementation. A calibration technique has been developed for these low-cost tri-axial accelerometers to determine bias, scale-factor and cross coupling factors, and a time-varying Kalman filter has been developed to estimate online dynamic bias and gravity of navigation system for mobile platforms (Batista, Silvestre et al. 2002). To determine scale and cross-axis errors, several tests have been carried out on different days in different environments for dynamic accelerometer calibration. Calibration of the accelerometer is validated before the usage in navigation (Batista, Silvestre et al. 2002).

#### *2.3.1.7 Calibration of MEMS accelerometer based on plane optical tracking technique and measurements*

Zhuxin et al. (2009) developed a calibration method to provide good parameters of sensor measurement. Since the system provides a high sampling rate, 200Hz, a simple filter is developed to reduce the errors from system vibration. The method averages every five data to provide an averaged value for the middle point as the coordinate providing smoother curves and better resolution. However, if the quantity of averaged points of the filter is too high, the information of the true movement will be loss (Zhuxin, Wejinya et al. 2009).

### 2.3.2 Inertial Navigation System Alignment

#### *2.3.2.1 Alignment Techniques*

The attitude of the inertial device can be given by the output of the gravity component when the outputs of the accelerometer are known perfectly.

The equation below presents the measurement of the gravity component from the accelerometers (Nebot 2005).

$$f_b = (C_b^n)^{-1} f_n \tag{2.23}$$

Where$C_b^n$ is orthogonal, the inverse is the transpose. Because the inertial unit is stationary, the measured acceleration is along the vertical axis (Nebot 2005).

$$f_n = [0 \quad 0 \quad -g]^T \tag{2.24}$$

Then, the equation will be:

$$\begin{bmatrix} f_{xT} \\ f_{yT} \\ f_{zT} \end{bmatrix} = \begin{bmatrix} \beta_c\gamma_c & \beta_c\gamma_s & -\beta_s \\ \theta_c\gamma_s + \theta_s\beta_s\gamma_c & \theta_c\gamma_c + \theta_s\beta_s\gamma_s & \theta_s\beta_c \\ \theta_s\gamma_s + \theta_c\beta_s\gamma_c & -\theta_s\gamma_c + \theta_c\beta_s\gamma_s & \theta_c\beta_c \end{bmatrix} \begin{bmatrix} 0 \\ 0 \\ -g \end{bmatrix}$$

Where the subscript T stands for the true acceleration unit because of gravity,

Thus:

$$f_{xT} = g \sin\beta \tag{2.25}$$

$$f_{yT} = -g \sin\theta \cos\beta \tag{2.26}$$

$$f_{zT} = -g \cos\theta \cos\beta \tag{2.27}$$

There are no perfect sensors; the higher the accuracy, the lower the error occurs. Therefore, the alignment accuracy can be obtained when the accuracy of the sensors is lower (Nebot 2005). A method called 'coarse alignment' used to determine alignment by rearranging the previous equations to determine the pitch β. Then the roll θ will be solved by substituting pitch θ into either equation (Nebot 2005).

When the coarse alignment method is not sufficiently accurate for the performance of navigation, an external source of alignment will be needed, such as a tilt sensor, GNSS attitude. Generally, the method of coarse alignment is implemented for rapid alignment, for example in missile applications, when no time is required for averaging the data of an external source (Nebot 2005).

Finally, the term r, which should be evaluated, stands for the heading of the vehicle. The heading is self-determined by gyrocompass (Nebot 2005). The output of the gyros is able to determine the devices of rotation of the Earth when the measurement of the attitude is determined by the measurement of initial position. However, it is possible to use an external source to find the initial heading when low cost gyros are implemented with high noise and low resolution of sensors (Nebot 2005).

#### *2.3.2.2 Accuracy of INS alignment*

Jie and Ruiping (2010) have mentioned that the accuracy of the alignment of INS affects the accuracy of a strapdown inertial navigation system. The state equation and observation equation were established on the basis of Kalman filter principle. The results display the algorithm, which is simply and effectively to approach the initial alignment (Jie and Ruiping 2010).

The sensor errors and alignment of an inertial navigation system affect the navigation solution. A celestial observation aided inertial navigation system, mounted on a space vehicle, depends on updated parameters from the INS. However, when the space vehicle is outside the dense atmospheric layer, errors of misalignment and gyro drift can be removed by celestial observations. A technique is presented to overcome the error of accumulated velocity and position. Thus, the navigation accuracy has been improved (Gul and Fang 2005).

# Chapter 3

# Modelling of Wireless Accelerometer Communication

In this chapter, a new wireless accelerometer communication design is presented. Currently, the majority of IMU accelerometers are designed with cable for data transmission. Some have been developed with wireless communications; however, the errors in such systems are significantly noticeable. In addition, the wireless communication device has been usually been fixed on the accelerometer and is not functional when implemented on other accelerometers. The following system enables these issues to be solved. A wireless communication mounted accelerometer has been designed, and a method of error reduction has been developed.

## 3.1 Hardware Configuration Design

The figure 3-1 displays the functional block diagram of the hardware configuration. The accelerometer that has been used in the system is OS 5000 IMU which is an off-the –shelf device from STM. In the system, this device has been added a Bluetooth adapter to communicate the computer wirelessly, it is also able to communicate the computer via cable, the process of the how the data transfers and be calibrated is displayed in the functional block diagram.

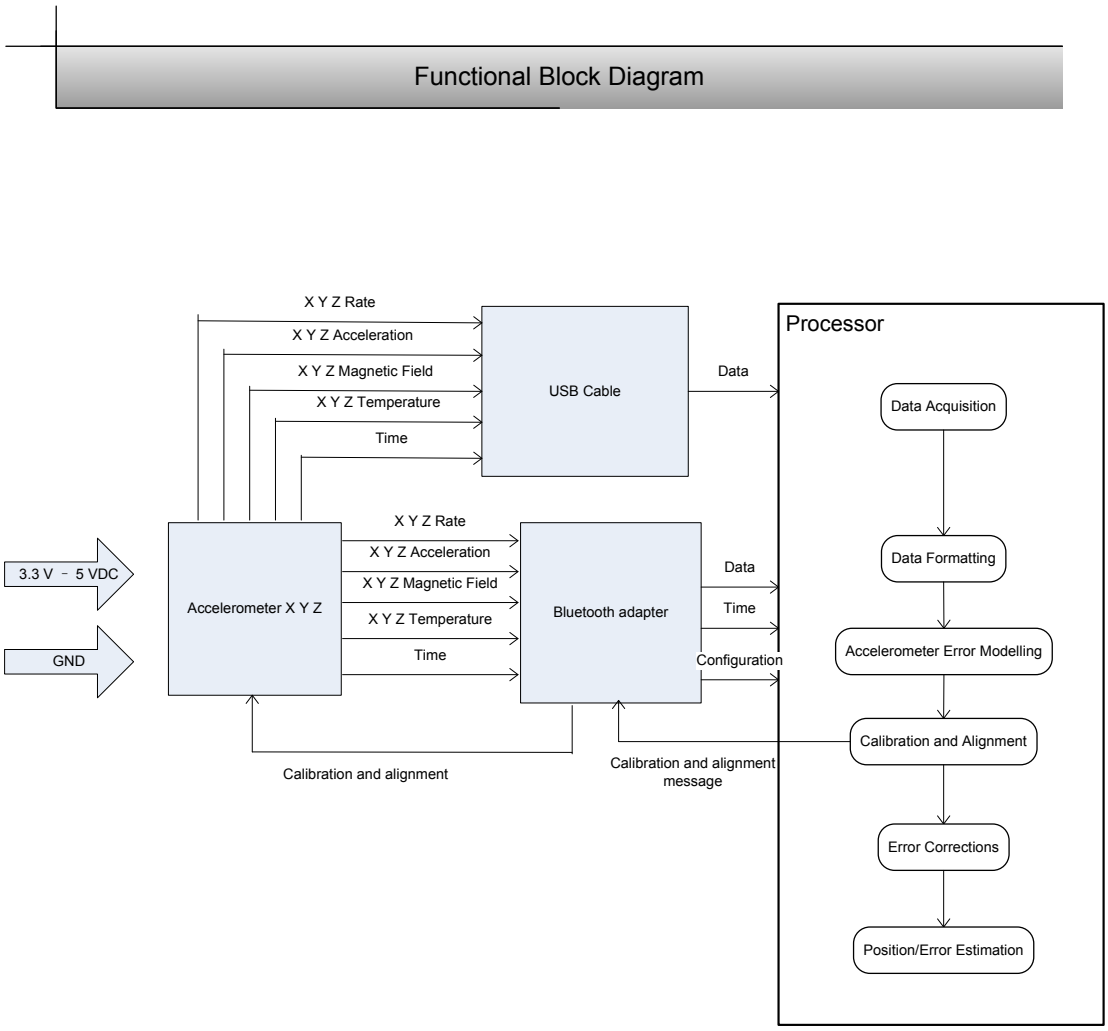


Figure 3-1: Functional Block Diagram of hardware configuration

The wireless inertial measurement unit is designed as in Figure 3-1. Three accelerometer sensors (X, Y, Z) are set up in three orthogonal axes. Data is transferred to the computer via a Bluetooth adapter which includes X, Y, Z acceleration, magnetic field, time and temperature. The same baud rate has been adjusted on both the Bluetooth adapter and the computer. When the acceleration operates, the computer converts raw data into readable data which is displayed on the screen synchronously. Error modelling is designed to estimate and reduce errors from wireless communication by comparing wireless communication data with the data from the same source via cable communication. In the error modelling process, a USB cable is connected to the computer; therefore, two sets of data have been transferred to the computer by different communication methods. Data

errors are addressed during the process and algorithms and error modelling has been developed to calibrate and align the system. The calibration and alignment message is transferred back to the accelerator. The acceleration setting can be adjusted during the calibrations, and updated raw data will again be sent to the computer via Bluetooth. When the errors have been estimated and corrected, the data will be implemented to determine the gyro-free INS position estimations.

## 3.2 Implementation of Wireless Accelerometer Communication

### 3.2.1 Inertial measurement unit specification

Os 5000 IMU has been used for the experiment. The 3 axis LIS331 accelerometer is from STM. The following tables represent the descriptions and specifications of the IMU(Oceanserver 2011):

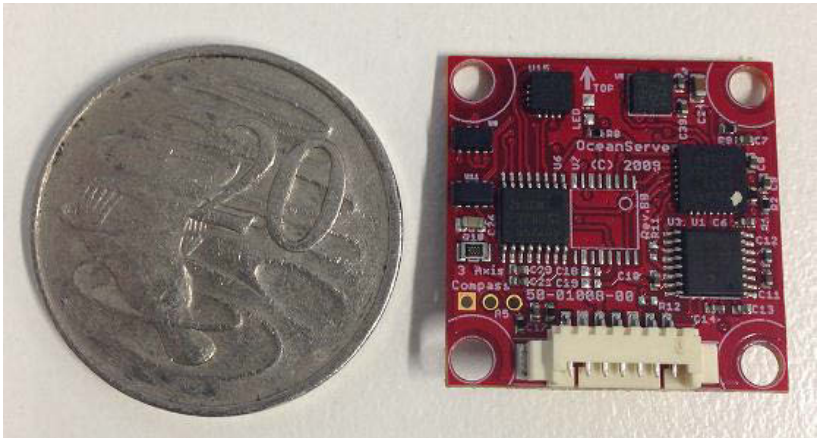


Figure 3-2: Ocean Server Inertial Measurement Unit, OS 5000 Series (Oceanserver 2011)

Table 3-1: Descriptions of IMU (Ocearserver 2011)

| Hardware | Descriptions |
|---|---|
| Magnetic sensors | 3 Axis magnetic Honeywell AMR sensors |
| Accelerometer | 3 Axis STM LIS331 accelerometer |
| Microprocessor | 50 MIPS processor supporting IEEE floating point operations |
| AD conversion | 24 bit differential sigma-delta converters |
| Compass accuracy | Weighs less than 2 grams weight |
| Inclination | 0.5 degrees nominal, 0.1 resolution |
| Temperature range | -40C to +85C operating, Humidity: 20-80% RH non-condensing |
| Weight | ~2 grams |
| Supply Voltage | 3.3V – 5VDC (Will operate with up to 15VDC using 3x the power) |
| Power consumption | 30ma at 3.3V |
| Serial Data Interface | RS-232C levels, TTL and USB 2.0 based on Variant 4800-115000 baud, 8 bit, 1 stop, no parity (19200 default) |
| Magnetic Compensation Routines | Hard Iron and Soft Iron calibrations supported, note: Soft iron |

To use wireless communication, IMU should connect to both battery power and Bluetooth adapter by using cable 19-00061-24 (serial and power connections). Figure 3-3 displays the setup of wireless communication. A laptop nearby can remotely communicate with IMU and gather raw data lists.

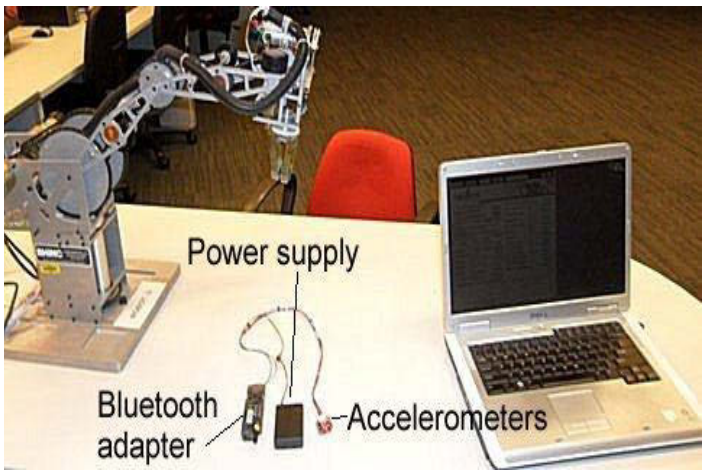


Figure 3-2: Prototype of wireless accelerometer unit

#### *3.2.1.1 Specifications*

The features of the IMU are displayed in table 3-2 (Oceanserver 2011):

Table 3-2: Features of IMU (Ocearserver 2011)

| Features |
|---|
| Digital SPI, I2C interfaces |
| Selectable full scale: from ±2g up to ±24g |
| < 0.25 mA current consumption in normal mode |
| < 10 µA current consumption in low-power mode |
| < 1µ current consumption in power-down mode |
| Resolution better than 1 mg |
| Ultra high stability over temperature: TYP 0.1 mg/°C |
| Operating temperature range: - 40°C to 85°C |
| Embedded self test |
| High shock survivability: 10,000g for 0.1 ms |
| Tiny size, 1” x 1”x 0.3”; weighs less than 2 grams weight |
| Precision compass accuracy, 0.5 degrees nominal, 0.1 resolution |
| Roll & Pitch full rotation (<1 degree (0-60 degrees)) |
| Tilt-compensated (electronically gimbaled) |
| Low power consumption, <20ma @3.3V |
| Hard and soft-iron compensation routines |
| Optional support for a high resolution depth or altitude sensor (24 bit A/D) |
| Serial Interface: RS232, USB or TTL |
| 50 MIPS processor supporting IEEE floating point math |
| Baud rate programmable: 4,800 to 115,000 baud |
| Rugged design (10,000 G shock survival) |
| Operating temperature: -20C to 70C (-40C to 85C storage) |
| ASCII sentence output in several formats; NMEA checksum |
| High data update rate to 40HZ |
| Support for True or Magnetic North output |
| 24 bit differential Analog to Digital converters from Analog Devices |

### 3.2.2 Cables (communication and power)

The description of different cables which have been implemented in the experiments is displayed in table 3-3 (Oceanserver 2011):

**Table 3-3: Descriptions of cables** (Oceanserver 2011)

| ID | Descriptions |
|---|---|
| 19-00061-24 | 24" OS5000-S Demo Kit Cable with Serial connection, Pressure and 3.6V battery power connection |
| 19-00062-24 | 24" OS5000-S/-T Series Pigtail Cable, 7 Pin connector, blunt cut |
| 19-00116-00 | Approx. 6' OS5000-US Demo Kit Cable with USB to 6 Pin connector |

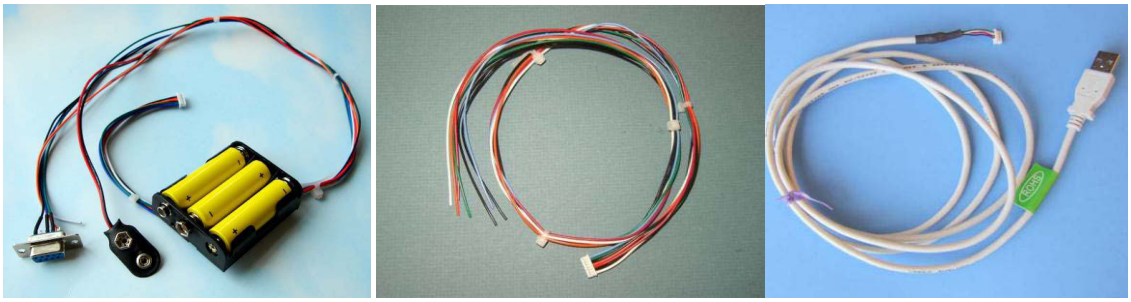

**Figure 3-3: Cables implemented in the experiments** (Oceanserver 2011)

### 3.2.3 Bluetooth Adapter Specification

The Bluetooth serial adapter, BluePort XP, is used in the experiments with an integrated power pack. It can connect to any legacy serial port at a rate of 232.4 kbps. The range of transmission is 100m (Rovingnetworks 2011). The size of the Bluetooth adapter is about 3.6" x 1.2" x 0.9" with 3.3V DC from integrated LiPoly battery. The Baud rate is from 1200 to 232 Kbps and there is no standard values and the data rate is 300Kbps. The Bluetooth version that it implemented is 2.1+EDR.

The table 3-4 represents the specification of the Bluetooth adaptor which I used in the system (Rovingnetworks 2011):

**Table 3-4: Specifications of Bluetooth** (Oceanserver 2011)

| ID | Descriptions |
|---|---|
| Bluetooth Versions | 2.1 + EDR, 2.0, 1.2, 1.1 |
| Data rate | 300 Kbps |
| Baud rate | 1200 to 232 Kbps and non-standard values |
| Frequency Band | 2.412 - 2.484 GHz |
| Modulation Techniques | FHSS/GFSK modulation, 79 channels at 1 MHz intervals |
| Profiles | SPP, DUN, HID, RFCOM, L2CAP, SDP |
| Supply voltage | 3.3V DC from integrated LiPoly battery. |
| Output power | +15dBm |
| Operating temperature | -40C to +85C |
| Interface | RS232, Bluetooth |
| Antenna | 1" or 4" external SMA antenna |
| Size | 3.6" x 1.2" x 0.9" |

### 3.2.4 Flexible Connection Modes of Bluetooth

The Bluetooth device used in the system is the BluePort-XP, displayed in the figure 3-4. It can create a virtual com port on the slave mode (Rovingnetworks 2011). If it is used as a terminal server, BluePort-XP will be automatically detected and connected to from a Bluetooth LAN access point. The application data can be transmitted over the network (Rovingnetworks 2011).

**Figure 3-4: Bluetooth adapter** (Rovingnetworks 2011)

## 3.3 Summary

In this chapter, the design and modelling of a wireless accelerometer unit have been presented, and the error modelling and model validation approach have been demonstrated in the functional block diagram. Three traditional accelerometers (X, Y, Z) are built in three orthogonal axes. A Bluetooth adaptor wirelessly and continuously transfers the raw acceleration measurements and communication configuration messages to a remote processor. The remote processor collects these acceleration readings and formats the data for later computing. An accelerometer error model was established using a modelling approach which will be presented in the next chapter. The remote processor returns the accelerometer calibration and positioning alignment information to the accelerometers wirelessly via the Bluetooth adaptor. At the start of every positioning mission, the accelerometers are calibrated and the initial positioning values are aligned. During a positioning mission, this unit continuously outputs the calibrated acceleration readings wirelessly, and computes the positioning information and estimates the positioning error continuously. This system is implemented using a MEMS IMU, a Bluetooth adaptor and a laptop as a remote processor. The figures below show these components of the wireless accelerometer unit before it is installed in a vehicle platform.

# Chapter 4

# Wireless Accelerometer Unit Error Modelling

This chapter presents the major contribution of this thesis: 'wireless accelerometer error modelling'. Bluetooth is one of mature wireless protocols. It is a reliable technology that I do not need to investigate if there is any error occurs during the data transmission. Theoretically, the data from wireless communication should be the same as the data from cable communication. However, Bluetooth is using short wavelength radio transmission, which has electromagnetic field. Inertial measurement unit is a high sensitive unit, any magnetic fields can interfere the accuracy of the output. Therefore, there is no error during the wireless communication, but the errors occur prior to the transmission. IMU is initially interfered by electromagnetic field from Bluetooth and then generates inaccurate data. These inaccurate data will be transferred to the computer wirelessly. The error modelling I have designed in my thesis is not just limited for these Bluetooth errors. It is a black box modeling. Error models have been separated into two sections, linear error modelling and nonlinear error modelling of the wireless inertial sensor. Both calibration and alignment have been designed for the particular models to minimise the value of errors. A gyro-free wireless communication inertial sensor has been prototyped and implemented for the sensor error calibration process. The approach for modelling the wireless inertial sensor errors and calibration is demonstrated in this chapter.

## 4.1 Experimental Method

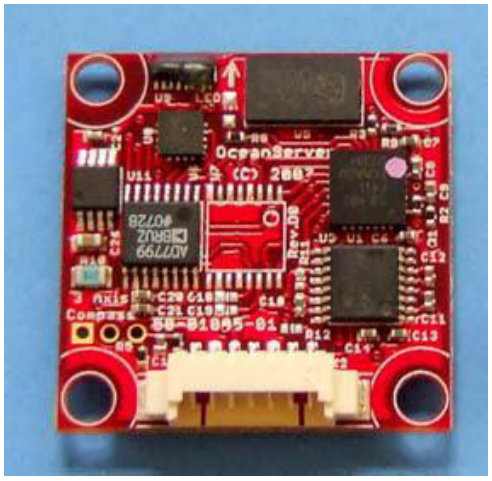

**Figure 4-1: Inertial Measurement Unit** (Oceanserver 2011)

In terms of the form and nature of the accelerometer system, it is appropriate to test either the complete system or just the measurement unit in the laboratory. Usually, when the development of a system has reached the point of laboratory testing, the characteristics of the component sensors used will be very well known and the purpose of the testing will be somewhat different from the objectives of the 'component tests'. However, one aim of checking the performance of the system is, for example, to determine whether the measurement of wireless communication behaves as predicted from the knowledge of the performance of the accelerometers. Sometimes, a manufacturer will wish to check that the units built on a production line will meet the design specification and the user will also wish to confirm that the inertial system will fulfil the requirements of a particular application. Typically, such tests involve wireless communications on a multi-axis platform. The system is rotated through a series of accurately known angles and positioned in different orientations with respect to the local gravity vector. The dominant sensor errors may then be determined from the static measurements of acceleration and turn rate taken in each

orientation of the unit. The unit under test is placed on a precision three axis platform, and a series of constant rate tests and multi-position tests are then used to allow the major sources of error to be identified.

### 4.1.1 Inertial Testing and Compensation

In order to obtain high performance results, a calibration and alignment has been processed. High accuracy ground truth data has been required to evaluate the estimated results produced by processing accelerometer data. The model of IMU OS5000 from OceanServer uses a 3-axisHoneywell AMR sensor and precision Tilt-compensated (electronically gimbaled) 3-axis accelerometer from ST Microelectronics which provides a precise accelerometer and rate for the testing and development of the inertial system. A tri-axial accelerometer, sampled at 0.5 Hz to 400 Hz using three MEMS LIS331DLF accelerometers, and containing a digital output motion sensor is an ultra-low-power high performance 3-axes “nano” accelerometer. The OS5000 is a high precision, low power consumption, high stability component in which resolution is better than 1 mg. It is able to communicate through both Serial and USB cables. Two different connections are available, and the IMU and the appropriate cable will be automatically detected (Oceanserver 2011). To locate magnetic north, earth’s magnetic field is considered to be an effect of the measurement of IMU (Oceanserver 2011). The earth’s magnetic field can be affected or offset by other magnetic fields when the IMU is mounted on certain devices or platforms. Sources of local magnetic fields can be ferrous metal, motor magnets and electric currents (Oceanserver 2011), and ‘soft-iron’ and ‘hard-iron’ are two sources of magnetic field distortion. Un-magnetized ferrous metal causes effects of ‘soft-iron’, whereas magnetized ferrous materials cause effects of ‘hard-iron’ near the IMU (Oceanserver 2011). The method, rotational calibration method is able to remove ‘hard-iron’ near IMU. To minimize the

impact of 'soft-iron' effects on the IMU, devices should be located away from such magnetic items. Soft-iron calibration is able to minimize the effects of soft-iron, this the measured data of distortion at a distance will be much more accurate with the implementation of soft iron correction (Oceanserver 2011).

### 4.1.2 Compass calibration process

1. To calibrate the IMU hardware, software has to be installed in the computer for reading data from the OceanServer device (Oceanserver 2011).

2. To take two separate measurements (X-Y and Z) for calibration, a Hyperterm window must open a virtual terminal, such as TeraTerm, in the calibration. The setting of the serial port should be: 19200 baud, 1 stop, no parity. The baud rate of the port should be adjusted to the same as that set on the Bluetooth adapter in the laboratory. Thus, the computer will start to output a string of data when it is connected to the sensor device (Oceanserver 2011).

3. Calibration of X, Y:

    1) The data of pitch and roll is checked and confirmed to ensure that each of them is no more than 1 degree and the platform is level. The area of experiment should be well away from hard-iron and soft-iron objects such as magnets, motors and wire with current that could disrupt the earth's magnetic field. The platform is fully rotated to confirm that the calibration process will remain at same level (Oceanserver 2011).

2) To calibrate X, Y, slowly rotate the platform for more than 20 seconds in at least one complete rotation. To obtain accurate magnetic sensing elements, the platform should be in as level a state as possible. Terminate the process after the device has been slowly rotated and the following output "…" is displayed by the software, which determines the values of maximum and minimum of X, Y (Oceanserver 2011).

3) If the platform is not kept level during calibration, the procedure must be repeated (Oceanserver 2011).

4. Calibration of Z axis: the Z axis is turned on its side by rotating the device 90 degrees.

1) The operational area of the experiment should be clear so that that there are no external soft iron and hard iron effects around the device, such as motors, magnets and wires with current. The calibration has to be carried out in the same area with the same earth's magnetic field, as the calibration for the X, Y axes (Oceanserver 2011).

2) Mode of Z calibration. The device should be slowly rotated 360 degrees to complete at least one rotation. More than 20 seconds time should be allowed for the rotation to obtain accurate magnetic sensing elements. The Z calibration should be processed in the same location as the X and Y calibration because this is important for tile compensation. The calibration procedure must be re-done if the platform is not level during the experiment (Oceanserver 2011).

### 4.1.3 Calibration of Soft Iron

Soft iron effects are caused by batteries, wires with current and other magnetic materials in the near field. The methods of the X, Y and Z calibration routines do not compensate for soft iron effects. Soft iron effects are generally much weaker than hard iron effects (Oceanserver 2011). A good IMU mounting location without soft iron structures should be chosen. Soft iron calibration should be run in cases where soft iron impacts sensors. Before the calibration process, the system with the IMU should be installed and calibrated. The declination has to be set to 0 before the soft iron calibrations. Four cardinal points need to be aligned according to an accurate reference magnetic compass, namely, 0˚ North, 90˚ East, 180˚ South, 270˚ West in a magnetic disturbance-free area. After the device and system have been properly aligned, the soft iron correction starts at 0˚ North with an <esc>$ command followed by entering 2 (Oceanserver 2011). The correction values will be generated once the calibration process has been run, and indicate that the soft iron calibration has been completed. The cardinal points in the system should be double checked. If the system is still not accurate compared to the ground true reference, the calibration process should be run again and each step should be checked carefully. The distance from the soft iron should be adjusted to generate a good result, if the magnetic field is too disturbed to allow accuracy of calibration (Oceanserver 2011).

## 4.2 Error Model

Two error modelling approaches are designed in this research. In the following sections, a linear error modelling approach is described. Wireless accelerometer modelling using nonlinear wireless accelerometer modelling is introduced in the second section is introduced in the second section.

### 4.2.1 Linear error model

This section presents the accelerometer error modelling approach and model results using the design and implementation on functional block diagram shown in Figure 3-1.

In the hardware configuration, three accelerometers are installed in three orthogonal axes x, y and z. Errors of accelerometers include: accelerometer bias, scale factor, misalignment of the three accelerometers' installation in three orthogonal axes, cross-axis effect, other random noises.

Considering these error components, the general accelerometer error r model for three accelerometers in axis-X, axis-Y, axis-Z are as following:

$$\begin{aligned}
\delta f_x &= b_x + S_{f_x} \times a_x + m_{y_x} \times a_y + m_{z_x} \times a_z + B_{x_y} \times a_x \times a_y + B_{x_z} \times a_x \times a_z + \eta_x \\
\delta f_y &= b_y + S_{f_y} \times a_y + m_{x_y} \times a_x + m_{z_y} \times a_z + B_{y_x} \times a_y \times a_x + B_{y_z} \times a_y \times a_z + \eta_y \\
\delta f_z &= b_z + S_{f_z} \times a_z + m_{x_z} \times a_x + m_{y_z} \times a_y + B_{z_x} \times a_z \times a_x + B_{z_y} \times a_z \times a_y + \eta_z
\end{aligned} \tag{4.1}$$

Where

$a_x, a_y, a_z$ are accelerations in axis-x, axis-y, and axis-z.

$\delta f_x, \delta f_y, \delta f_z$ are accelerometer errors in axis-x, axis-y, and axis-z.

bx, by, bz are accelerometer bias in axis-x, axis-y, and axis-z.

Sf_x, Sf_y, Sf_z are scale factors of accelerometer x, y and z.

my_x, mz-x, mx_y, mz_y, mx_z, my_z are error coefficients for accelerometers' installation and misalignment errors.

Bx_y, Bx_z, By_x, By_z, Bz_x, Bz_y represent cross-axis error coefficients

$\eta_x, \eta_y, \eta_z$ are random noises on accelerometers' signals in axis-x, axis-y, and axis-z.

To model equation 4.1, a 6-position testing is designed.

The six-position configuration of the accelerometers is:

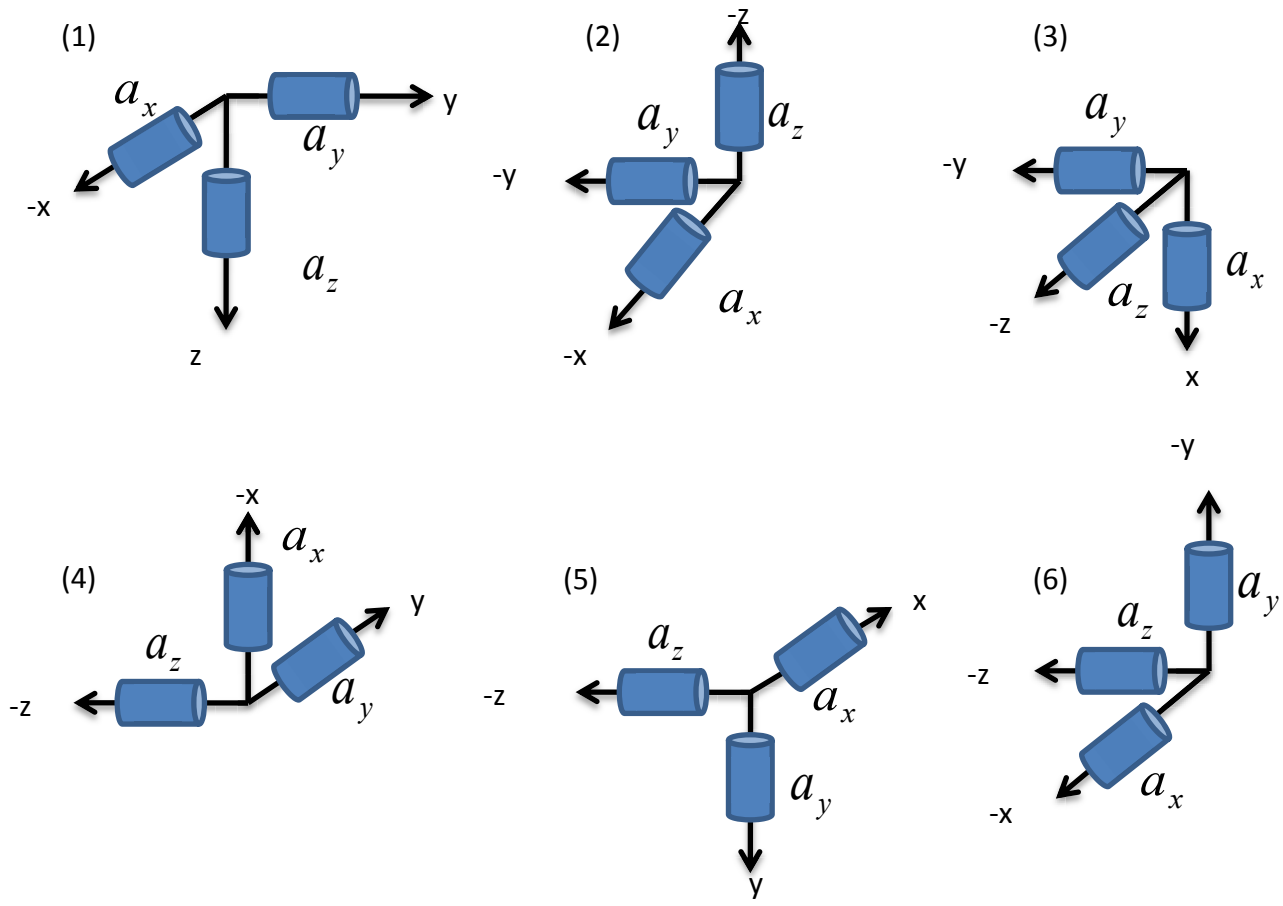


Figure 4-2: 6-positions testing

The specific forces on the three accelerometers in these six positions are as in Figure 4-2. Accelerometer measurements are collected in the six positions. Accelerometer outputs measured in the six positions are compared with the specific forces in Figure 4-2.

From the experiments, it was found that the cross-axis errors make little contribution to the overall errors. The cross-axis error coefficients Bx_y, Bx_z, By_x, By_z, Bz_x, Bz_y can therefore be ignored during the modelling process. The accelerometer error model can be simplified as following:

$$\begin{aligned}
\delta f_x &= b_x + S_{f_x} \times a_x + m_{y_x} \times a_y + m_{z_x} \times a_z + \eta_x \\
\delta f_y &= b_y + S_{f_y} \times a_y + m_{x_y} \times a_x + m_{z_y} \times a_z + \eta_y \\
\delta f_z &= b_z + S_{f_z} \times a_z + m_{x_z} \times a_x + m_{y_z} \times a_y + \eta_z
\end{aligned} \tag{4.2}$$

Model parameters are calculated using the following approach.

In position 1, accelerometer x and y are on the horizontal plain. Accelerometer z is vertically in line with the gravity direction. The specific forces in 3 axes in position 1 are

$$\begin{aligned}
a_x(1) &= 0 \\
a_y(1) &= 0 \\
a_z(1) &= g
\end{aligned} \tag{4.3}$$

The accelerometers' measurements in 3 axes are $\tilde{a}_x(1), \tilde{a}_y(1), \tilde{a}_z(1)$.

The accelerometer errors in 3 axes are:

$$\begin{aligned}
\delta f_x(1) &= \tilde{a}_x(1) - a_x(1) \\
\delta f_y(1) &= \tilde{a}_y(1) - a_y(1) \\
\delta f_z(1) &= \tilde{a}_z(1) - a_z(1)
\end{aligned} \tag{4.4}$$

Substituting (4.3) to (4.4), replacing the left side of (4.2) with (4.4), and applying (4.3) in (4.2), we have:

$$\begin{aligned}
b_x + m_{z_x} \times g + \eta_x &= -\tilde{a}_x(1) \\
b_y + m_{z_y} \times g + \eta_y &= \tilde{a}_y(1) \\
b_z + S_{f_z} \times g + \eta_z &= \tilde{a}_z(1) - g
\end{aligned} \tag{4.5}$$

In position 2, the specific forces are

$$\begin{aligned} a_x(2) &= 0 \\ a_y(2) &= 0 \\ a_z(2) &= -g \end{aligned} \tag{4.6}$$

The accelerometers' measurements in 3 axes are: $\tilde{a}_x(2), \tilde{a}_y(2), \tilde{a}_z(2)$ .Using the same approach as in Position 1, we have:

$$\begin{aligned} b_x + m_{z\_x} \times (-g) + \eta_x &= -\tilde{a}_x(2) \\ b_y + m_{z\_y} \times (-g) + \eta_y &= -\tilde{a}_y(2) \\ b_z + S_{f\_z} \times (-g) + \eta_z &= -g - \tilde{a}_z(2) \end{aligned} \tag{4.7}$$

Applying the same procedure in Positions 1 and 2, the error model parameters and accelerometer measurements of positions 3, 4, 5 and 6 are derived as follows:

Position 3:

$$\begin{aligned} b_x + S_{f\_x} \times (g) + \eta_x &= \tilde{a}_x(3) - g \\ b_y + m_{x\_y} \times (g) + \eta_y &= -\tilde{a}_y(3) \\ b_z + m_{x\_z} \times (g) + \eta_z &= -\tilde{a}_z(3) \end{aligned} \tag{4.8}$$

Position 4:

$$\begin{aligned} b_x + S_{f\_x} \times (-g) + \eta_x &= -g - \tilde{a}_x(4) \\ b_y + m_{x\_y} \times (-g) + \eta_y &= \tilde{a}_y(4) \\ b_z + m_{x\_z} \times (-g) + \eta_z &= -\tilde{a}_z(4) \end{aligned} \tag{4.9}$$

Position 5:

$$\begin{aligned} b_x + m_{y\_x} \times (g) + \eta_x &= \tilde{a}_x(5) \\ b_y + S_{f\_y} \times (g) + \eta_y &= \tilde{a}_y(5) - g \\ b_z + m_{y\_z} \times (g) + \eta_z &= -\tilde{a}_z(5) \end{aligned} \tag{4.10}$$

Position 6:

$$\begin{aligned} b_x + m_{y\_x} \times (-g) + \eta_x &= -\tilde{a}_x(6) \\ b_y + S_{f\_y} \times (-g) + \eta_y &= -g - \tilde{a}_y(6) \\ b_z + m_{y\_z} \times (-g) + \eta_z &= -\tilde{a}_z(6) \end{aligned} \tag{4.11}$$

The measurement errors of sensors are dependent on the physical operational principle of the sensor itself. The accelerometer unit previously introduced has been operated in several calibration experiments. The calibration results show that the cross-axis and quadratic coefficient errors do not change significantly in the laboratory, which validates the calibration of the accelerometer prior to the using the navigation system. Therefore, the experiments focus on the method of how to determine the bias and scale factor errors between wireless communications and cable. After determining the errors of bias and scale factor, error modeling is able to be calculated to reduce such errors in wireless communication in 3 axes in 6 positions. The diagrams of validations are displayed in this chapter to present the improvement of the data.

## Position 1

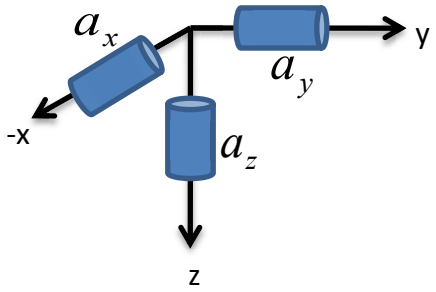


Figure 4-3: Position 1 system position

$$\begin{aligned} a_x(1) &= 0 \\ a_y(1) &= 0 \\ a_z(1) &= g \end{aligned} \tag{4.13}$$

$$\begin{aligned} b_x + m_{z\_x} \times (-g) + \eta_x &= -\tilde{a}_x(1) \\ b_y + m_{z\_y} \times (-g) + \eta_y &= -\tilde{a}_y(1) \\ b_z + S_{f\_z} \times (-g) + \eta_z &= -g - \tilde{a}_z(1) \end{aligned} \tag{4.14}$$

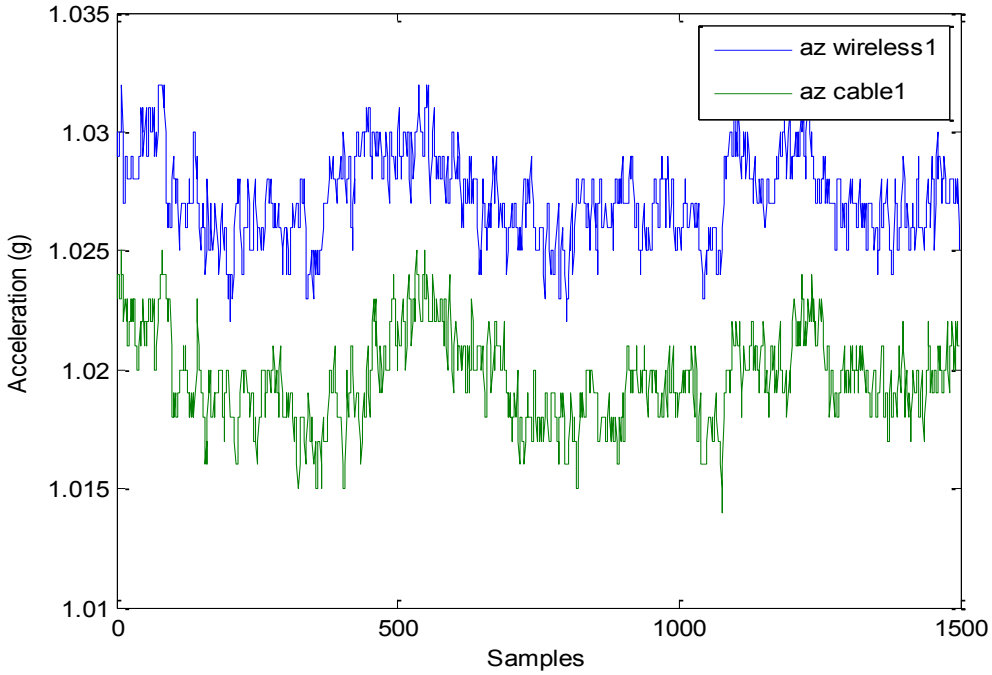


Figure 4-4: Accelerations of wireless and cable in linear model

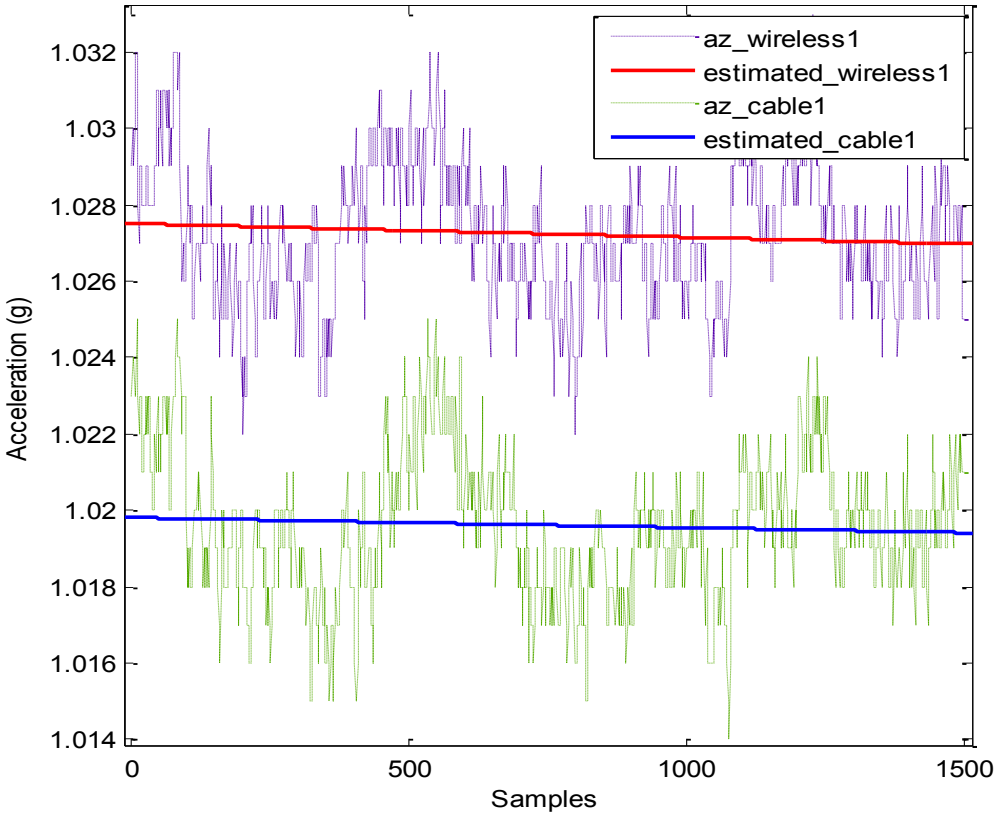


Figure 4-5: Position 1 Estimated accelerations of wireless and cable in linear model

Linear model wireless position 1:

f(x) = p1*x + p2

Coefficients (with 95% confidence bounds):

p1 = -3.572e-007 (-5.693e-007, -1.45e-007)

p2 = 1.028 (1.027, 1.028) (4.15)

Linear model cable position 1:

f(x) = p1*x + p2

Coefficients (with 95% confidence bounds):

p1 = -2.628e-007 (-4.858e-007, -3.979e-008)

p2 = 1.02 (1.02, 1.02) (4.16)

**Table 4-1: Position 1 linear model results for Ax, Ay and Az in both wireless mode and cable mode**

| Position 1 | | | | | | |
|---|---|---|---|---|---|---|
| | Ax | | Ay | | Az | |
| | Wireless | Cable | Wireless | Cable | Wireless | Cable |
| p1 | 7.13E-08 | 7.86E-08 | 1.19E-07 | 2.15E-08 | -3.57E-07 | -2.63E-07 |
| p2 | 0.002365 | 0.001136 | 0.005484 | 0.004991 | 1.028 | 1.02 |

Figure 4-3 displays the position 1 of the system and the directions of three axes (X, Y and Z). Where accelerations on X axis and Y axis are 0; and acceleration on Z axis is g.

Figure 4-4 displays 1500 samples of two different accelerations at the same system position on Z axis in a static state. The green data presents the acceleration of cable communication, whereas the blue data presents the acceleration of Bluetooth wireless communication.

Figure 4-5 displays the estimated data of two different accelerations on Z axis at the same system position on Z axis in a static state. Two accelerations have been estimated by using curve fitting. In terms of the equations from 4.7 to 4.11, curve fitting equation has been designed as f(x) = p1*x + p2 as a linear model, where p1 can be looked as scale factor, p2 can be looked as bias. The curve fitting method is able to present the track of accelerations.

Table 4-1 clearly displays the difference and comparison of the data of cable communication and wireless communication at position 1.

## Position 2

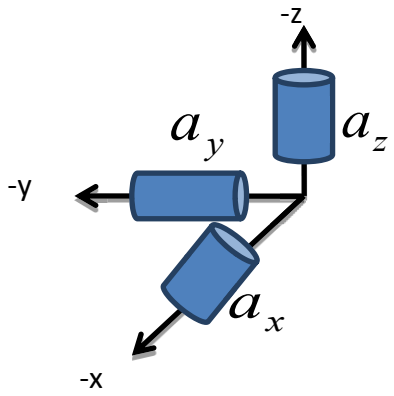


Figure 4-6: Position 2 system position

$$\begin{aligned} a_x(2) &= 0 \\ a_y(2) &= 0 \\ a_z(2) &= -g \end{aligned} \tag{4.17}$$

$$\begin{aligned} b_x + m_{z\_x} \times (-g) + \eta_x &= -\tilde{a}_x(2) \\ b_y + m_{z\_y} \times (-g) + \eta_y &= -\tilde{a}_y(2) \\ b_z + S_{f\_z} \times (-g) + \eta_z &= -g - \tilde{a}_z(2) \end{aligned} \tag{4.18}$$

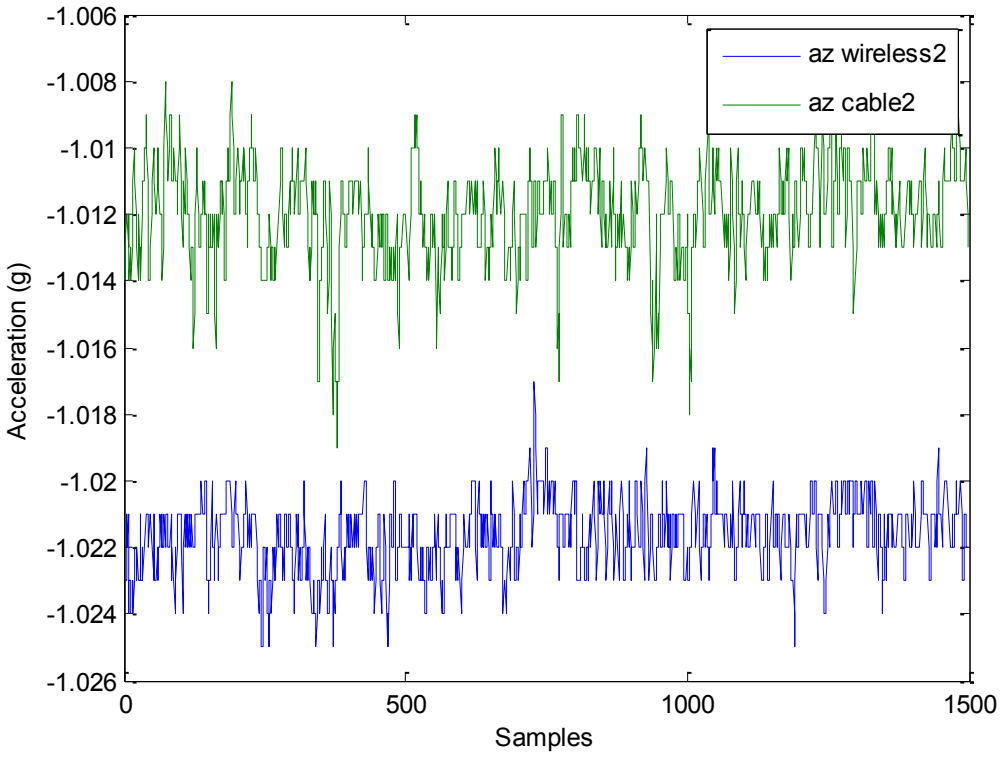


Figure 4-7: Position 2 Accelerations of wireless and cable in linear model

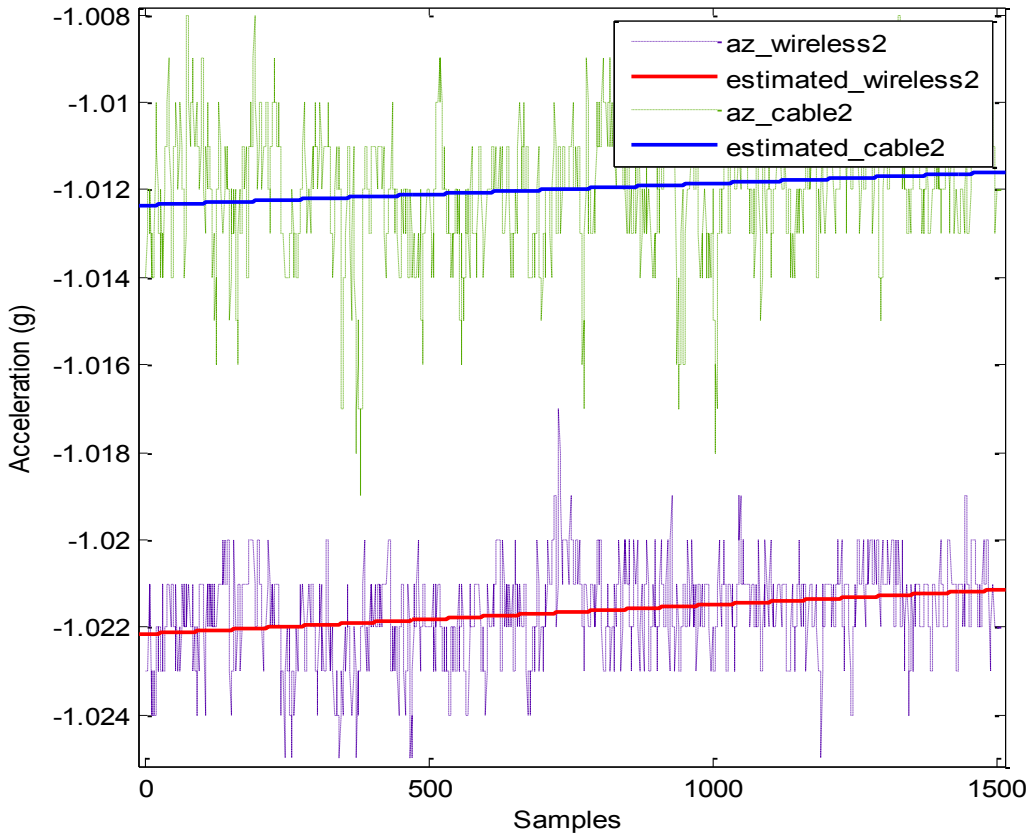


Figure 4-8: Position 2 Estimated accelerations of wireless and cable in linear model

Linear model wireless position 2:

f(x) = p1*x + p2

Coefficients (with 95% confidence bounds):

p1 = 6.675e-007 (5.464e-007, 7.887e-007)

p2 = -1.022 (-1.022, -1.022) (4.19)

Linear model cable position 2:

f(x) = p1*x + p2

Coefficients (with 95% confidence bounds):

p1 = 4.997e-007 (3.273e-007, 6.722e-007)

p2 = -1.012 (-1.013, -1.012) (4.20)

**Table 4-2: Position 2 linear model results for Ax, Ay and Az in both wireless mode and cable mode**

| Position 2 | | | | | | |
|---|---|---|---|---|---|---|
| | Ax | | Ay | | Az | |
| | Wireless | Cable | Wireless | Cable | Wireless | Cable |
| p1 | -1.26E-08 | 6.64E-08 | 1.44E-07 | 4.92E-07 | 6.68E-07 | 5.00E-07 |
| p2 | -6.00E-05 | 0.002028 | 0.007696 | 0.006505 | -1.022 | -1.012 |

Figure 4-6 displays the position 2 of the system and the directions of three axes (X, Y and Z). Where accelerations on X axis and Y axis are 0; and acceleration on Z axis is -g.

Figure 4-7 displays 1500 samples of two different accelerations at the same system position on Z axis in a static state. The green data presents the acceleration of cable communication, whereas the blue data presents the acceleration of Bluetooth wireless communication.

Figure 4-8 displays the estimated data of two different accelerations on Z axis at the same system position on Z axis in a static state. Two accelerations have been estimated by using curve fitting. As mentioned in system position 1, curve fitting equation has been designed as f(x) = p1*x + p2 as a linear model, where p1 can be looked as scale factor, p2 can be looked as bias. The curve fitting method is able to present the track of accelerations. Table 4-2 clearly displays the difference and comparison of the data of cable communication and wireless communication at position 2.

## Position 3

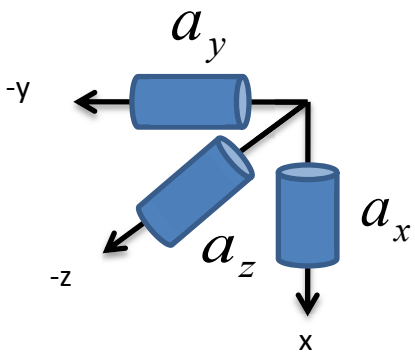


Figure 4-9: Position 3 system position

$$\begin{aligned} a_x(3) &= g \\ a_y(3) &= 0 \\ a_z(3) &= 0 \end{aligned} \tag{4.21}$$

$$\begin{aligned} b_x + S_{f\_x} \times (g) + \eta_x &= \tilde{a}_x(3) - g \\ b_y + m_{x\_y} \times (g) + \eta_y &= -\tilde{a}_y(3) \\ b_z + m_{x\_z} \times (g) + \eta_z &= -\tilde{a}_z(3) \end{aligned} \tag{4.22}$$

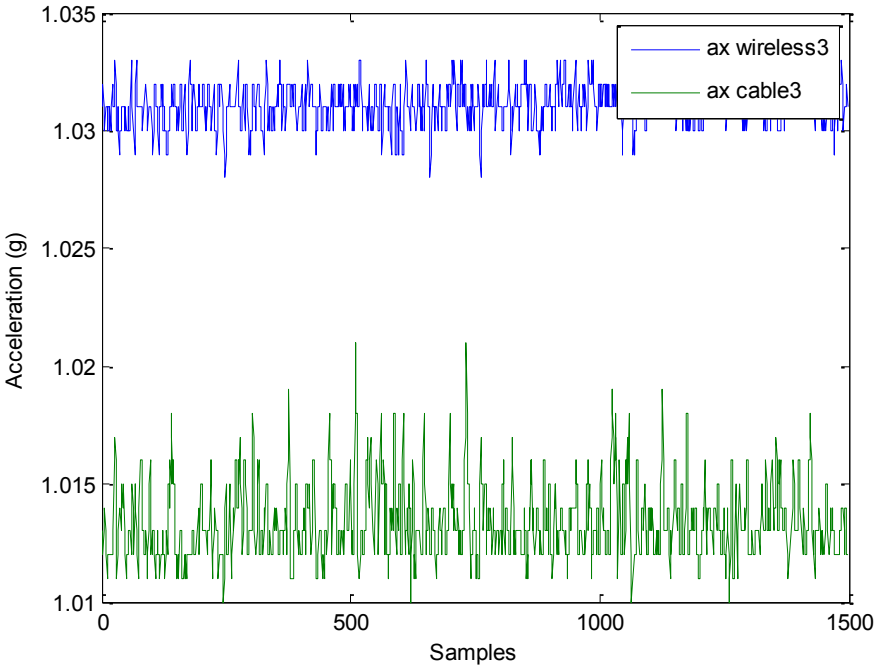


Figure 4-10: Position 3 Accelerations of wireless and cable in linear model

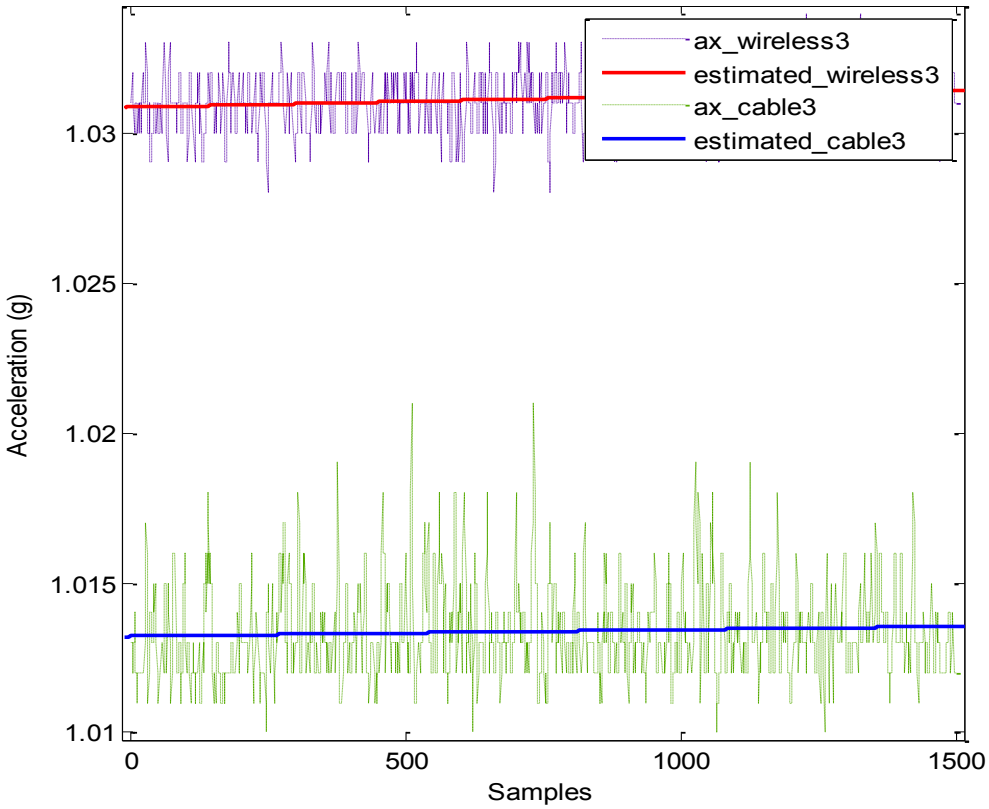


Figure 4-11: Position 3 Estimated accelerations of wireless and cable in linear model

Linear model wireless position 3:

f(x) = p1*x + p2

Coefficients (with 95% confidence bounds):

p1 = 3.892e-007 (2.875e-007, 4.908e-007)

p2 = 1.031 (1.031, 1.031) (4.23)

Linear model cable position 3:

f(x) = p1*x + p2

Coefficients (with 95% confidence bounds):

p1 = 2.196e-007 (3.811e-008, 4.011e-007)

p2 = 1.013 (1.013, 1.013) (4.24)

**Table 4-3: Position 3 linear model results for Ax, Ay and Az in both wireless mode and cable mode**

| Position 3 | | | | | | |
|---|---|---|---|---|---|---|
| | Ax | | Ay | | Az | |
| | Wireless | Cable | Wireless | Cable | Wireless | Cable |
| p1 | 3.89E-07 | 2.20E-07 | 1.02E-06 | 4.39E-07 | 1.84E-07 | 3.02E-07 |
| p2 | 1.03E+00 | 1.013 | 0.01471 | -0.00873 | -0.00036 | 0.000392 |

Figure 4-9 displays the position 3 of the system and the directions of three axes (X, Y and Z). Where accelerations on Y axis and Z axis are 0; and acceleration on X axis is g.

Figure 4-10 displays 1500 samples of two different accelerations on X axis at the same system position on X axis in a static state. The green data presents the acceleration of cable communication, whereas the blue data presents the acceleration of Bluetooth wireless communication.

Figure 4-11 displays the estimated data of two different accelerations at the same system position on X axis in a static state. Two accelerations have been estimated by using curve fitting. As mentioned in system position 1, curve fitting equation has been designed as f(x) = p1*x + p2 as a linear model, where p1 can be looked as scale factor, p2 can be looked as bias. The curve fitting method is able to present the track of accelerations. Table 4-3 clearly displays the difference and comparison of the data of cable communication and wireless communication at position 3

## Position 4

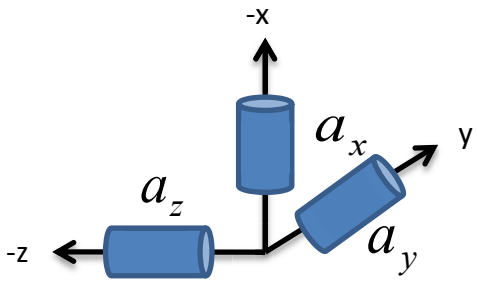


Figure 4-12: Position 4 system position

$$\begin{aligned} a_x(4) &= -g \\ a_y(4) &= 0 \\ a_z(4) &= 0 \end{aligned} \tag{4.25}$$

$$
\begin{aligned}
b_x + S_{f\_x} \times (-g) + \eta_x &= -g - \tilde{a}_x(4) \\
b_y + m_{x\_y} \times (-g) + \eta_y &= \tilde{a}_y(4) \\
b_z + m_{x\_z} \times (-g) + \eta_z &= -\tilde{a}_z(4)
\end{aligned}
\tag{4.26}
$$

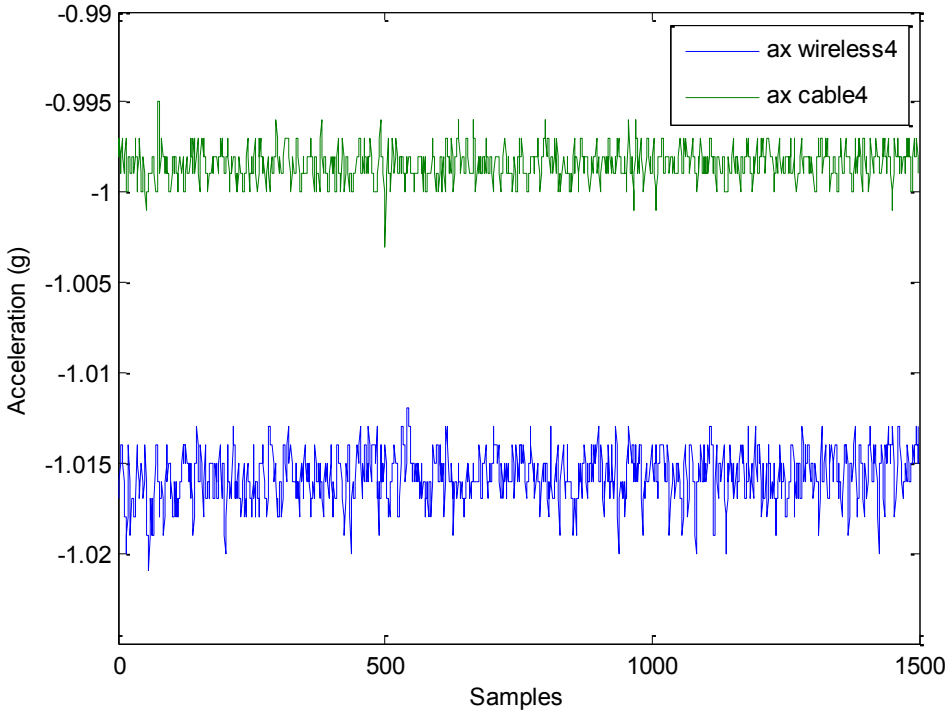


Figure 4-13: Position 4 Accelerations of wireless and cable in linear model

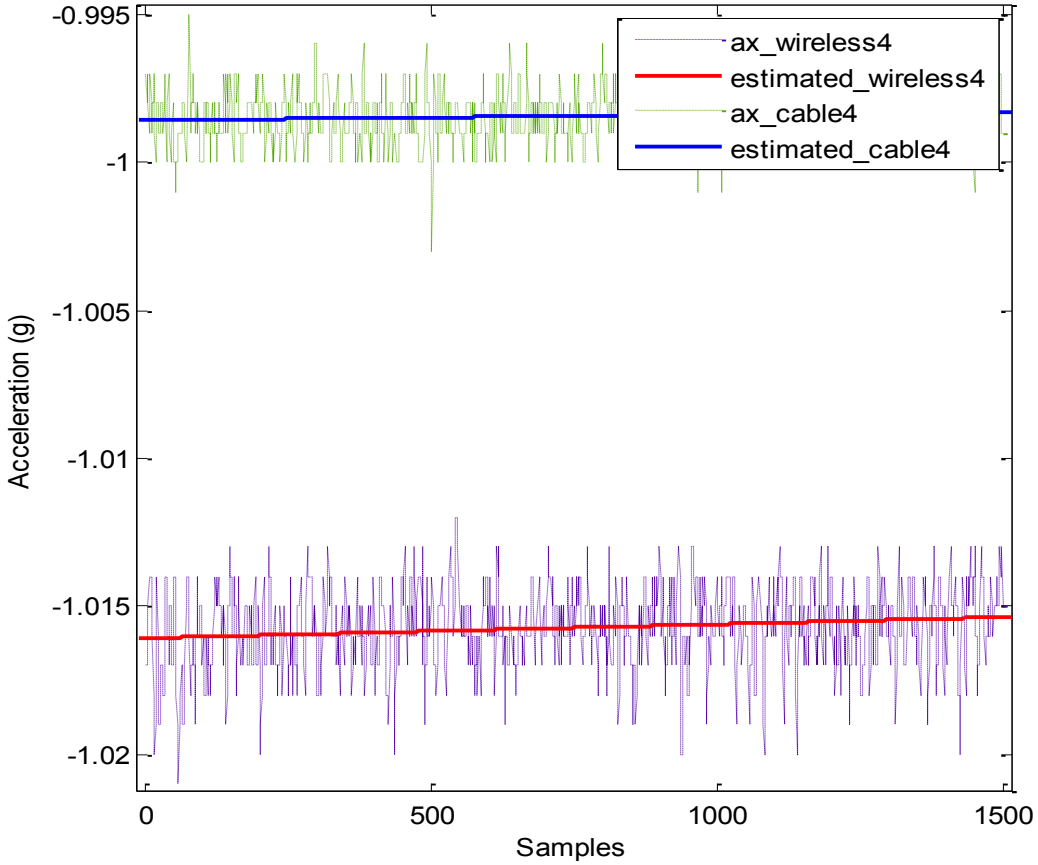


Figure 4-14: Position 4 Estimated accelerations of wireless and cable in linear model

Linear model wireless position 4:

f(x) = p1*x + p2

Coefficients (with 95% confidence bounds):

p1 = 4.714e-007 (3.13e-007, 6.299e-007)

p2 = -1.016 (-1.016, -1.016) (4.27)

Linear model cable position 4:

f(x) = p1*x + p2

Coefficients (with 95% confidence bounds):

p1 = 1.952e-007 (8.937e-008, 3.011e-007)

p2 = -0.9986 (-0.9987, -0.9985) (4.28)

**Table 4-4: Position 4 linear model results for Ax, Ay and Az in both wireless mode and cable mode**

| Position4 | | | | | | |
|---|---|---|---|---|---|---|
| | Ax | | Ay | | Az | |
| | wireless | Cable | Wireless | Cable | Wireless | Cable |
| p1 | 3.51E-07 | 1.95E-07 | 3.62E-07 | 2.47E-07 | 5.37E-07 | -1.09E-06 |
| p2 | -1.016 | -0.9986 | -0.01122 | 0.01316 | 0.01002 | 0.004893 |

Figure 4-12 displays the position 4 of the system and the directions of three axes (X, Y and Z). Where accelerations on Y axis and Z axis are 0; and acceleration on X axis is -g.

Figure 4-13 displays 1500 samples of two different accelerations at the same system position on X axis in a static state. The green data presents the acceleration of cable communication, whereas the blue data presents the acceleration of Bluetooth wireless communication.

Figure 4-14 displays the estimated data of two different accelerations at the same system position on X axis in a static state. Two accelerations have been estimated by using curve fitting. As mentioned in system position 1, curve fitting equation has been designed as f(x) = p1*x + p2 as a linear model, where p1 can be looked as scale factor, p2 can be looked as bias. The curve fitting method is able to present the track of accelerations. Table 4-4 clearly displays the difference and comparison of the data of cable communication and wireless communication at position 4.

## Position 5

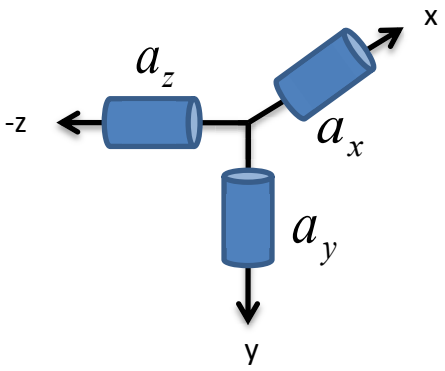


Figure 4-15: Position 5 system position

$$\begin{aligned} a_x(5) &= 0 \\ a_y(5) &= g \\ a_z(5) &= 0 \end{aligned} \tag{4.29}$$

$$\begin{aligned} b_x + m_{y\_x} \times (g) + \eta_x &= \tilde{a}_x(5) \\ b_y + S_{f\_y} \times (g) + \eta_y &= \tilde{a}_y(5) - g \\ b_z + m_{y\_z} \times (g) + \eta_z &= -\tilde{a}_z(5) \end{aligned} \tag{4.30}$$

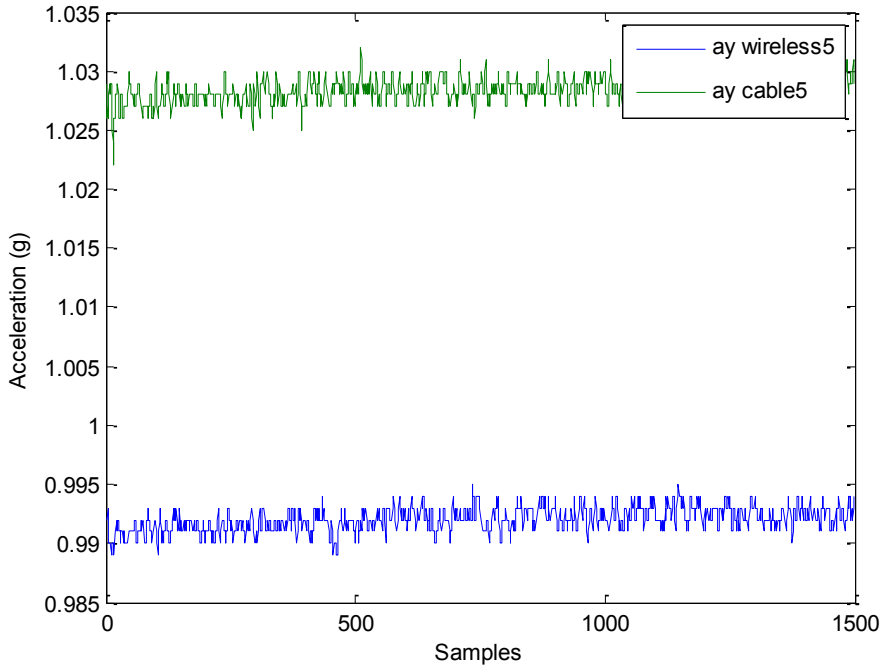


Figure 4-16: Position 5 Accelerations of wireless and cable in linear model

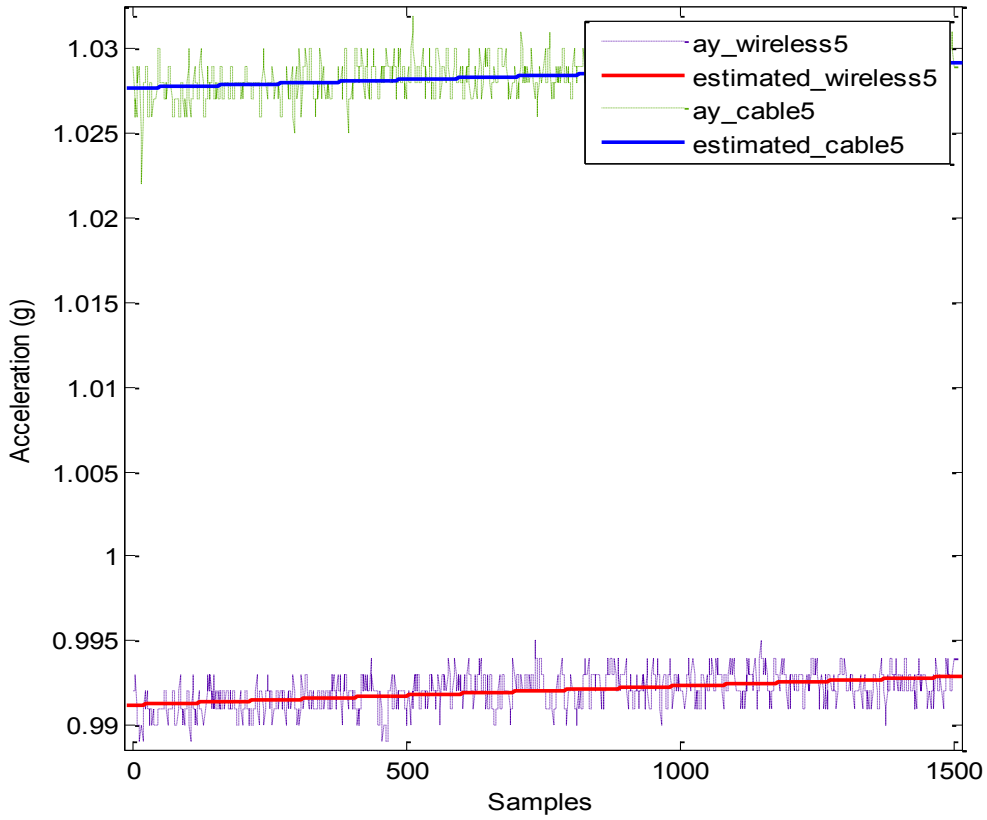


Figure 4-17: Position 5 Estimated accelerations of wireless and cable in linear model

Linear model wireless position 5:

f(x) = p1*x + p2

Coefficients (with 95% confidence bounds):

p1 = 1.107e-006 (1.001e-006, 1.213e-006)

p2 = 0.9912 (0.9911, 0.9913) (4.31)

Linear model cable position 5:

f(x) = p1*x + p2

Coefficients (with 95% confidence bounds):

p1 = 9.729e-007 (8.599e-007, 1.086e-006)

p2 = 1.028 (1.028, 1.028) (4.32)

**Table 4-5: Position 5 linear model results for Ax, Ay and Az in both wireless mode and cable mode**

| Position 5 | | | | | | |
|---|---|---|---|---|---|---|
| | Ax | | Ay | | Az | |
| | Wireless | Cable | Wireless | Cable | Wireless | Cable |
| p1 | 5.69E-07 | 2.87E-07 | 1.11E-06 | 9.73E-07 | 2.87E-07 | -8.13E-07 |
| p2 | -0.01068 | 0.01454 | 0.9912 | 1.028 | -0.0004 | -7.13E-05 |

Figure 4-15 displays the position 5 of the system and the directions of three axes (X, Y and Z). Where accelerations on X axis and Z axis are 0; and acceleration on Y axis is g.

Figure 4-16 displays 1500 samples of two different accelerations at the same system position on Y axis in a static state. The green data presents the acceleration of cable communication, whereas the blue data presents the acceleration of Bluetooth wireless communication.

Figure 4-17 displays the estimated data of two different accelerations at the same system position on Y axis in a static state. Two accelerations have been estimated by using curve fitting. As mentioned in system position 1, curve fitting equation has been designed as f(x) = p1*x + p2 as a linear model, where p1 can be looked as scale factor, p2 can be looked as bias. The curve fitting method is able to present the track of accelerations. Table 4-5 clearly displays the difference and comparison of the data of cable communication and wireless communication at position 5.

## Position 6

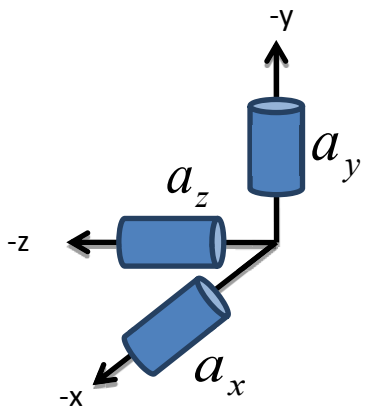


Figure 4-18: Position 6 system position

$$\begin{aligned} a_x(6) &= 0 \\ a_y(6) &= -g \\ a_z(6) &= 0 \end{aligned} \tag{4.33}$$

$$
\begin{aligned}
b_x + m_{y\_x} \times (-g) + \eta_x &= -\tilde{a}_x(6) \\
b_y + S_{f\_y} \times (-g) + \eta_y &= -g - \tilde{a}_y(6) \\
b_z + m_{y\_z} \times (-g) + \eta_z &= -\tilde{a}_z(6)
\end{aligned}
\tag{4.34}
$$

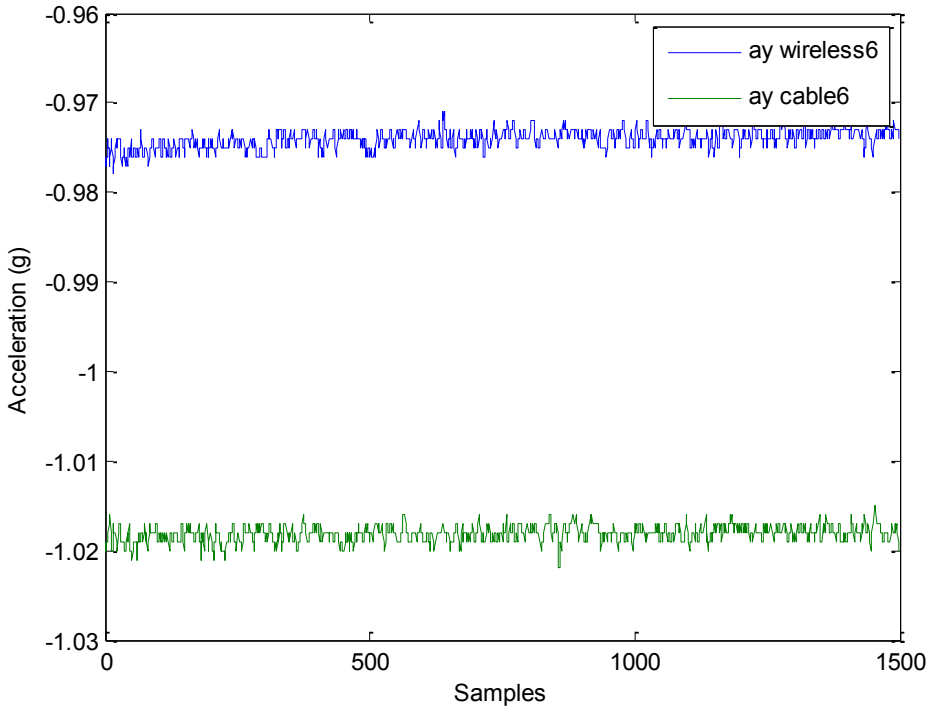


Figure 4-19: Position 6 Accelerations of wireless and cable in linear model

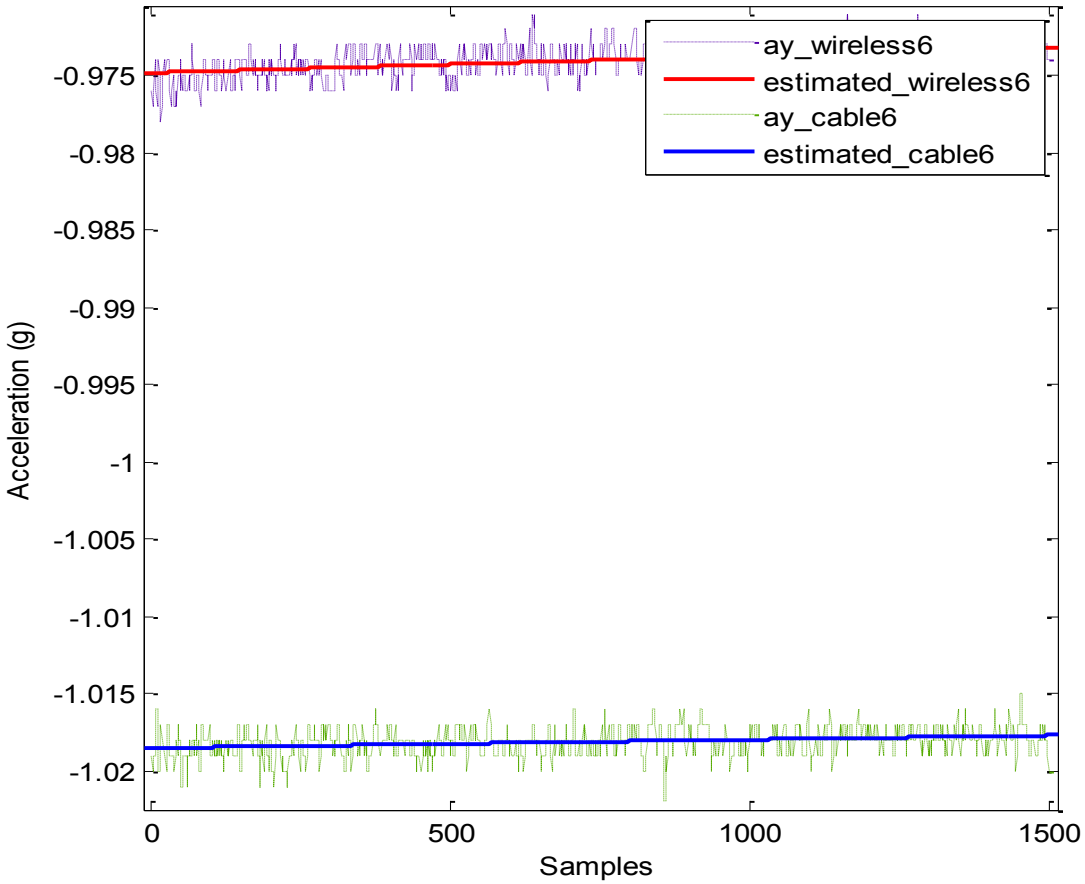


Figure 4-20: Position 6 Estimated accelerations of wireless and cable in linear model

Linear model wireless position 6:

f(x) = p1*x + p2

Coefficients (with 95% confidence bounds):

p1 = 1.072e-006 (9.692e-007, 1.174e-006)

p2 = -0.9748 (-0.9749, -0.9747) (4.35)

Linear model cable position 6:

f(x) = p1*x + p2

Coefficients (with 95% confidence bounds):

p1 = 5.454e-007 (4.427e-007, 6.481e-007)

p2 = -1.019 (-1.019, -1.018) (4.36)

**Table 4-6: Position 6 linear model results for Ax, Ay and Az in both wireless mode and cable mode**

| Position6 | | | | | | |
|---|---|---|---|---|---|---|
| | Ax | | Ay | | Az | |
| | Wireless | Cable | Wireless | Cable | Wireless | Cable |
| p1 | 5.09E-07 | 2.13E-07 | 6.07E-07 | 5.45E-07 | -1.37E-07 | -1.22E-06 |
| p2 | 0.01332 | -0.01118 | -0.9748 | -1.019 | 0.007826 | 0.00852 |

Figure 4-18 displays the position 6 of the system and the directions of three axes (X, Y and Z). Where accelerations on X axis and Z axis are 0; and acceleration on Y axis is -g.

Figure 4-19 displays 1500 samples of two different accelerations at the same system position on Y axis in a static state. The green data presents the acceleration of cable communication, whereas the blue data presents the acceleration of Bluetooth wireless communication.

Figure 4-20 displays the estimated data of two different accelerations at the same system position on Y axis in a static state. Two accelerations have been estimated by using curve fitting. As mentioned in system position 1, curve fitting equation has been designed as f(x) = p1*x + p2 as a linear model, where p1 can be looked as scale factor, p2 can be looked as bias. The curve fitting method is able to present the track of accelerations. Table 4-6 clearly displays the difference and comparison of the data of cable communication and wireless communication at position 6.

### 4.2.2 Nonlinear Error Modelling

The equation that has been implemented into nonlinear error modelling is:

$$f(x) = \mathrm{a}_0 + \mathrm{a}_1 * \sin(\mathrm{x} * \mathrm{w}) \tag{4.37}$$

Similar to the linear model, $\mathrm{a}_0$ stands for bias, $\mathrm{a}_1$ stands for scale factors. w stands for the angular frequency of the function. The purpose of implementing the nonlinear error modelling is to validate the accuracy of linear error modelling and to confirm that the coefficients of errors are determined. Moreover, using nonlinear error modelling enables comparison compare with the linear error modelling to improve the accuracy of the system. After inputting the raw data to the equation through 6 positions, the results are displayed:

**Position 1**

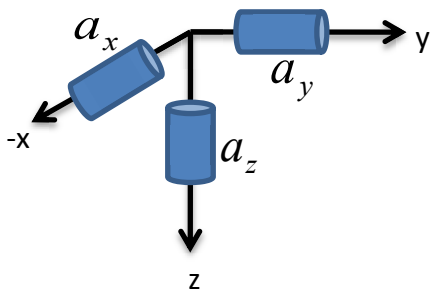


Figure 4-21: Position 1 system position

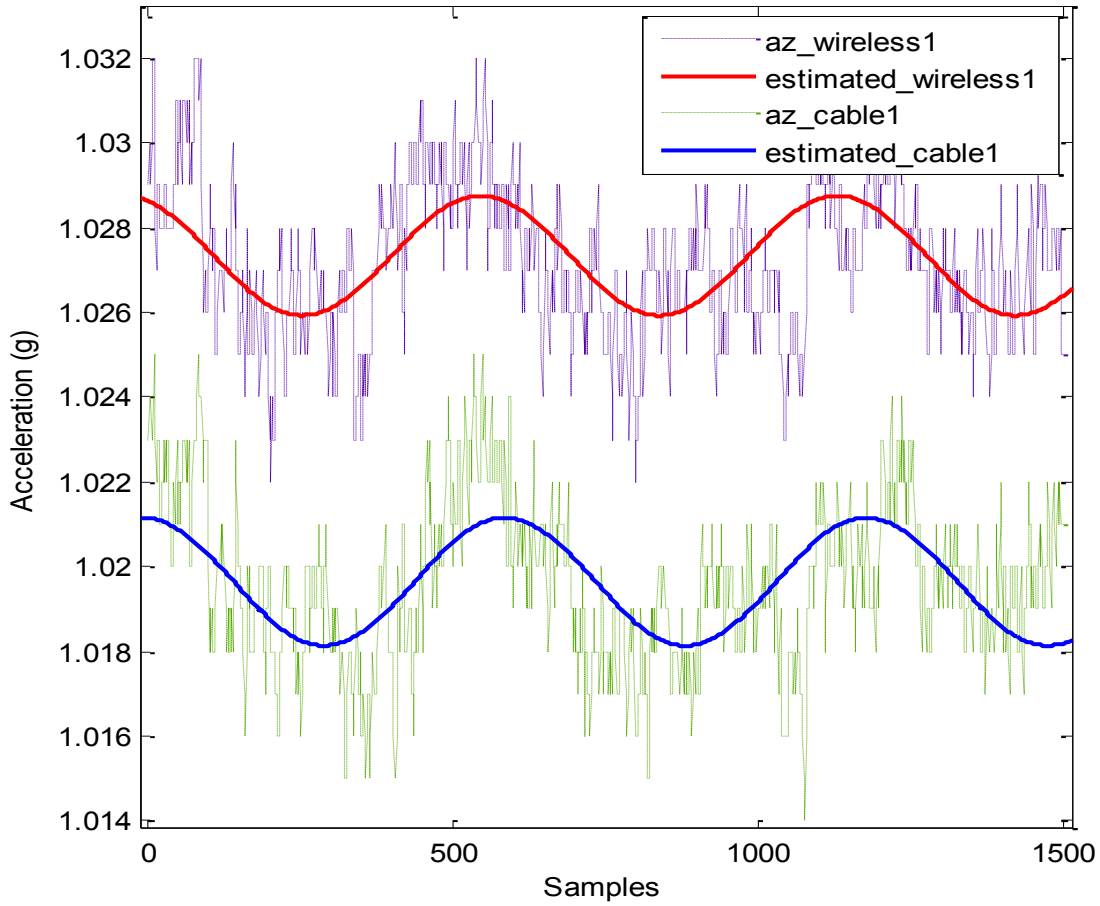


Figure 4-21: Position 1 Estimated accelerations of wireless and cable in nonlinear model

Nonlinear model wireless position 1:

f(x) = a0 + a1*sin(x*w)

Coefficients (with 95% confidence bounds):

a0 = 1.027 (1.027, 1.027)

a1 = 0.001412

w = -0.4133 (4.38)

Nonlinear model cable position 1:

f(x) = a0 + a1*sin(x*w)

Coefficients (with 95% confidence bounds):

a0 = 1.02 (1.02, 1.02)

a1 = 0.001507

w = -0.0803 (4.39)

Figure 4-22 displays the position 1 of the system and the directions of three axes (X, Y and Z). Where accelerations on X axis and Y axis are 0; and acceleration on Z axis is g. There are 1500 samples of two different accelerations at the same system position on Z axis in a static state. The green data presents the acceleration of cable communication, whereas the blue data presents the acceleration of Bluetooth wireless communication. The data of two different accelerations have been estimated at the same system position on Z axis in a static state by using nonlinear error modelling. Two accelerations have been estimated by using nonlinear curve fitting. The purpose of this figure is to clearly display the difference and comparison of the data of cable communication and wireless communication at position 1.

## Position 2

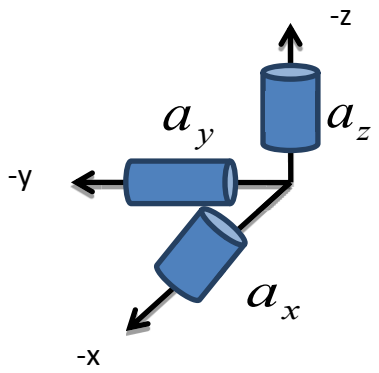


Figure 4-23: Position 2 system position

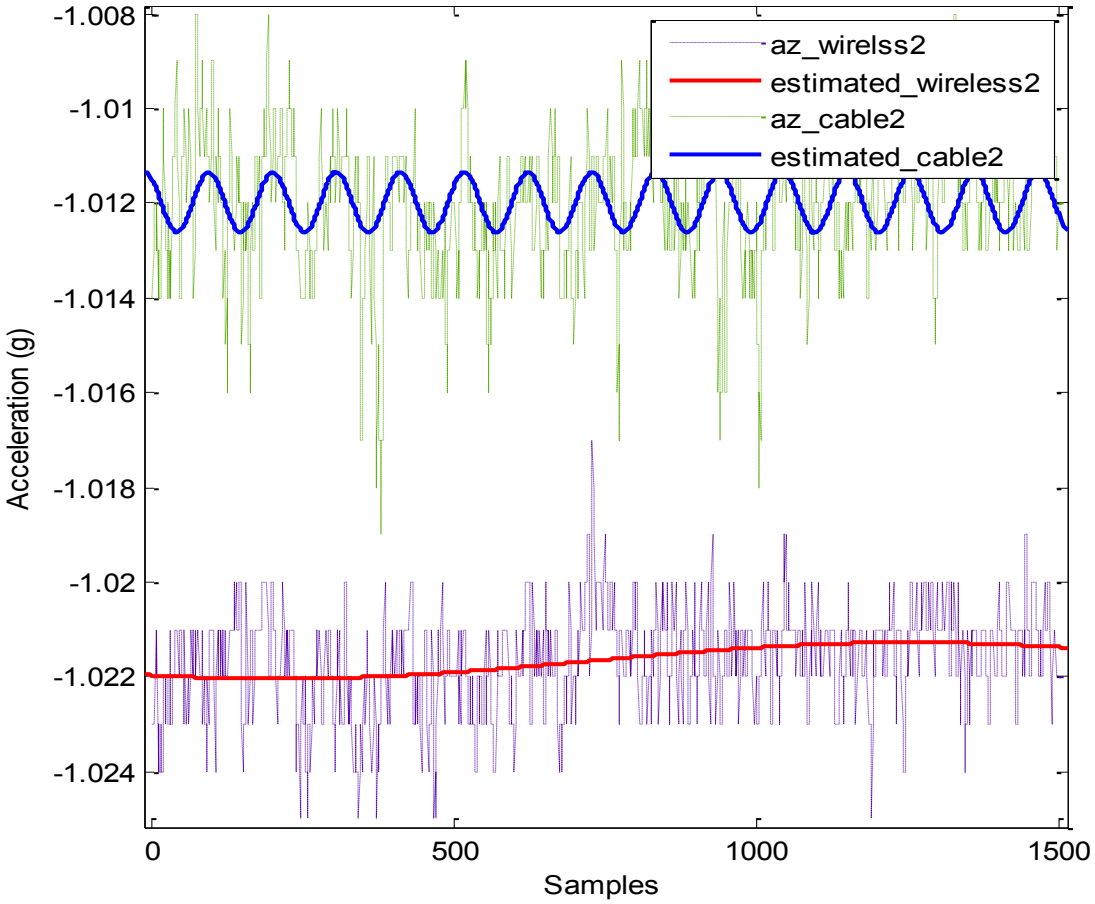


Figure 4-22: Position 2 Estimated accelerations of wireless and cable in nonlinear model

Nonlinear model wireless position 2:

f(x) = a0 + a1*sin(x*w)

Coefficients (with 95% confidence bounds):

a0 = -1.022 (-1.022, -1.022)

a1 = 0.0003826

w = -0.636 (4.40)

Nonlinear model cable position 2:

f(x) = a0 + a1*sin(x*w)

Coefficients (with 95% confidence bounds):

a0 = -1.012 (-1.012, -1.012)

a1 = 0.0006371

w = -0.706 (4.41)

Figure 4-24 displays the position 2 of the system and the directions of three axes (X, Y and Z). Where accelerations on X axis and Y axis are 0; and acceleration on Z axis is -g. There are 1500 samples of two different accelerations at the same system position on Z axis in a static state. The green data presents the acceleration of cable communication, whereas the blue data presents the acceleration of Bluetooth wireless communication. The data of two different accelerations have been estimated at the same system position on Z axis in a static state by using nonlinear error modelling. Two accelerations have been estimated by using nonlinear curve fitting. The purpose of this figure is to clearly display the difference and comparison of the data of cable communication and wireless communication at position 2.

## Position 3

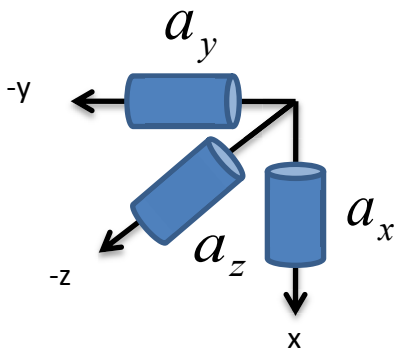


Figure 4-25: Position 3 system position

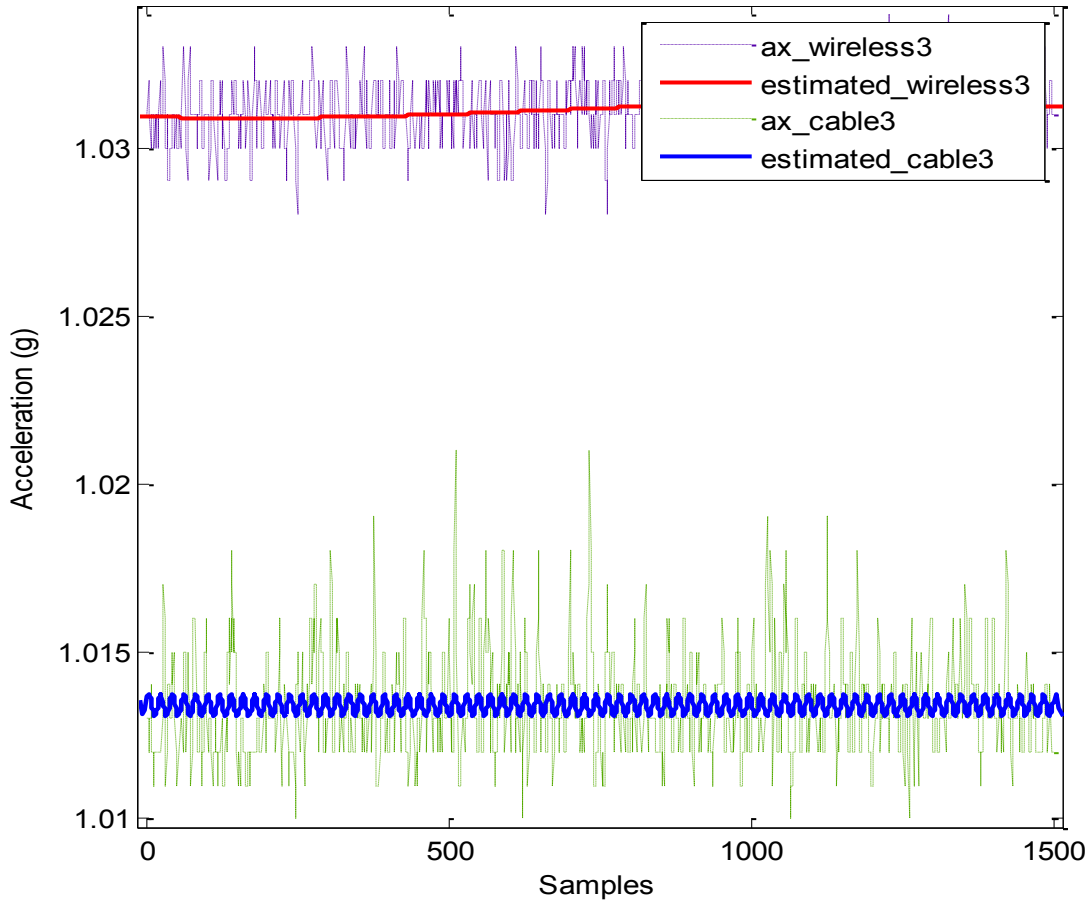


Figure 4-23: Position 3 Estimated accelerations of wireless and cable in nonlinear model

Nonlinear model wireless position 3:

f(x) = a0 + a1*sin(x*w)

Coefficients (with 95% confidence bounds):

a0 = 1.031 (1.031, 1.031)

a1 = 0.00023409

w = -0.536 (4.42)

Nonlinear model cable position 3:

f(x) = a0 + a1*sin(x*w)

Coefficients (with 95% confidence bounds):

a0 = 1.013 (1.013, 1.013)

a1 = 0.00024831

w = 1.299 (4.43)

Figure 4-26 displays the position 3 of the system and the directions of three axes (X, Y and Z). Where accelerations on Y axis and Z axis are 0; and acceleration on X axis is g. There are 1500 samples of two different accelerations at the same system position on X axis in a static state. The green data presents the acceleration of cable communication, whereas the blue data presents the acceleration of Bluetooth wireless communication. The data of two different accelerations have been estimated at the same system position on X axis in a static state by using nonlinear error modelling. Two accelerations have been estimated by using nonlinear curve fitting. The purpose of this figure is to clearly display the difference and comparison of the data of cable communication and wireless communication at position 3.

## Position 4

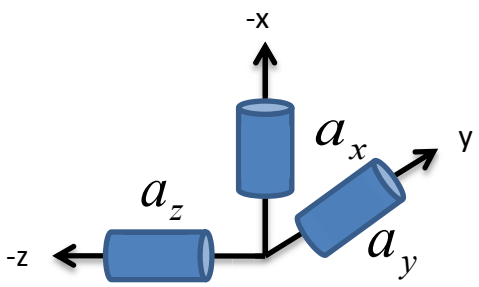


Figure 4-27: Position 4 system position

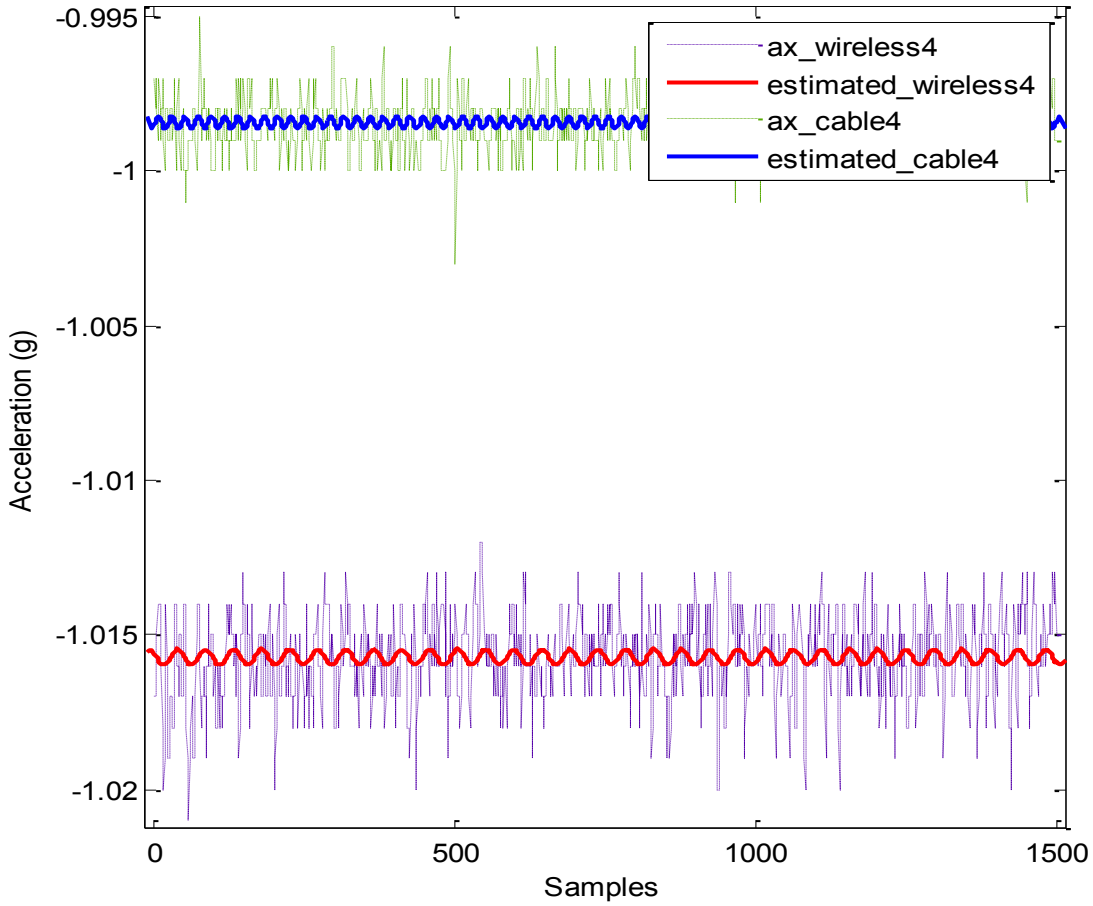


Figure 4-24: Position 4 Estimated accelerations of wireless and cable in nonlinear model

Nonlinear model wireless position 4:

f(x) = a0 + a1*sin(x*w)

Coefficients (with 95% confidence bounds):

a0 = -1.016 (-1.016, -1.016)

a1 = 0.00025808

w = -1.024 (4.44)

Nonlinear model cable position 4:

f(x) = a0 + a1*sin(x*w)

Coefficients (with 95% confidence bounds):

a0 = -0.9984 (-0.9985, -0.9984)

a1 = 0.00020331

w = 0.0891 (4.45)

Figure 4-28 displays the position 4 of the system and the directions of three axes (X, Y and Z). Where accelerations on Y axis and Z axis are 0; and acceleration on X axis is -g. There are 1500 samples of two different accelerations at the same system position on X axis in a static state. The green data presents the acceleration of cable communication, whereas the blue data presents the acceleration of Bluetooth wireless communication. The data of two different accelerations have been estimated at the same system position on X axis in a static state by using nonlinear error modelling. Two accelerations have been estimated by using nonlinear curve fitting. The purpose of this figure is to clearly display the difference and comparison of the data of cable communication and wireless communication at position 4.

## Position 5

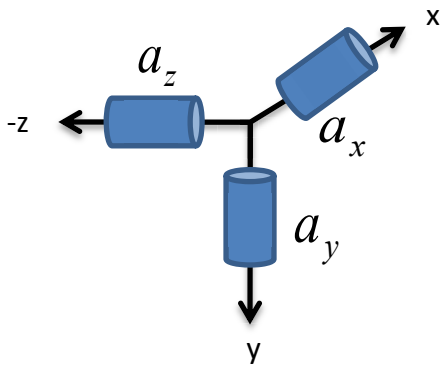


Figure 4-29: Position 5 system position

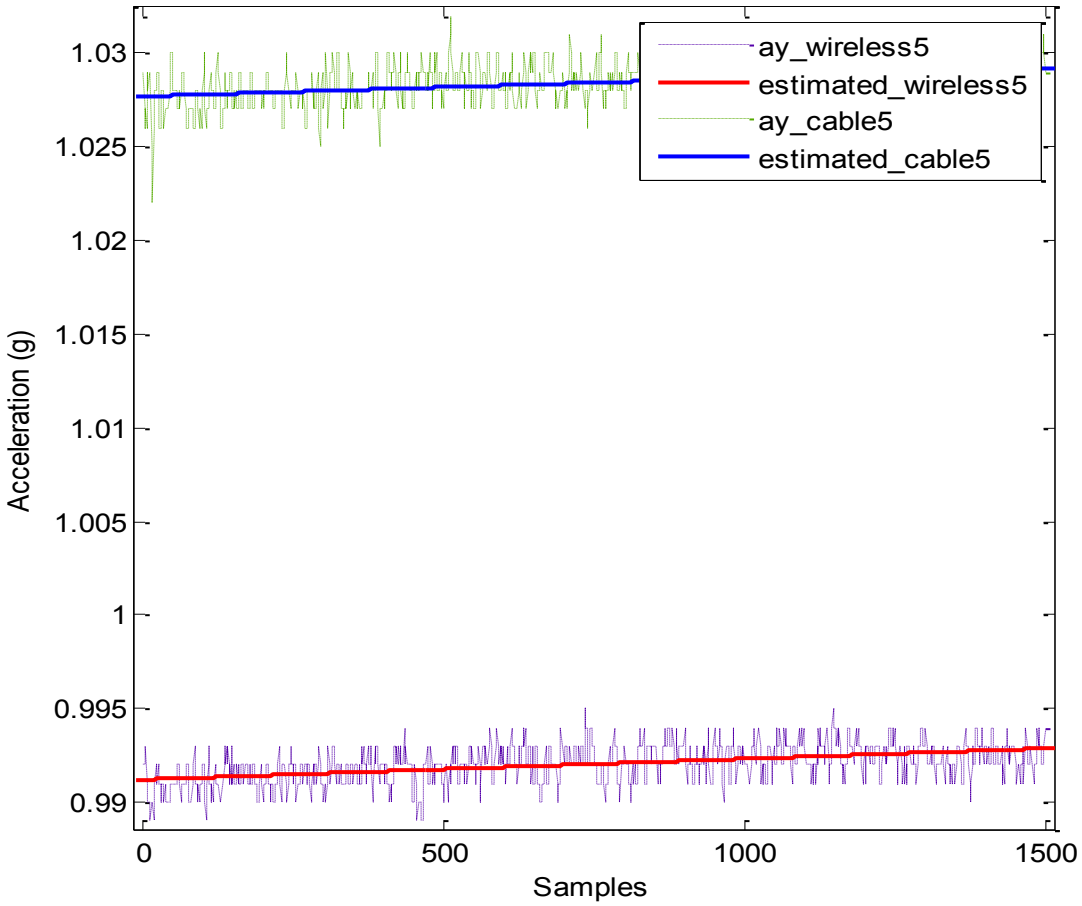


Figure 4-25: Position 5 Estimated accelerations of wireless and cable in nonlinear model

Nonlinear model wireless position 5:

f(x) = a0 + a1*sin(x*w)

Coefficients (with 95% confidence bounds):

a0 = 0.9907 (0.9875, 0.9939)

a1 = 0.001837

w = 1.4969 (4.46)

Nonlinear model cable position 5:

f(x) = a0 + a1*sin(x*w)

Coefficients (with 95% confidence bounds):

a0 = 1.027 (1.015, 1.039)

a1 = 0.0019316

w = 1.5002 (4.47)

Figure 4-30 displays the position 5 of the system and the directions of three axes (X, Y and Z). Where accelerations on X axis and Z axis are 0; and acceleration on Y axis is g. There are 1500 samples of two different accelerations at the same system position on Y axis in a static state. The green data presents the acceleration of cable communication, whereas the blue data presents the acceleration of Bluetooth wireless communication. The data of two different accelerations have been estimated at the same system position on Y axis in a static state by using nonlinear error modelling. Two accelerations have been estimated by using nonlinear curve fitting. The purpose of this figure is to clearly display the difference and comparison of the data of cable communication and wireless communication at position 5.

## Position 6

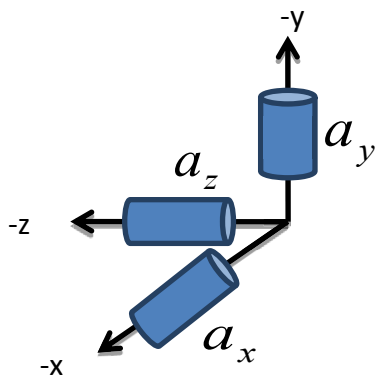


Figure 4-31: Position 6 system position

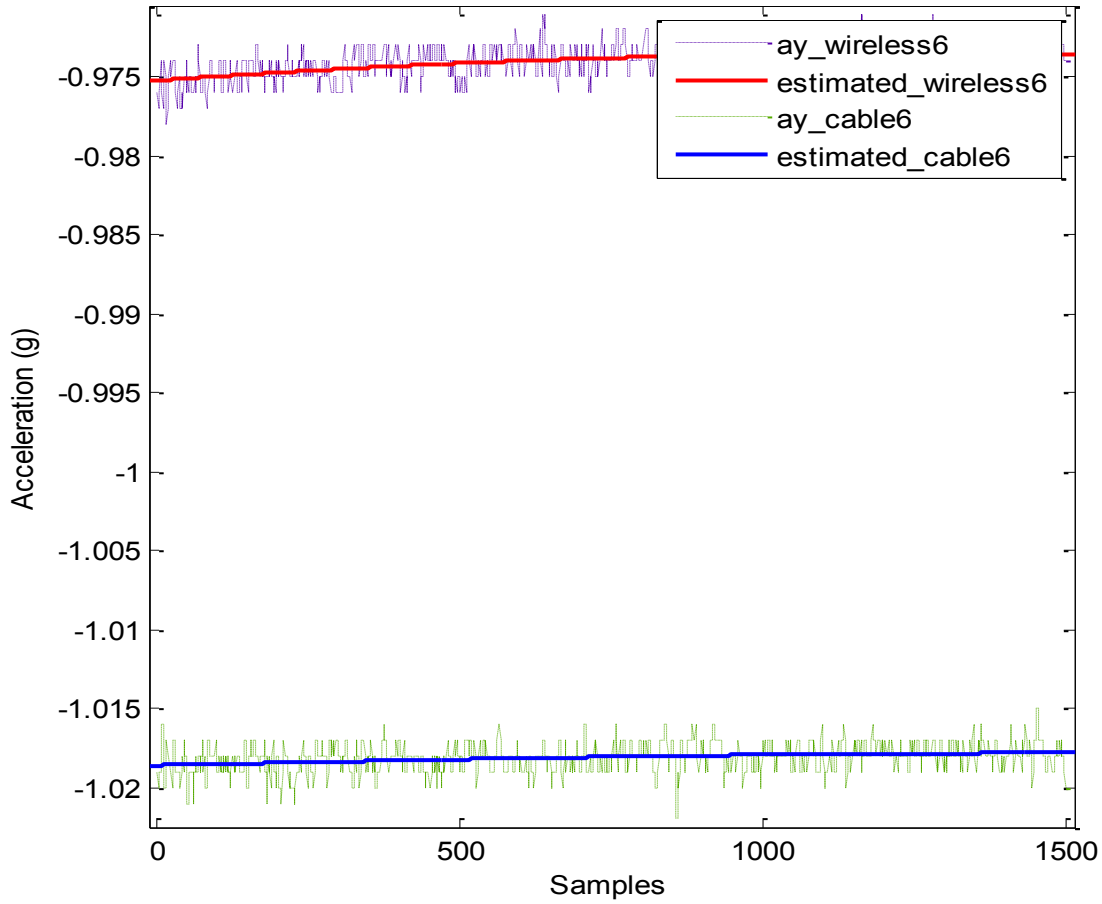


Figure 4-26: Position 6 Estimated accelerations of wireless and cable in nonlinear model

Nonlinear model wireless position 6:

f(x) = a0 + a1*sin(x*w)

Coefficients (with 95% confidence bounds):

a0 = -1.028 (-1.019, -1.037)

a1 = 0.0007352

w = 1.3611 (4.48)

Nonlinear model cable position 6:

f(x) = a0 + a1*sin(x*w)

Coefficients (with 95% confidence bounds):

a0 = -1.018 (-1.021, -1.016)

a1 = 0.00066341

w = 1.3995 (4.49)

Figure 4-32 displays the position 6 of the system and the directions of three axes (X, Y and Z). Where accelerations on X axis and Z axis are 0; and acceleration on Y axis is -g. There are 1500 samples of two different accelerations at the same system position on Y axis in a static state. The green data presents the acceleration of cable communication, whereas the blue data presents the acceleration of Bluetooth wireless communication. The data of two different accelerations have been estimated at the same system position on Y axis in a static state by using nonlinear error modelling. Two accelerations have been estimated by using nonlinear curve fitting. The purpose of this figure is to clearly display the difference and comparison of the data of cable communication and wireless communication at position 6.

## 4.3 Evolution of Errors Estimate

After determining the system errors by using both linear error modelling and nonlinear error modelling, the data can be estimated and calibrated as in the figures 4-33 to figures 4-44, this is the validation of the error modelling system which displays that the error modelling reduces the error and improve the accuracy of the system.

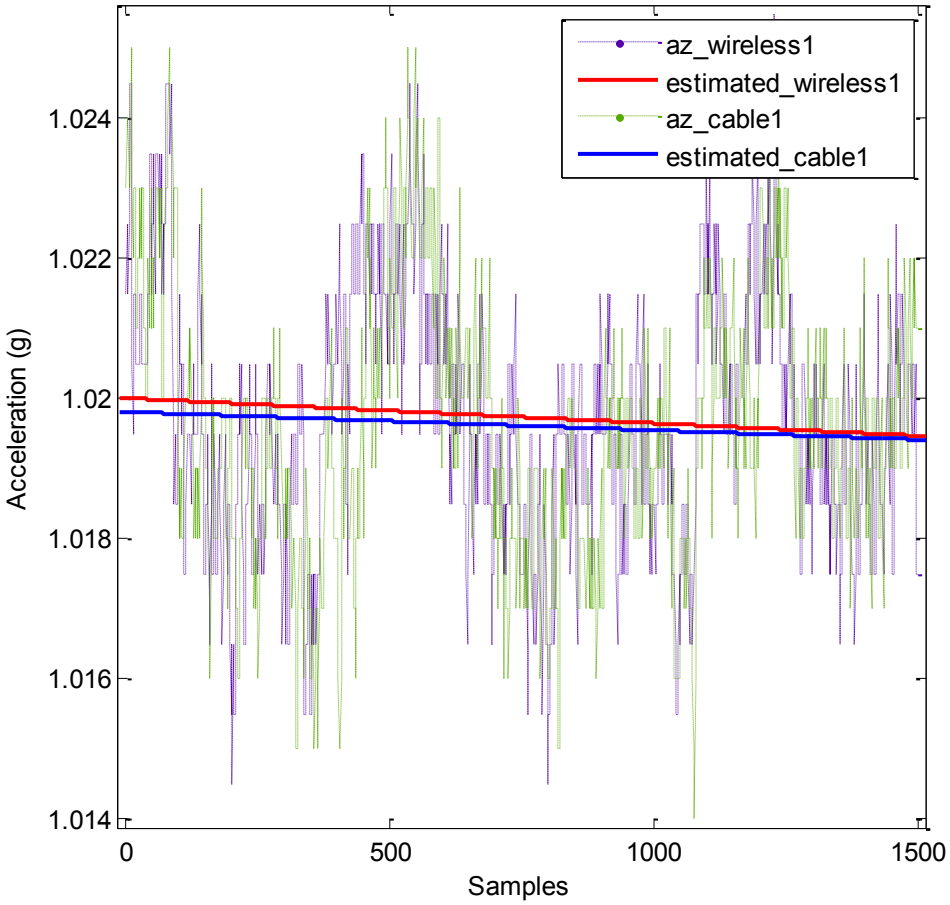


Figure 4-27: Position 1 Evolution of estimated errors in linear model

In figure 4-33, both wireless data and cable data of the acceleration on axis -Z have been displayed as two straight lines which have been processed by curve fitting in linear error modelling. This diagram validates that, after error modelling applied, the data from wireless communication is very close to the data from cable communication. It clearly displays that errors have been reduced.

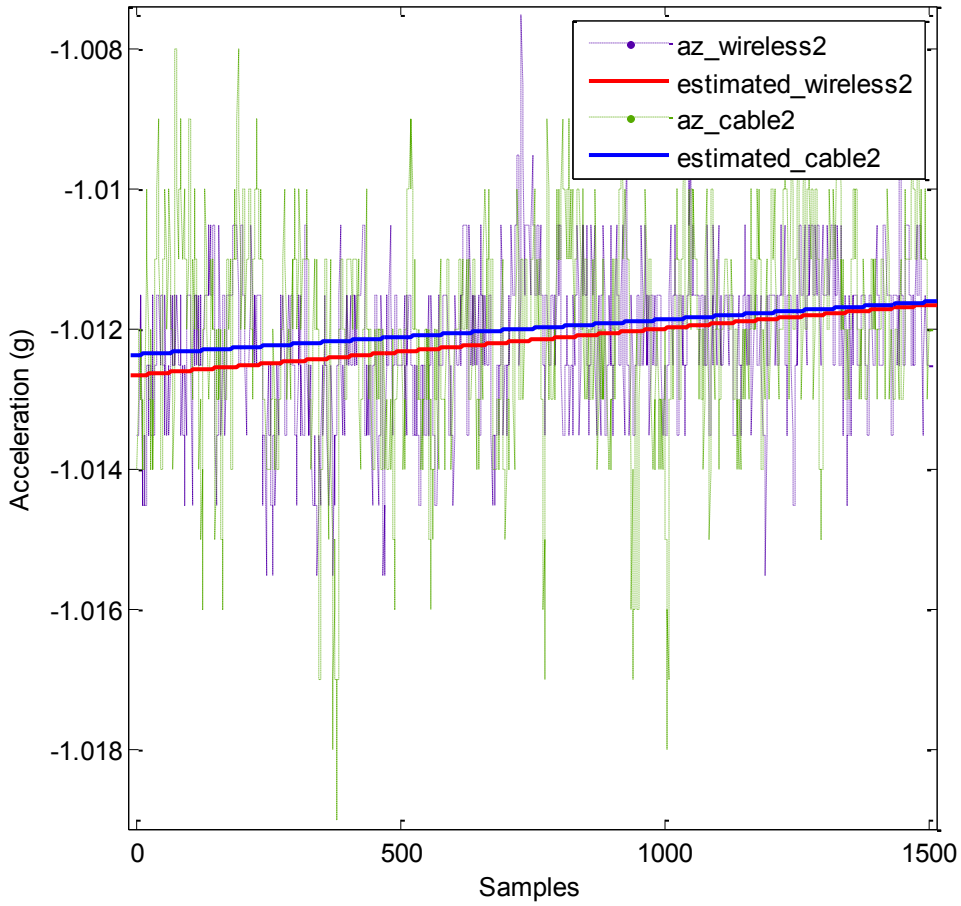


Figure 4-28: Position 2 Evolution of estimated errors in linear model

In figure 4-34, both wireless data and cable data of the acceleration on axis -Z have been displayed as two straight lines which have been processed by curve fitting in linear error modelling. This diagram validates that, after error modelling applied, the data from wireless communication is very close to the data from cable communication. It clearly displays that errors have been reduced.

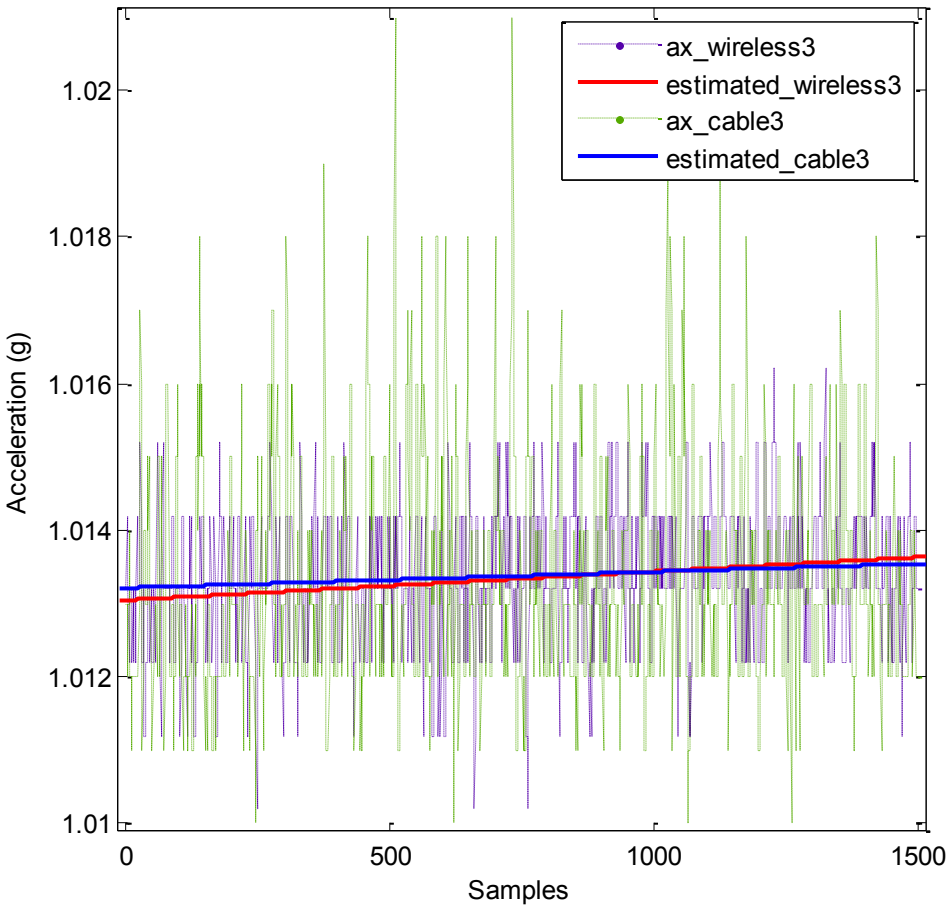


Figure 4-29: Position 3 Evolution of estimated errors in linear model

In figure 4-35, both wireless data and cable data of the acceleration on axis X have been displayed as two straight lines which have been processed by curve fitting in linear error modelling. This diagram validates that, after error modelling applied, the data from wireless communication is very close to the data from cable communication. It clearly displays that errors have been reduced.

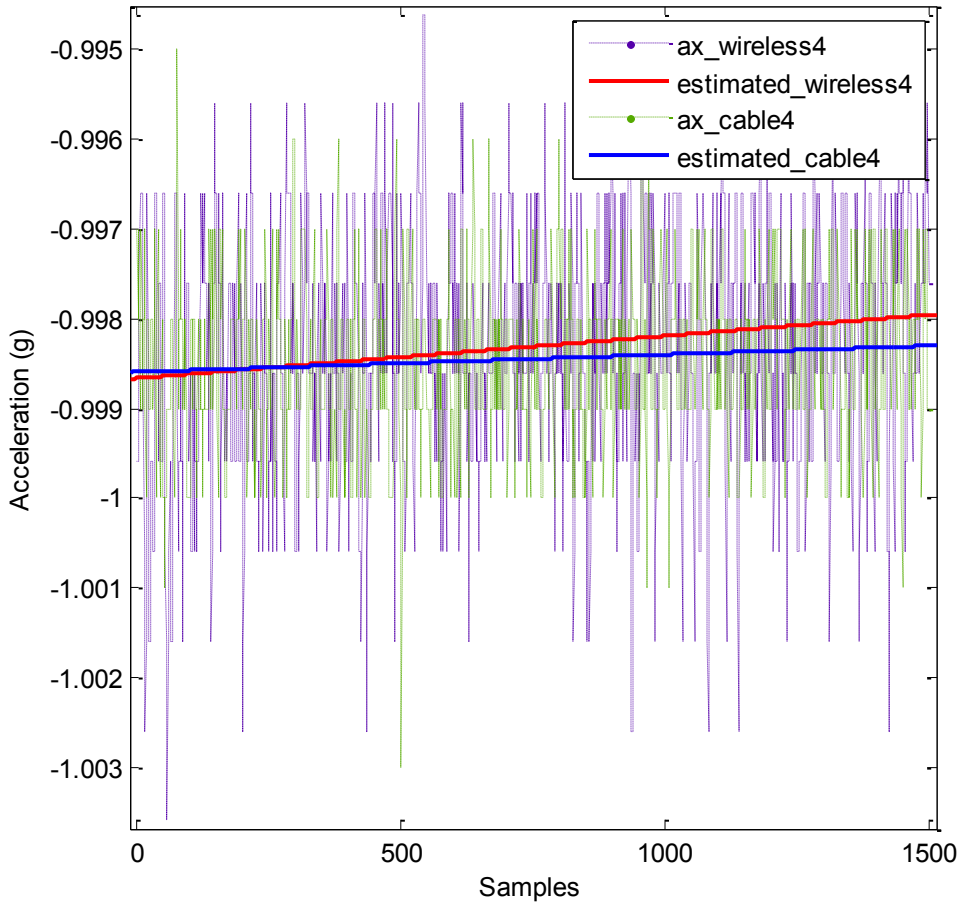


Figure 4-30: Position 4 Evolution of estimated errors in linear model

In figure 4-36, both wireless data and cable data of the acceleration on axis -X have been displayed as two straight lines which have been processed by curve fitting in linear error modelling. This diagram validates that, after error modelling applied, the data from wireless communication is very close to the data from cable communication. It clearly displays that errors have been reduced.

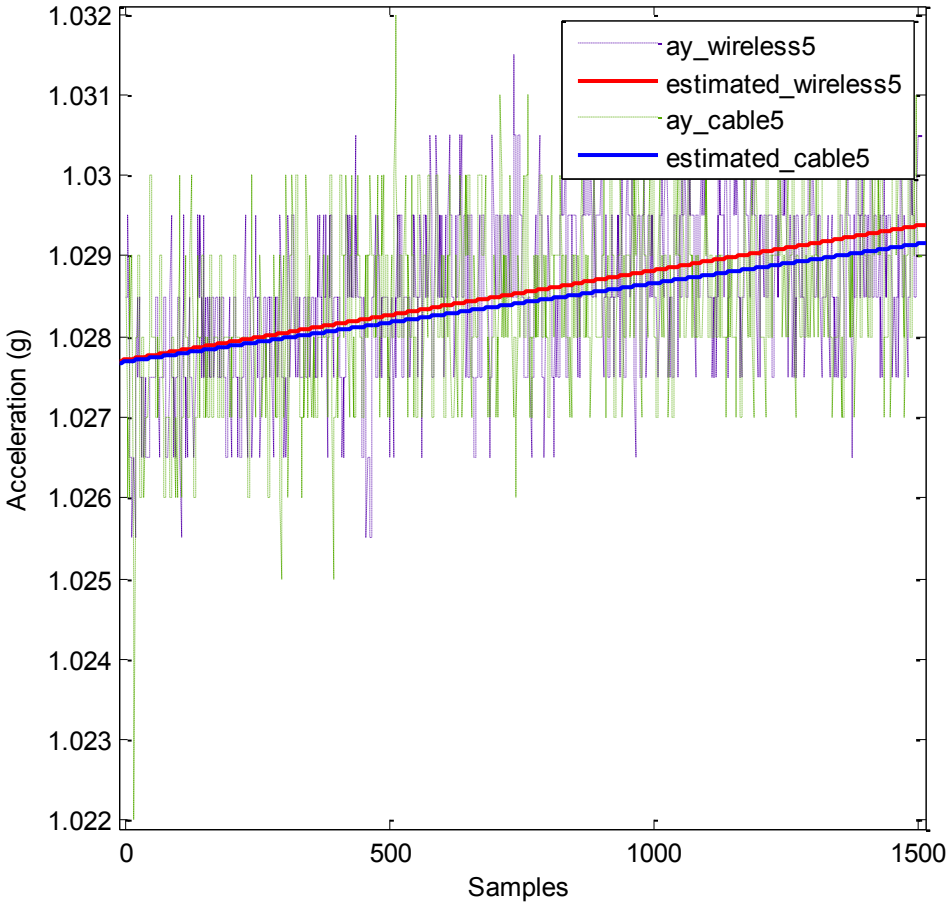


Figure 4-31: Position 5 Evolution of estimated errors in linear model

In this figure 4-37, both wireless data and cable data of the acceleration on axis Y have been displayed as two straight lines which have been processed by curve fitting in linear error modelling. This diagram validates that, after error modelling applied, the data from wireless communication is very close to the data from cable communication. It clearly displays that errors have been reduced.

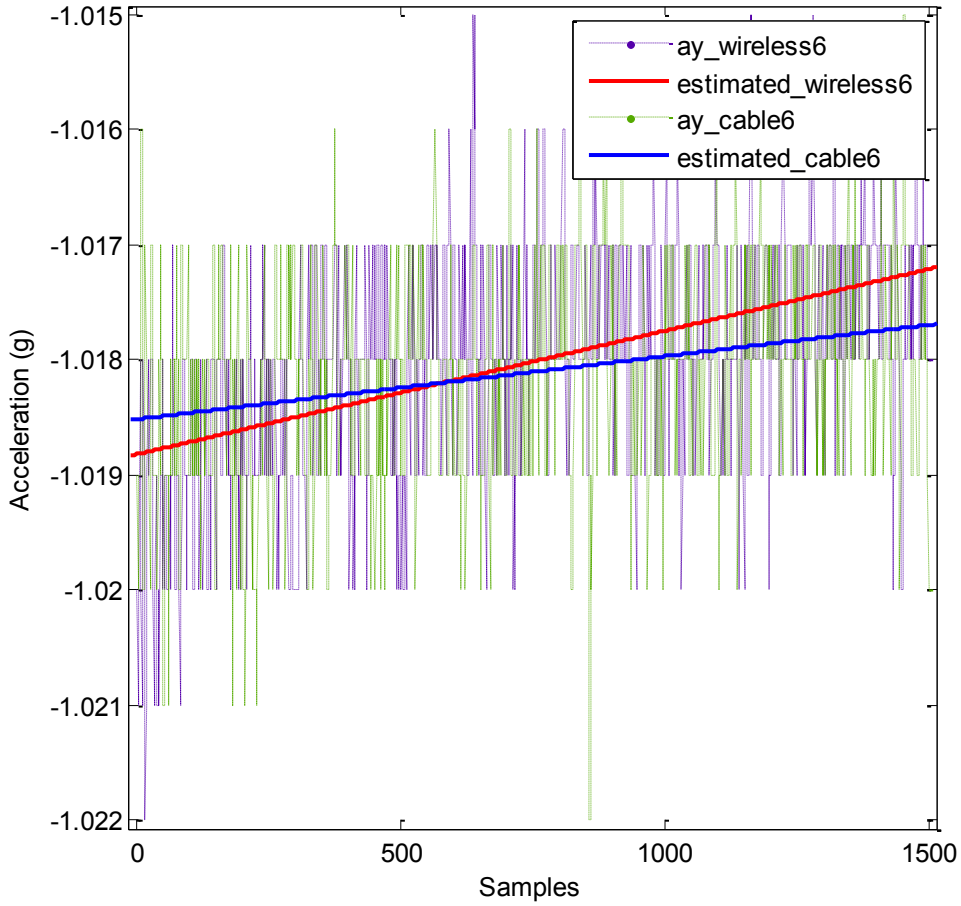


Figure 4-32: Position 6 Evolution of estimated errors in linear model

In figure 4-38, both wireless data and cable data of the acceleration on axis -Y have been displayed as two straight lines which have been processed by curve fitting in linear error modelling. This diagram validates that, after error modelling applied, the data from wireless communication is very close to the data from cable communication. It clearly displays that errors have been reduced.

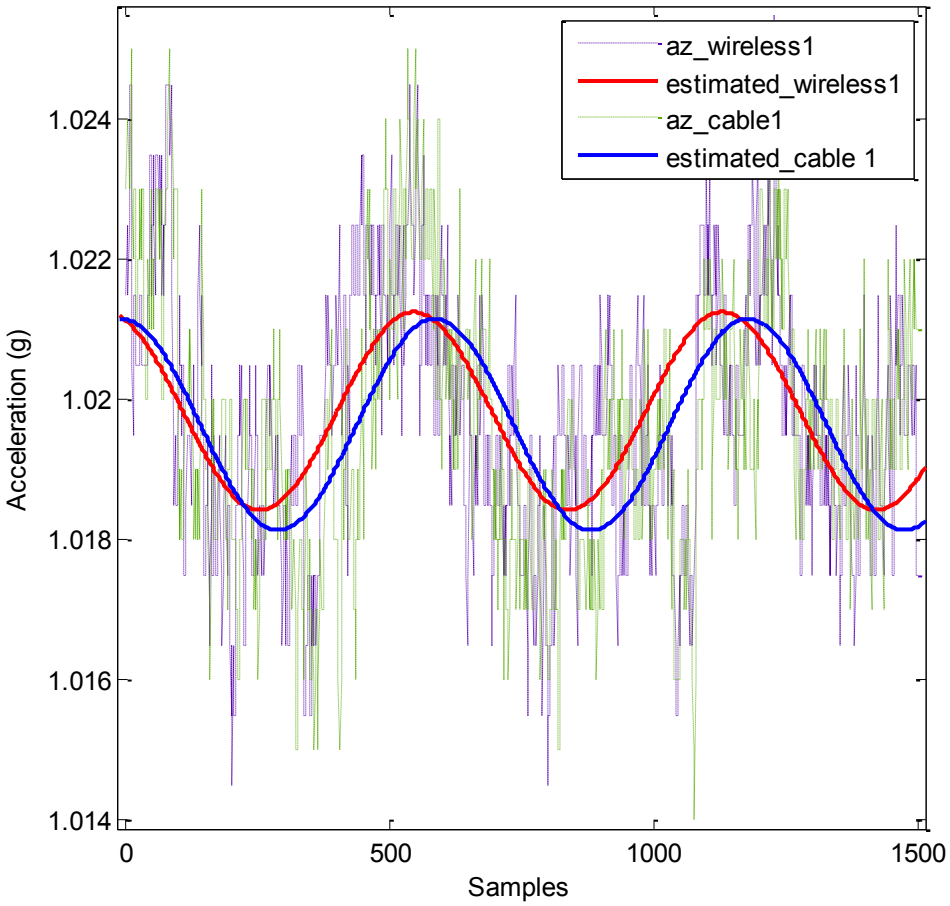


Figure 4-33: Position 1 Evolution of estimated errors in nonlinear model

In figure 4-39, both wireless data and cable data of the acceleration on axis Z have been displayed as two straight lines which have been processed by curve fitting in nonlinear error modelling. This diagram validates that, after error modelling applied, the data from wireless communication is very close to the data from cable communication. It clearly displays that errors have been reduced.

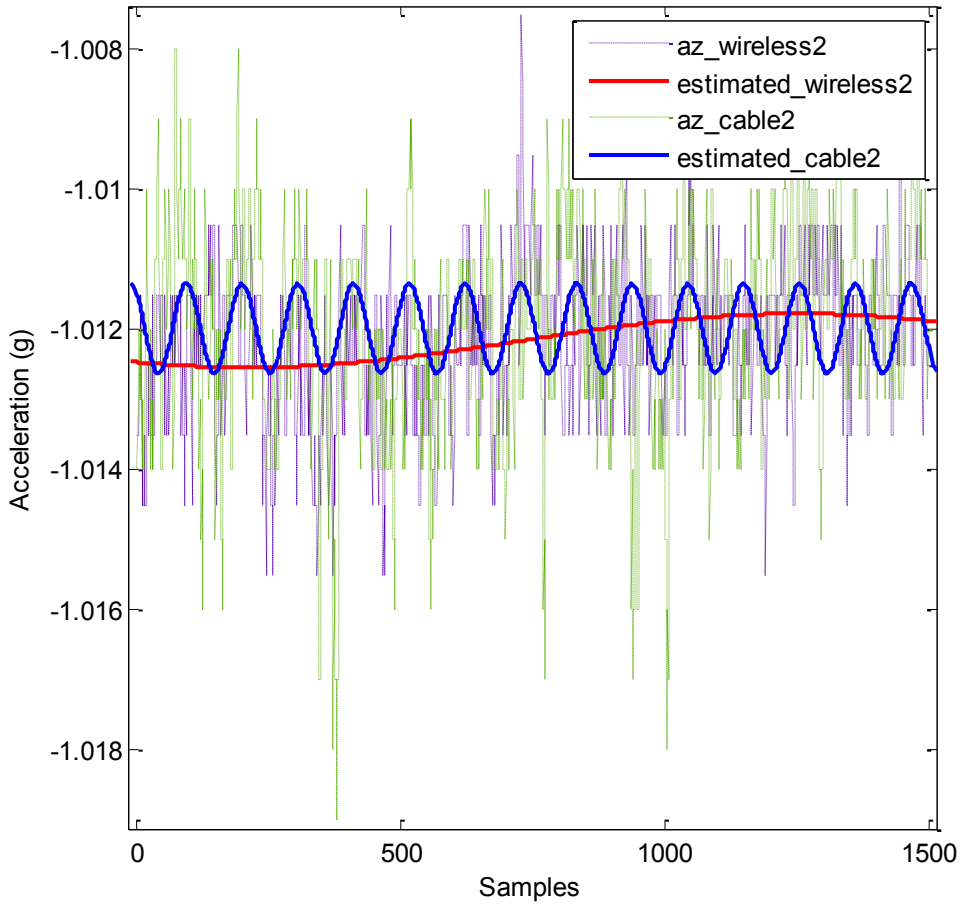


Figure 4-34: Position 2 Evolution of estimated errors in nonlinear model

In figure 4-40, both wireless data and cable data of the acceleration on axis -Z have been displayed as two straight lines which have been processed by curve fitting in nonlinear error modelling. This diagram validates that, after error modelling applied, the data from wireless communication is very close to the data from cable communication. It clearly displays that errors have been reduced.

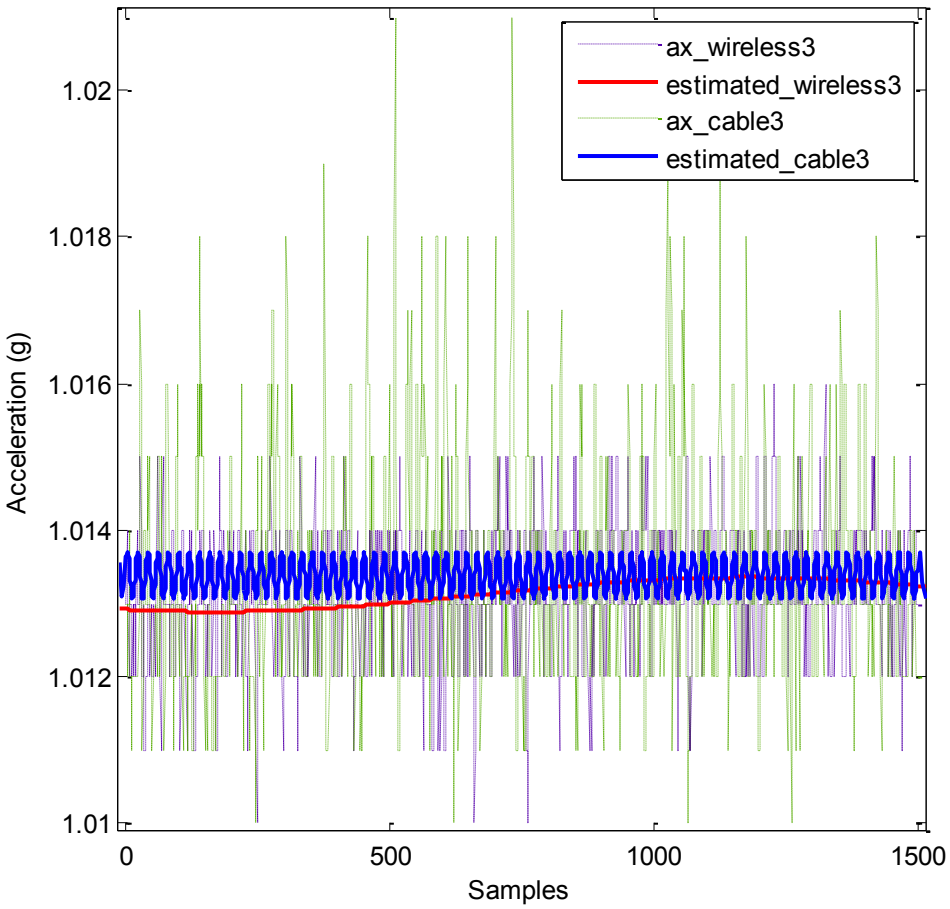


Figure 4-35: Position 3 Evolution of estimated errors in nonlinear model

In figure 4-41, both wireless data and cable data of the acceleration on axis X have been displayed as two straight lines which have been processed by curve fitting in nonlinear error modelling. This diagram validates that, after error modelling applied, the data from wireless communication is very close to the data from cable communication. It clearly displays that errors have been reduced.

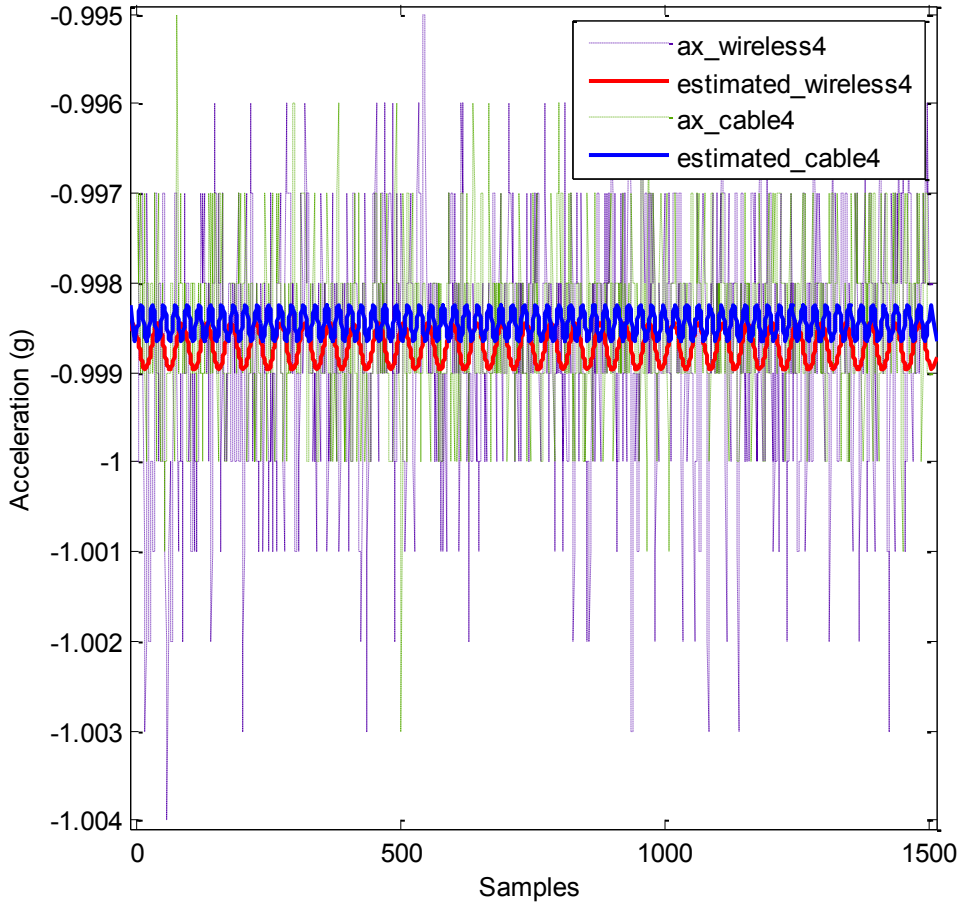


Figure 4-36: Position 4 Evolution of estimated errors in nonlinear model

In figure 4-42, both wireless data and cable data of the acceleration on axis -X have been displayed as two straight lines which have been processed by curve fitting in nonlinear error modelling. This diagram validates that, after error modelling applied, the data from wireless communication is very close to the data from cable communication. It clearly displays that errors have been reduced.

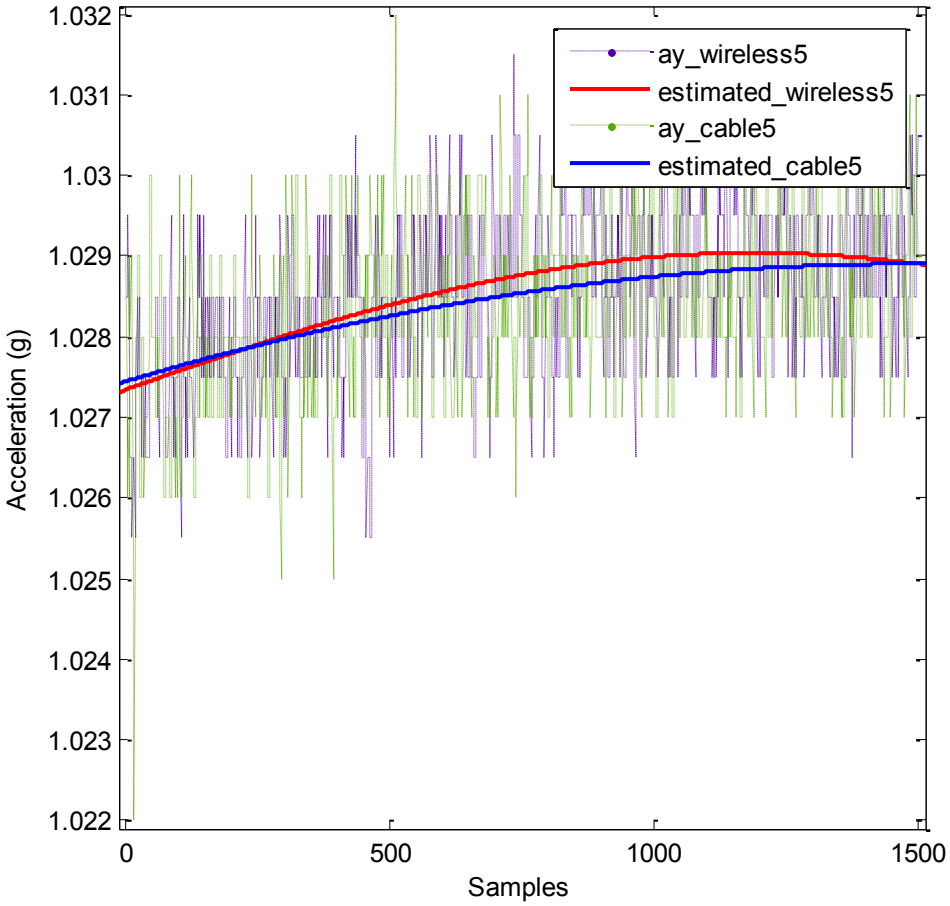


Figure 4-37: Position 5 Evolution of estimated errors in nonlinear model

In figure 4-43, both wireless data and cable data of the acceleration on axis Y have been displayed as two straight lines which have been processed by curve fitting in nonlinear error modelling. This diagram validates that, after error modelling applied, the data from wireless communication is very close to the data from cable communication. It clearly displays that errors have been reduced.

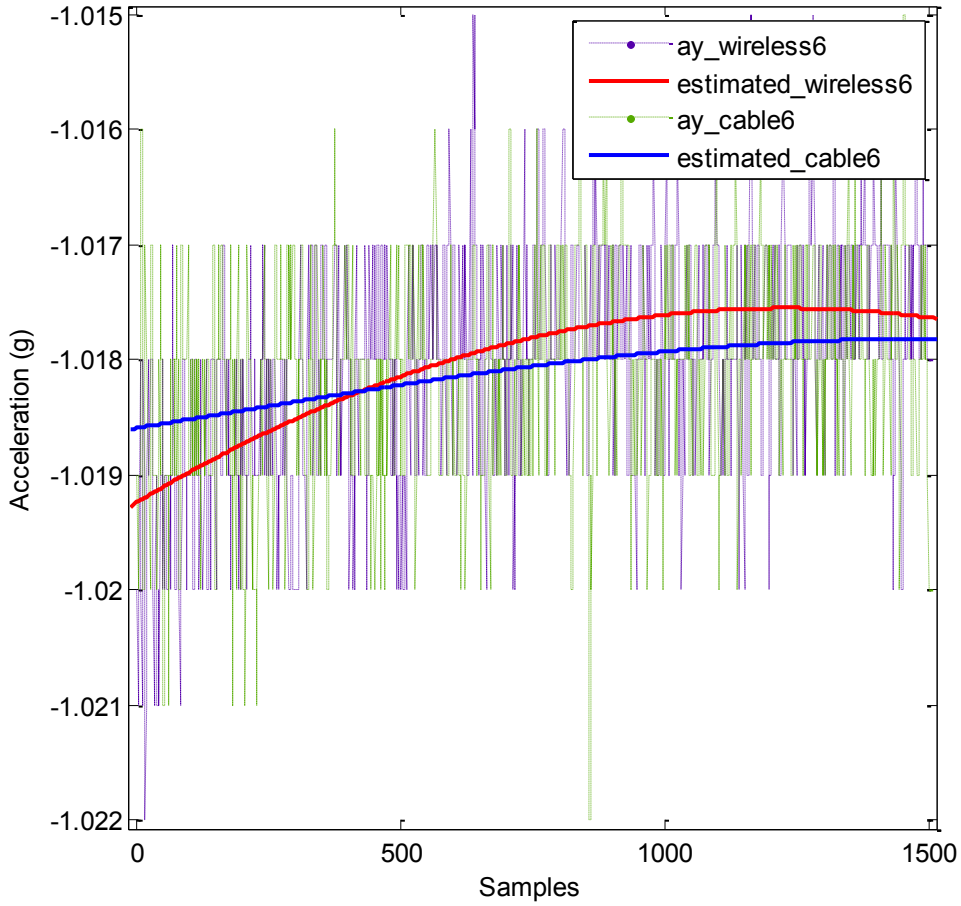


Figure 4-38: Position 6 Evolution of estimated errors in nonlinear model

In figure 4-44, both wireless data and cable data of the acceleration on axis -Y have been displayed as two straight lines which have been processed by curve fitting in nonlinear error modelling. This diagram validates that, after error modelling applied, the data from wireless communication is very close to the data from cable communication. It clearly displays that errors have been reduced.

In the linear error modelling, running regression using (4.5), (4.7), (4.8), (4.9), (4.10) and (4.11), the error model coefficients are obtained as in the table 4-7 and table 4-8:

Table 4-7: Error coefficients of linear model in wireless mode

| Error items | Coefficients | |
|---|---|---|
| bias | *bx* | 0.0234 |
| | *by* | -0.017 |
| | *bz* | 0.0244 |
| Scale factor | *Sf_x* | 0.0077 |
| | *Sf_y* | 0.009 |
| | *Sf_z* | 0.0028 |
| coefficients for accelerometers' installation and misalignment errors | *my_x* | 0.0017 |
| | *mz_x* | -0.0012 |
| | *mx_y* | -0.0023 |
| | *mz_y* | 0.0067 |
| | *mx_z* | 0.0053 |
| | *my_z* | 0.004 |

Table 4-8: Error coefficients of linear model in cable mode

| Error items | Coefficients | |
|---|---|---|
| bias | *bx* | 0.0059 |
| | *by* | -0.0233 |
| | *bz* | 0.0158 |
| Scale factor | *Sf_x* | 0.0075 |
| | *Sf_y* | 0.0052 |
| | *Sf_z* | 0.0038 |
| coefficients for accelerometers' installation and misalignment errors | *my_x* | 0.0019 |
| | *mz_x* | 0.00044163 |
| | *mx_y* | -0.0025 |
| | *mz_y* | 0.0059 |
| | *mx_z* | 0.0017 |
| | *my_z* | 0.0041 |

In the nonlinear error modelling, running the equation (4.37), the error model coefficients are obtained as in the table 4-9 and 4-10:

Table 4-9: Error coefficients of nonlinear model in wireless mode

| Error items | Coefficients | |
|---|---|---|
| Bias | *bx* | 0.0235 |
| | *by* | -0.00935 |
| | *bz* | 0.0245 |
| Scale factor | *Sf_x* | 0.000246 |
| | *Sf_y* | 0.00129 |
| | *Sf_z* | 0.000897 |

Table 4-10: Error coefficients of nonlinear model in cable mode

| Error items | Coefficients | |
|---|---|---|
| bias | *bx* | 0.00572 |
| | *by* | -0.0225 |
| | *bz* | 0.0163 |
| Scale factor | *Sf_x* | 0.000225 |
| | *Sf_y* | 0.00129 |
| | *Sf_z* | 0.00107 |

## 4.4 Summary

This chapter has presented the two error modellings: linear error modelling and nonlinear error modelling. Both contain different algorithms and figures, but the results of both modellings are very close. The main method focused on in this thesis is linear error modelling, because it is able to determine more coefficients of the system. After determining all the errors, the raw data should be processed and updated by error modelling so that the errors in the system can be minimised. A curve fitting method is eventually implemented in the plotting to estimate a group of data which has been processed by error modelling. Validations have been done as evolutions of the estimated errors. All the diagrams with curve fitting clearly present the result of error reducing by using error modelling. The data from the cable communication has not been processed by error modelling. The reason for this is that, for the purpose of this thesis, the data from the cable communication is regarded as the original data. Since wireless communication has been used in this system, it is very important to determine the difference between the cable communication data and the wireless communication data, so that the errors from the wireless communication can be discovered and estimated. Nevertheless, as long as the error modelling has been validated, it can be implemented in any INS. Therefore, the error modelling can even be used to estimate the errors from cable communications as well to upgrade the accuracy of the system. Nonlinear error modelling is the method which is able to test and validate the linear error modelling. The angular frequency w does not appear to affect the system errors and therefore is not a great cause for concern. However, in future research, nonlinear error modelling will no longer be the preferred validation method as it is possible to display more curves to determine more unknown errors from the estimated waves.

# Chapter 5

# Experimental results in a low cost gyro-free inertial navigation system

## 5.1 Low Cost Gyro-Free Inertial Navigation System

This wireless inertial measurement unit is used to build a wireless low cost gyro-free inertial navigation system (INS). The experimental results using this low cost INS have validated the system design in Chapter 3 and IMU modelling results shown in Chapter 4.

A gyro-free inertial navigation system is an accelerometers based navigation system. It is designed to decrease the production cost, operation cost, body size and power consumption of the system by exclusion of gyroscopes from the inertial system. Nevertheless, navigation data is delivered at sufficient accuracy for the inertial system with the error modelling shown in chapter 4.

The experiments have been setup in the information communication technology laboratory. Laptop is used to receive the real-time inertial data from the INS remotely within a range of 50 meters from the INS. This experiment is able to validate the error modelling on a low cost gyro-free inertial navigation system in a dynamic environment. The accelerates from three axes X, Y, Z can be recorded by both cable and wireless communication. After all the calculations, position and ranges will be computed by using accelerates. Comparing with the data from ground true, diagrams will clearly present errors and how much it can be improved by an error modelling system in a dynamic environment.

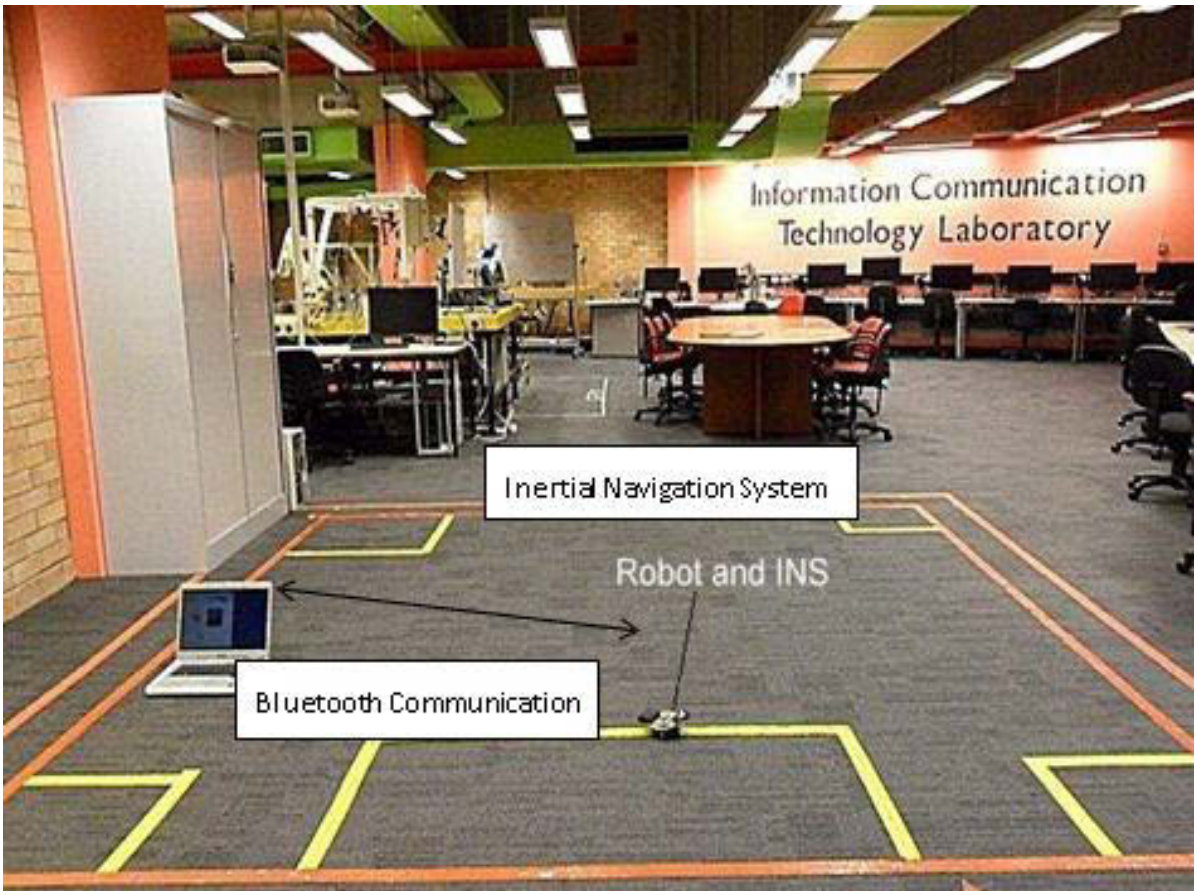


**Figure 5-1:** Testing the error modelling of IMU wireless communication in physical environment

## 5.2 Experiment Procedures

Test case description:

The purpose of this experiment is to validate that the errors have been estimated and reduced by error modelling in a dynamic wireless gyro-free inertial system.

Step 1

A track has been setup on the smooth ground. Inertial sensors and Bluetooth adopter have been mounted on a moving platform. The IMU has been turned on for 2 hours in order to get a stable data as the data of inertial sensor increases when the temperature of the system increases. Laptop has been put aside for data recording and monitoring.

Step 2

The platform should move alone the tracks from the origin point. X and Y axes have been determined according to the tracks. Initial calibration and alignment has been set before the experiment to remove software iron and hard iron effects. The robotic platform should move with a free random velocity as the error modelling should be applied in any situation.
When the robot moves the accelerations of X and Y should be measured and estimated. Acceleration Z should be zero as it is vertical here for reference.

Step 3

After accelerations have been collected, calculations have been done automatically through the matlab. The velocities of X and Y are determined by integrating the accelerations. Moreover, second integration should be processed to determine the actually distances and positions of X and Y.

Step 4

All the raw data of wireless communication INS has been plot including acceleration and position by matlab. Comparing the raw data with the actual ground true position, the difference in between is apparent. At this stage, error modelling which we developed in chapter 4 has been implemented. Algorithms have been reformed by removing the coefficients of errors such as bias and scale factor. The results of the estimated data has been plot, the errors have been minimised significantly.

## 5.3 Analysis of Experimental Results

The test in previous chapter shows the difference between blue tooth data and cable data in residual biases, scale factor and random noise. The data I measured is much different from the data which has been expected. The residual biases of the Bluetooth are larger than the one of the cable. These kinds of errors can be reduced by the adjustment of the algorithm. The errors will be fixed into the algorithm and the results have been integrated accurately.

The dynamic positioning experimental results using this wireless accelerometer unit has been demonstrated.

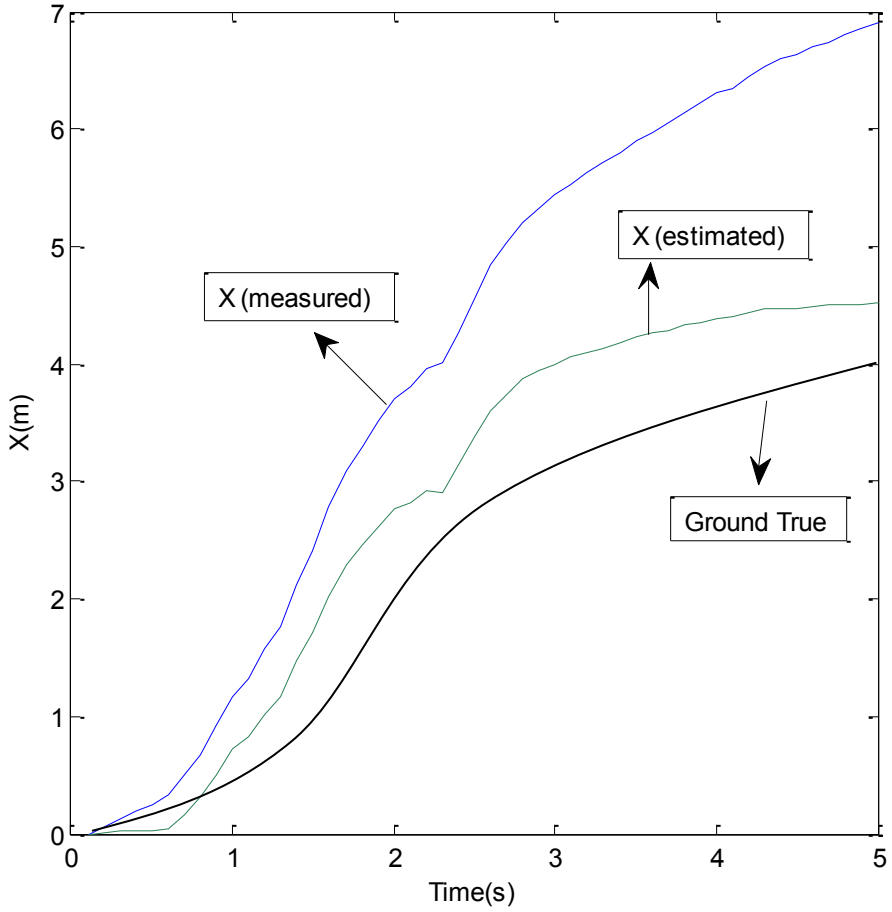


Figure 5-2: Position in axis X. X (measured) shows the position X without error modelling. X (estimated) shows the position X using error modelling.

X (measured) : Positioning data using direct wireless accelerometer measurements without error modelling.

X (estimated) : Positioning data using wireless accelerometer measurements with error modelling.

In Figure 5-2, the coordinate X (measured) is calculated using directly measured wireless acceleration without error modeling, and the accelerations are double integrated to compute position X. The curve of X (measured) shows that the vehicle moves in a curve

from 0 to 7 meters. The coordinate X (estimated) is calculated using the estimated accelerations by applying the error model from previous chapter with coefficients of errors. The curve of the coordinate X (estimated) shows that the vehicle moves from 0 to 4.5 meters in axis-X. The line of ground true displays the real-time data of the position on X axis which is 4 meters. Therefore, comparing with the data of ground true, the errors of X (estimated) are much smaller than the errors of X (measured).

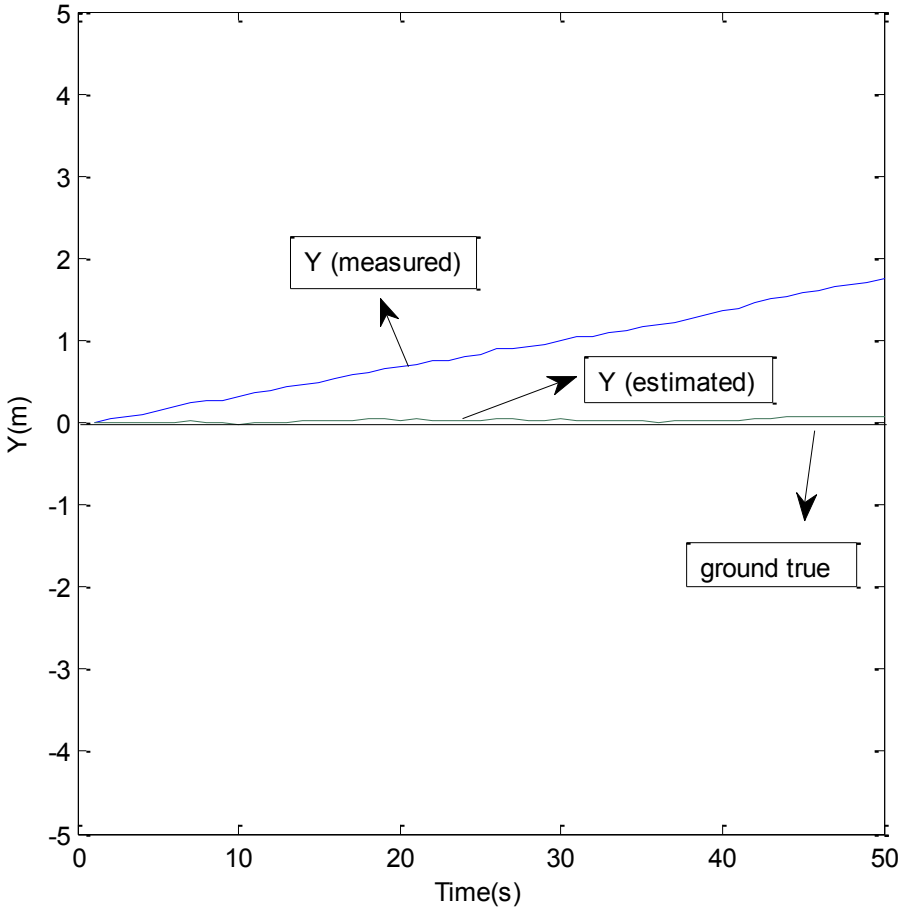


Figure 5-3: Position in axis Y. Y (measured) shows the position Y without error modelling. Y (estimated) shows the position Y using error modelling.

Y (measured) : Positioning data using direct wireless accelerometer measurements without error modelling.

Y (estimated) : Positioning data using wireless accelerometer measurements with error modelling.

The computed coordinates in axis Y using two types of data sets are illustrated in Figure 5-3. The curve of the coordinate Y calculated by using directly measured accelerations illustrate the unit is moving from 0 to 1.8 meters. The coordinate Y calculated by using the accelerations with error modelling in previous chapter shows a much flatter curve. The ground true has been displayed on the figure which shows that coordinate Y is around 0 meter within the positioning period. Therefore, the position accuracy using estimated acceleration with modelling is much higher than using measured acceleration without error modelling.

To conclude, the positioning curves in axis X and Y demonstrate that the error modelling is successful in a short positioning time.

From the coordinate error trend in Figure 5-2 and Figure 5-3, it can be seen that the coordinate error grows over time. The major remaining errors are caused by the double integration process of errors in the device resolution and random noises. The random noises are illustrated in the error model. This again implicates the characteristics and constraints of using a low cost gyro-free inertial measurement unit with only three accelerometers. Further analysis of these constraints will be the focus of a future research direction.

# Chapter 6

# Conclusions

## 6.1 Introduction

This chapter presents a conclusion and contribution of the thesis and addresses the potential for future research. Section 6.2 presents contribution of this thesis, Section 6.3 presents the future research topics based on review of the thesis. Section 6.4 contains concluding remarks of the thesis. Section 6.5 contains the bibliography.

## 6.2 Contributions

During the research work, a new wireless accelerometer communication has been designed. Low cost accelerometers have been provided to minimise the cost, power consumption and size of the system. An integrated IMEM accelerometer system with Bluetooth communication is implemented to achieve a real-time data processing and remote monitoring. However, as we all know, IMU is a high precise magnetic sensitive device, Bluetooth is using short-wavelength radio transmissions, when a Bluetooth device mounted on IMU, magnetic field interfere the accuracy of IMU sensor. Therefore, IMU generates error occurred data by using Bluetooth. Therefore, a 'wireless accelerometer error modelling' has been designed to correct the errors. The error models are separated into two sections: the linear error modeling and the nonlinear error modeling wireless inertial sensor. Both calibration and alignment have been designed for the particular models to minimize the value of errors. A gyro-free wireless communication inertial sensor has been prototyped and implemented for the sensor error calibration process. The approach for modeling the wireless inertial sensor errors and calibration is demonstrated.

## 6.2.1 Publication

A paper has been presented in an international conference in this research area:

> Zhengyu Yu, 'Design and implementation of an economical Inertial Measurement Unit', paper presented to the Asia-Pacific Conference on Computer Aided System Engineering (APCASE) IEEE conference, Bali, Indonesia, 10-12 February 2014.

***Abstract***- This paper presents a modelling of new generation wireless inertial measurement units. A new algorithm simulation is introduced to develop the accuracy in a wireless inertial navigation system. Design, implementation and validation have been displayed in the system. A linear modelling has been designed to distinguish between the data from cable communication and the data from wireless communication. According to the linear modelling, errors are detected. Simulations are used to reduce and correct the errors by matlab.

A paper has been published in an international conference in this research area:

> Zhengyu Yu, Xiaoying Kong, and Tich Phuoc Tran 2012, 'Development of a low cost wireless Inertial Measurement Unit', paper presented to the *International Conference on Engineering and ICT (ICEI2012)*, Melaka, Malaysia, 4-6 April 2012.

***Abstract***- This paper presents a development process of a wireless inertial measurement unit (IMU). A wireless communication configuration is designed for this unit. Low cost micro-electro-mechanical-systems (MEMS) accelerometers are used in the hardware prototyping. Wireless measurement errors are modelled as a black box and calibrated at the remote processor end. A simplified multi-position testing approach is designed in wireless IMU error modelling. A gyro-free inertial navigation system (INS) is prototyped

using this wireless IMU. Gyro-free INS experiments present an improved accuracy level by using the error modelling in this work.

## 6.3 Future Research

As illustrated in this thesis, the positioning errors of the gyro-free INS grow over time in the integration process. In future research, external sensors, such as, infrared ray, laser scanner and camera could be integrated to aid positioning. Using more accelerometers to build a full gyro-free INS would be a worthwhile topic for future research and development. The theory of a 6-accellerometer INS confirms the feasibility of such a system. A 6-accelerometer INS has been introduced by Chen, which has one accelerometer at the centre of each face of a cube. The rotational acceleration of the cube can be determined from the measurement of six accelerations (Chen, Lee et al. 1994). The development of a wireless communication based gyro-free INS using more MEMS accelerometers will be my next research project. The current wireless accelerometer unit was prototyped by integrating OEM components. For its future development, the hardware part could be improved in size and weight by building in-house- developed components.

## 6.4 Concluding Remarks

The main good of this work was to discover a more accurate and reliable modelling for wireless communication in inertial navigation system. The data from cable communication is the original data from IMU, calibrations and alignments have been completed prior to the experiments. It is not the prefect data but it is the best data. The data from cable could have some tiny errors because of disadvantages of low cost component. This still can be accepted as it is the common issue from all low cost devices. However, after adding a wireless device on the system, figures clearly display that there is a small difference between the data from wireless communication and the original data. This is the main point to design an error modelling to correct the difference. Error modelling generates six sets of new algorithms in six positions. These new algorithms are able to determine different errors, such as bias, scale and misalignment errors, by using three accelerometers in x, y and z axes. When errors have been

detected by thousands sets of samples, the original algorithms are modified specifically for each position to reduce the errors. Estimated data figures are plotted; these figures clearly display the results of the error modelling that errors have been corrected or minimized. Since the new algorithm has been designed for IMUs, this method can also be used on other IMU devices to correct the data as long as the data has been interfered by external device. Finally, a gyro-free INS has been demonstrated in a dynamic environment to display that the error modelling is successful in a short positioning time.

## 6.5 Bibliography

Barshan, B. and H. F. Durrant-Whyte (1995). "Inertial navigation systems for mobile robots." Robotics and Automation, IEEE Transactions on **11**(3): 328-342.

Batista, P., C. Silvestre, et al. (2002). "Accelerometer Calibration and Dynamic Bias and Gravity Estimation: Analysis, Design, and Experimental Evaluation." Control Systems Technology, IEEE Transactions on **19**(5): 1128-1137.

Bryson, M. and S. Sukkarieh (2007). "Building a Robust Implementation of Bearing-only Inertial SLAM for a UAV." Journal of Field Robotics **24**(1-2): 113-143.

Camps, F., S. Harasse, et al. (2009). Numerical calibration for 3-axis accelerometers and magnetometers. Electro/Information Technology, 2009. eit '09. IEEE International Conference on.

Chen, J.-H., S.-C. Lee, et al. (1994). "Gyroscope free strapdown inertial measurement unit by six linear accelerometers." Journal of Guidance, Control, and Dynamics **17**(2): 286-290.

Feng, S., X. Wen, et al. Enhancement of the Aided Inertial Navigation System for an AUV via micronavigation. OCEANS 2010.

Gao, J., P. Webb, et al. (2003). "Error reduction for an inertial-sensor-based dynamic parallel kinematic machine positioning system." Measurement Science and Technology **14**(5): 543.

Grewal, M. S. (2007). Fundamentals of Satellite and Inertial Navigation. Global positioning systems, inertial navigation, and integration, Hoboken, N.J. : Wiley-Interscience**:** 10-11.

Gul, F. and J. Fang (2005). Correction technique for velocity and position error of inertial navigation system by celestial observations. Emerging Technologies, 2005. Proceedings of the IEEE Symposium on.

Guobin, C., X. Jiangning, et al. (2010). Error Analysis and Simulation of the Dual-Axis Rotation-Dwell Autocompensating Strapdown Inertial Navigation System. Measuring Technology and Mechatronics Automation (ICMTMA), 2010 International Conference on.

Hung, J. C., J. R. Thacher, et al. (1989). Calibration of accelerometer triad of an IMU with drifting <e1>Z </e1>-accelerometer bias. Aerospace and Electronics Conference, 1989. NAECON 1989., Proceedings of the IEEE 1989 National.

Jie, L. and T. Ruiping (2010). Initial alignment technology of strapdown inertial navigation system based-on stationary base. Intelligent Control and Information Processing (ICICIP), 2010 International Conference on.

Liduan, W., Y. Ping, et al. (2008). High performance strapdown inertial navigation system algorithms for space flight. Systems and Control in Aerospace and Astronautics, 2008. ISSCAA 2008. 2nd International Symposium on.

Liu, H. and G. Pang (1999). Accelerometer for mobile robot positioning. Industry Applications Conference, 1999. Thirty-Fourth IAS Annual Meeting. Conference Record of the 1999 IEEE.

Lueck, F. W. a. R. (2002). A Quick Method for Calibrating Accelerometers. Rockland Scientific Internation Inc.: 1-2.

Lupton, T. and S. Sukkarieh (2008). Removing scale biases and ambiguity from 6DoF monocular SLAM using inertial. Robotics and Automation, 2008. ICRA 2008. IEEE International Conference on.

Nebot, E. (2005). Navigation System Design. Centre of Excellence for Autonomous Systems. NSW, The University of Sydney: 75-77.

Oceanserver (2011, Dec 20 2011). "Compass Products." Retrieved Nov 12, 2011, from http://www.oceanserver-store.com/compass.html.

Olivares, A., G. Olivares, et al. (2009). High-efficiency low-cost accelerometer-aided gyroscope calibration. Test and Measurement, 2009. ICTM '09. International Conference on.

Qu, P., L. Fu, et al. (2009). Design of inertial navigation system based on micromechanical gyroscope and accelerometer. Control and Decision Conference, 2009. CCDC '09. Chinese.

Rovingnetworks (2011, Dec 12 2011). "RS232 to Bluetooth serial adapter with rechargeable battery." Retrieved Oct 15, 2011, from http://www.g2microsystems.com/products/RN_220XP.

Titterton, D. H. D. H. (2004). Accelerometer and multi-sensor technology. Strapdown inertial navigation technology, Stevenage : Institution of Electrical Engineers, c2004. **5:** 153-154.

Titterton, D. H. D. H. (2004). Accelerometer and multi-sensor technology. Strapdown inertial navigation technology, Stevenage : Institution of Electrical Engineers, c2004. **5:** 156-159.

Titterton, D. H. D. H. (2004). MEMS inertial sensors. Strapdown inertial navigation technology, Stevenage : Institution of Electrical Engineers, c2004. **5:** 205-206.

Trujillo, D. M. (1982). A new approach to the integration of accelerometer data. Earthquake engineering and structural dynamics. **10:** 529–535.

Vectornav (2011). "Inertial Navigation." Retrieved Oct 03, 2011, from http://www.vectornav.com/index.php?option=com_content&view=article&id=27&Itemid=11.

Wikipedia (2011). "Bluetooth." Retrieved Nov 11, 2011, from http://en.wikipedia.org/wiki/Bluetooth.

Zhuxin, D., U. C. Wejinya, et al. (2009). Calibration of MEMS accelerometer based on plane optical tracking technique and measurements. Nano/Micro Engineered and Molecular Systems, 2009. NEMS 2009. 4th IEEE International Conference on.

# Appendix

## Sample of data set in Position 1 (cable)

| Acc. X | Acc. Y | Acc. Z | Acc. X | Acc. Y | Acc. Z | Acc. X | Acc. Y | Acc. Z |
|---|---|---|---|---|---|---|---|---|
| 0.001 | 0.005 | 1.023 | 0.001 | 0.005 | 1.02 | 0.001 | 0.004 | 1.023 |
| 0.001 | 0.006 | 1.024 | 0.001 | 0.005 | 1.02 | 0 | 0.004 | 1.023 |
| 0.001 | 0.007 | 1.024 | 0.002 | 0.005 | 1.02 | 0.001 | 0.005 | 1.023 |
| 0.002 | 0.007 | 1.024 | 0.001 | 0.005 | 1.021 | 0 | 0.005 | 1.023 |
| 0.002 | 0.006 | 1.023 | 0.001 | 0.005 | 1.022 | 0 | 0.005 | 1.024 |
| 0.002 | 0.006 | 1.023 | 0.001 | 0.004 | 1.021 | 0.001 | 0.005 | 1.024 |
| 0.003 | 0.005 | 1.023 | 0.002 | 0.004 | 1.022 | 0 | 0.005 | 1.025 |
| 0.001 | 0.004 | 1.023 | 0.002 | 0.004 | 1.022 | 0.001 | 0.005 | 1.024 |
| 0 | 0.005 | 1.025 | 0.001 | 0.005 | 1.022 | 0 | 0.006 | 1.024 |
| 0.001 | 0.004 | 1.024 | 0.002 | 0.005 | 1.023 | 0.001 | 0.005 | 1.024 |
| 0.001 | 0.004 | 1.024 | 0.001 | 0.005 | 1.023 | 0.001 | 0.006 | 1.024 |
| 0.001 | 0.005 | 1.023 | 0.001 | 0.004 | 1.021 | 0 | 0.005 | 1.024 |
| 0.002 | 0.004 | 1.022 | 0.002 | 0.004 | 1.022 | 0.001 | 0.005 | 1.024 |
| 0.002 | 0.006 | 1.023 | 0.002 | 0.005 | 1.022 | 0.001 | 0.005 | 1.024 |
| 0.002 | 0.006 | 1.023 | 0.001 | 0.005 | 1.022 | 0.001 | 0.004 | 1.023 |
| 0.002 | 0.005 | 1.023 | 0.001 | 0.005 | 1.021 | 0.002 | 0.005 | 1.023 |
| 0.002 | 0.005 | 1.023 | 0 | 0.005 | 1.022 | 0.001 | 0.005 | 1.022 |
| 0.002 | 0.004 | 1.022 | 0 | 0.004 | 1.022 | 0 | 0.005 | 1.023 |
| 0.001 | 0.005 | 1.023 | 0 | 0.004 | 1.022 | 0 | 0.005 | 1.023 |
| 0.001 | 0.005 | 1.021 | 0 | 0.005 | 1.023 | 0 | 0.005 | 1.023 |
| 0.001 | 0.005 | 1.021 | 0.001 | 0.005 | 1.023 | 0 | 0.005 | 1.023 |
| 0.001 | 0.006 | 1.021 | 0.001 | 0.005 | 1.023 | 0 | 0.005 | 1.023 |
| 0.002 | 0.005 | 1.022 | 0.001 | 0.006 | 1.023 | 0.001 | 0.005 | 1.021 |
| 0.001 | 0.005 | 1.022 | 0.001 | 0.005 | 1.023 | 0.001 | 0.005 | 1.02 |
| 0.002 | 0.005 | 1.022 | 0 | 0.005 | 1.022 | 0.001 | 0.004 | 1.02 |
| 0.002 | 0.005 | 1.023 | 0.001 | 0.005 | 1.022 | 0.001 | 0.004 | 1.018 |
| 0.002 | 0.005 | 1.022 | 0.001 | 0.005 | 1.023 | 0 | 0.004 | 1.018 |
| 0.002 | 0.005 | 1.023 | 0.001 | 0.005 | 1.022 | 0.001 | 0.004 | 1.019 |
| 0.002 | 0.005 | 1.022 | 0.001 | 0.006 | 1.023 | 0.001 | 0.004 | 1.018 |
| 0.001 | 0.005 | 1.023 | 0.001 | 0.006 | 1.022 | 0.002 | 0.004 | 1.019 |
| 0.001 | 0.005 | 1.023 | 0.001 | 0.006 | 1.021 | 0.002 | 0.005 | 1.019 |
| 0.001 | 0.005 | 1.023 | 0 | 0.005 | 1.02 | 0.002 | 0.005 | 1.019 |
| 0.001 | 0.005 | 1.022 | 0.001 | 0.004 | 1.02 | 0.002 | 0.005 | 1.018 |
| 0.002 | 0.005 | 1.021 | 0.001 | 0.004 | 1.02 | 0.002 | 0.006 | 1.018 |
| 0.002 | 0.005 | 1.021 | 0 | 0.004 | 1.021 | 0.002 | 0.006 | 1.018 |
| 0.002 | 0.004 | 1.021 | 0.001 | 0.004 | 1.022 | 0.002 | 0.006 | 1.019 |
| 0.002 | 0.005 | 1.021 | 0.001 | 0.004 | 1.023 | 0.002 | 0.006 | 1.019 |

| Acc. X | Acc. Y | Acc. Z | Acc. X | Acc. Y | Acc. Z | Acc. X | Acc. Y | Acc. Z |
|---|---|---|---|---|---|---|---|---|
| 0.002 | 0.005 | 1.02 | 0.001 | 0.004 | 1.018 | 0.001 | 0.005 | 1.02 |
| 0.002 | 0.005 | 1.02 | 0.002 | 0.005 | 1.018 | 0.001 | 0.004 | 1.02 |
| 0.002 | 0.004 | 1.02 | 0.002 | 0.005 | 1.017 | 0 | 0.004 | 1.02 |
| 0.002 | 0.005 | 1.02 | 0.002 | 0.006 | 1.016 | 0.001 | 0.004 | 1.018 |
| 0.001 | 0.005 | 1.02 | 0.001 | 0.006 | 1.017 | 0.001 | 0.005 | 1.018 |
| 0.001 | 0.005 | 1.02 | 0.001 | 0.005 | 1.016 | 0.001 | 0.005 | 1.018 |
| 0.001 | 0.005 | 1.02 | 0 | 0.005 | 1.018 | 0.001 | 0.006 | 1.018 |
| 0 | 0.005 | 1.021 | 0 | 0.005 | 1.018 | 0 | 0.005 | 1.018 |
| 0.001 | 0.005 | 1.02 | 0 | 0.005 | 1.019 | 0.001 | 0.005 | 1.018 |
| 0.001 | 0.006 | 1.02 | 0 | 0.006 | 1.02 | 0 | 0.005 | 1.018 |
| 0.001 | 0.006 | 1.021 | 0.001 | 0.005 | 1.019 | 0 | 0.004 | 1.018 |
| 0.001 | 0.006 | 1.02 | 0.001 | 0.005 | 1.02 | 0.001 | 0.004 | 1.017 |
| 0.001 | 0.006 | 1.02 | 0.001 | 0.005 | 1.019 | 0 | 0.004 | 1.017 |
| 0 | 0.006 | 1.02 | 0.001 | 0.005 | 1.018 | 0.001 | 0.004 | 1.016 |
| 0 | 0.006 | 1.02 | 0.001 | 0.005 | 1.018 | 0.002 | 0.004 | 1.016 |
| 0.001 | 0.005 | 1.019 | 0.001 | 0.005 | 1.018 | 0.002 | 0.005 | 1.016 |
| 0.001 | 0.005 | 1.019 | 0.001 | 0.005 | 1.018 | 0.002 | 0.005 | 1.016 |
| 0.002 | 0.004 | 1.018 | 0.001 | 0.005 | 1.018 | 0.002 | 0.004 | 1.016 |
| 0.002 | 0.005 | 1.018 | 0.001 | 0.005 | 1.019 | 0.002 | 0.005 | 1.017 |
| 0.002 | 0.005 | 1.019 | 0.002 | 0.005 | 1.018 | 0.002 | 0.005 | 1.018 |
| 0.002 | 0.005 | 1.018 | 0.002 | 0.004 | 1.019 | 0.002 | 0.005 | 1.018 |
| 0.002 | 0.005 | 1.019 | 0.002 | 0.005 | 1.019 | 0.001 | 0.006 | 1.018 |
| 0.002 | 0.004 | 1.019 | 0.002 | 0.005 | 1.019 | 0.001 | 0.005 | 1.019 |
| 0.001 | 0.004 | 1.018 | 0.002 | 0.006 | 1.019 | 0.001 | 0.005 | 1.019 |
| 0.001 | 0.004 | 1.019 | 0.002 | 0.006 | 1.019 | 0.001 | 0.004 | 1.02 |
| 0.001 | 0.005 | 1.019 | 0.001 | 0.006 | 1.019 | 0.001 | 0.004 | 1.02 |
| 0.001 | 0.005 | 1.018 | 0.001 | 0.006 | 1.02 | 0.001 | 0.004 | 1.02 |
| 0.001 | 0.006 | 1.019 | 0 | 0.006 | 1.02 | 0.001 | 0.004 | 1.02 |
| 0 | 0.005 | 1.019 | 0 | 0.006 | 1.02 | 0.002 | 0.004 | 1.019 |
| 0 | 0.006 | 1.019 | 0.001 | 0.006 | 1.02 | 0.002 | 0.004 | 1.019 |
| 0 | 0.006 | 1.02 | 0.001 | 0.006 | 1.02 | 0.002 | 0.004 | 1.02 |
| 0 | 0.006 | 1.022 | 0.002 | 0.006 | 1.02 | 0.001 | 0.004 | 1.02 |
| 0 | 0.005 | 1.023 | 0.002 | 0.006 | 1.02 | 0.001 | 0.004 | 1.02 |
| 0.001 | 0.004 | 1.022 | 0.001 | 0.005 | 1.019 | 0.001 | 0.005 | 1.02 |
| 0.001 | 0.005 | 1.021 | 0 | 0.005 | 1.019 | 0.001 | 0.005 | 1.019 |
| 0.001 | 0.005 | 1.02 | 0 | 0.004 | 1.018 | 0.001 | 0.006 | 1.019 |
| 0.002 | 0.005 | 1.02 | 0 | 0.004 | 1.018 | 0.001 | 0.005 | 1.019 |
| 0.002 | 0.005 | 1.02 | 0 | 0.004 | 1.017 | 0.001 | 0.005 | 1.019 |
| 0.002 | 0.004 | 1.02 | 0.001 | 0.004 | 1.019 | 0.002 | 0.005 | 1.019 |
| 0.002 | 0.005 | 1.02 | 0.001 | 0.005 | 1.019 | 0.002 | 0.005 | 1.019 |
| 0.002 | 0.005 | 1.019 | 0.002 | 0.005 | 1.019 | 0.002 | 0.005 | 1.018 |
| 0.001 | 0.006 | 1.019 | 0.002 | 0.005 | 1.019 | 0.001 | 0.005 | 1.019 |
| 0.001 | 0.005 | 1.018 | 0.001 | 0.005 | 1.02 | 0.001 | 0.005 | 1.019 |

## Sample of data set in Position 2 (cable)

| Acc. X | Acc. Y | Acc. Z | Acc. X | Acc. Y | Acc. Z | Acc. X | Acc. Y | Acc. Z |
|---|---|---|---|---|---|---|---|---|
| 0.003 | 0.006 | -1.014 | 0.002 | 0.005 | -1.011 | 0.002 | 0.004 | -1.009 |
| 0.003 | 0.007 | -1.013 | 0.002 | 0.006 | -1.012 | 0.002 | 0.003 | -1.01 |
| 0.004 | 0.008 | -1.013 | 0.002 | 0.006 | -1.014 | 0.002 | 0.004 | -1.011 |
| 0.004 | 0.008 | -1.012 | 0.002 | 0.006 | -1.014 | 0.002 | 0.006 | -1.011 |
| 0.003 | 0.008 | -1.012 | 0.003 | 0.006 | -1.014 | 0.001 | 0.007 | -1.011 |
| 0.003 | 0.007 | -1.012 | 0.002 | 0.005 | -1.014 | 0.002 | 0.007 | -1.011 |
| 0.002 | 0.007 | -1.013 | 0.002 | 0.006 | -1.013 | 0.002 | 0.007 | -1.01 |
| 0.002 | 0.005 | -1.012 | 0.002 | 0.007 | -1.012 | 0.002 | 0.006 | -1.011 |
| 0.002 | 0.006 | -1.014 | 0.002 | 0.006 | -1.011 | 0.002 | 0.005 | -1.011 |
| 0.002 | 0.006 | -1.014 | 0.002 | 0.005 | -1.011 | 0.001 | 0.005 | -1.011 |
| 0.003 | 0.006 | -1.013 | 0.002 | 0.004 | -1.01 | 0.001 | 0.005 | -1.011 |
| 0.004 | 0.007 | -1.014 | 0.002 | 0.004 | -1.01 | 0.001 | 0.006 | -1.011 |
| 0.004 | 0.007 | -1.014 | 0.002 | 0.005 | -1.01 | 0.001 | 0.007 | -1.012 |
| 0.003 | 0.006 | -1.013 | 0.002 | 0.006 | -1.011 | 0.002 | 0.005 | -1.011 |
| 0.003 | 0.005 | -1.013 | 0.002 | 0.008 | -1.012 | 0.002 | 0.006 | -1.01 |
| 0.002 | 0.005 | -1.013 | 0.002 | 0.006 | -1.012 | 0.002 | 0.007 | -1.01 |
| 0.002 | 0.008 | -1.011 | 0.002 | 0.006 | -1.012 | 0.002 | 0.007 | -1.009 |
| 0.002 | 0.008 | -1.01 | 0.002 | 0.007 | -1.011 | 0.003 | 0.008 | -1.009 |
| 0.002 | 0.01 | -1.011 | 0.002 | 0.006 | -1.011 | 0.003 | 0.008 | -1.011 |
| 0.002 | 0.01 | -1.011 | 0.002 | 0.007 | -1.01 | 0.003 | 0.007 | -1.012 |
| 0.002 | 0.009 | -1.012 | 0.002 | 0.008 | -1.011 | 0.003 | 0.008 | -1.012 |
| 0.002 | 0.008 | -1.013 | 0.002 | 0.008 | -1.012 | 0.002 | 0.007 | -1.013 |
| 0.002 | 0.008 | -1.013 | 0.002 | 0.008 | -1.012 | 0.002 | 0.006 | -1.011 |
| 0.002 | 0.007 | -1.013 | 0.002 | 0.008 | -1.012 | 0.002 | 0.006 | -1.011 |
| 0.003 | 0.007 | -1.014 | 0.003 | 0.006 | -1.012 | 0.002 | 0.005 | -1.011 |
| 0.002 | 0.007 | -1.014 | 0.003 | 0.007 | -1.012 | 0.002 | 0.007 | -1.012 |
| 0.002 | 0.007 | -1.012 | 0.003 | 0.007 | -1.013 | 0.002 | 0.007 | -1.012 |
| 0.002 | 0.007 | -1.014 | 0.004 | 0.006 | -1.014 | 0.002 | 0.007 | -1.01 |
| 0.001 | 0.007 | -1.013 | 0.003 | 0.007 | -1.013 | 0.002 | 0.007 | -1.011 |
| 0.001 | 0.007 | -1.013 | 0.003 | 0.007 | -1.012 | 0.002 | 0.007 | -1.011 |
| 0.002 | 0.006 | -1.014 | 0.002 | 0.007 | -1.01 | 0.001 | 0.009 | -1.011 |
| 0.002 | 0.006 | -1.012 | 0.002 | 0.008 | -1.008 | 0.002 | 0.007 | -1.012 |
| 0.001 | 0.005 | -1.012 | 0.003 | 0.006 | -1.008 | 0.002 | 0.007 | -1.012 |
| 0.001 | 0.006 | -1.011 | 0.003 | 0.006 | -1.008 | 0.002 | 0.008 | -1.012 |
| 0.001 | 0.006 | -1.011 | 0.003 | 0.006 | -1.009 | 0.001 | 0.006 | -1.013 |
| 0.001 | 0.007 | -1.011 | 0.003 | 0.006 | -1.01 | 0.001 | 0.006 | -1.014 |
| 0.002 | 0.008 | -1.01 | 0.002 | 0.006 | -1.011 | 0.001 | 0.006 | -1.013 |
| 0.001 | 0.009 | -1.01 | 0.002 | 0.006 | -1.011 | 0.001 | 0.006 | -1.013 |
| 0.001 | 0.008 | -1.01 | 0.002 | 0.006 | -1.01 | 0.002 | 0.007 | -1.013 |
| 0.002 | 0.008 | -1.009 | 0.001 | 0.005 | -1.01 | 0.001 | 0.008 | -1.015 |
| 0.002 | 0.007 | -1.01 | 0.002 | 0.005 | -1.009 | 0.002 | 0.007 | -1.014 |

| Acc. X | Acc. Y | Acc. Z | Acc. X | Acc. Y | Acc. Z | Acc. X | Acc. Y | Acc. Z |
|---|---|---|---|---|---|---|---|---|
| 0.002 | 0.005 | -1.016 | 0.002 | 0.008 | -1.012 | 0.002 | 0.007 | -1.011 |
| 0.002 | 0.005 | -1.015 | 0.002 | 0.008 | -1.013 | 0.003 | 0.008 | -1.01 |
| 0.002 | 0.005 | -1.012 | 0.003 | 0.009 | -1.013 | 0.003 | 0.008 | -1.011 |
| 0.002 | 0.004 | -1.012 | 0.003 | 0.007 | -1.012 | 0.003 | 0.007 | -1.01 |
| 0.002 | 0.006 | -1.011 | 0.002 | 0.007 | -1.011 | 0.003 | 0.007 | -1.01 |
| 0.002 | 0.006 | -1.011 | 0.003 | 0.007 | -1.011 | 0.003 | 0.006 | -1.011 |
| 0.001 | 0.005 | -1.01 | 0.003 | 0.006 | -1.011 | 0.003 | 0.006 | -1.011 |
| 0.001 | 0.006 | -1.011 | 0.002 | 0.007 | -1.012 | 0.002 | 0.007 | -1.012 |
| 0.002 | 0.006 | -1.012 | 0.002 | 0.007 | -1.012 | 0.002 | 0.005 | -1.012 |
| 0.002 | 0.005 | -1.012 | 0.002 | 0.007 | -1.011 | 0.002 | 0.007 | -1.013 |
| 0.002 | 0.005 | -1.013 | 0.002 | 0.008 | -1.012 | 0.002 | 0.007 | -1.012 |
| 0.002 | 0.004 | -1.013 | 0.001 | 0.008 | -1.013 | 0.002 | 0.007 | -1.011 |
| 0.001 | 0.005 | -1.013 | 0.001 | 0.006 | -1.014 | 0.002 | 0.008 | -1.011 |
| 0.002 | 0.005 | -1.013 | 0.001 | 0.006 | -1.014 | 0.002 | 0.007 | -1.01 |
| 0.002 | 0.005 | -1.012 | 0.002 | 0.005 | -1.013 | 0.002 | 0.007 | -1.01 |
| 0.003 | 0.007 | -1.012 | 0.002 | 0.005 | -1.012 | 0.002 | 0.007 | -1.01 |
| 0.003 | 0.006 | -1.011 | 0.002 | 0.007 | -1.011 | 0.002 | 0.007 | -1.009 |
| 0.003 | 0.007 | -1.011 | 0.002 | 0.007 | -1.011 | 0.002 | 0.008 | -1.01 |
| 0.002 | 0.008 | -1.012 | 0.001 | 0.008 | -1.01 | 0.002 | 0.006 | -1.01 |
| 0.003 | 0.007 | -1.012 | 0.002 | 0.008 | -1.011 | 0.002 | 0.005 | -1.01 |
| 0.002 | 0.007 | -1.011 | 0.002 | 0.007 | -1.011 | 0.002 | 0.005 | -1.011 |
| 0.002 | 0.008 | -1.012 | 0.001 | 0.005 | -1.01 | 0.002 | 0.005 | -1.011 |
| 0.003 | 0.008 | -1.012 | 0.002 | 0.005 | -1.011 | 0.003 | 0.006 | -1.011 |
| 0.002 | 0.008 | -1.015 | 0.001 | 0.004 | -1.009 | 0.002 | 0.008 | -1.011 |
| 0.004 | 0.007 | -1.015 | 0.002 | 0.005 | -1.008 | 0.001 | 0.008 | -1.011 |
| 0.004 | 0.006 | -1.015 | 0.003 | 0.006 | -1.009 | 0.001 | 0.008 | -1.01 |
| 0.003 | 0.006 | -1.014 | 0.002 | 0.007 | -1.009 | 0.001 | 0.009 | -1.011 |
| 0.003 | 0.006 | -1.012 | 0.002 | 0.007 | -1.01 | 0.002 | 0.008 | -1.011 |
| 0.002 | 0.008 | -1.013 | 0.002 | 0.007 | -1.011 | 0.002 | 0.008 | -1.012 |
| 0.002 | 0.008 | -1.013 | 0.001 | 0.005 | -1.011 | 0.002 | 0.006 | -1.012 |
| 0.003 | 0.008 | -1.012 | 0.002 | 0.006 | -1.012 | 0.002 | 0.006 | -1.013 |
| 0.002 | 0.008 | -1.013 | 0.002 | 0.006 | -1.012 | 0.002 | 0.005 | -1.013 |
| 0.002 | 0.007 | -1.013 | 0.002 | 0.006 | -1.011 | 0.002 | 0.006 | -1.013 |
| 0.002 | 0.008 | -1.012 | 0.002 | 0.007 | -1.011 | 0.002 | 0.007 | -1.013 |
| 0.002 | 0.007 | -1.013 | 0.002 | 0.007 | -1.01 | 0.002 | 0.006 | -1.014 |
| 0.002 | 0.006 | -1.012 | 0.002 | 0.008 | -1.01 | 0.002 | 0.006 | -1.014 |
| 0.002 | 0.005 | -1.015 | 0.002 | 0.008 | -1.01 | 0.002 | 0.006 | -1.014 |
| 0.002 | 0.003 | -1.015 | 0.002 | 0.008 | -1.011 | 0.001 | 0.006 | -1.014 |
| 0.001 | 0.004 | -1.015 | 0.001 | 0.008 | -1.012 | 0.001 | 0.008 | -1.014 |
| 0.001 | 0.004 | -1.016 | 0.001 | 0.009 | -1.011 | 0.001 | 0.008 | -1.014 |
| 0 | 0.006 | -1.013 | 0.001 | 0.007 | -1.011 | 0.001 | 0.009 | -1.014 |
| 0 | 0.007 | -1.012 | 0.001 | 0.007 | -1.011 | 0.002 | 0.009 | -1.014 |
| 0.001 | 0.007 | -1.013 | 0.002 | 0.007 | -1.011 | 0.002 | 0.009 | -1.014 |

## Sample of data set in Position 3 (cable)

| Acc. X | Acc. Y | Acc. Z | Acc. X | Acc. Y | Acc. Z | Acc. X | Acc. Y | Acc. Z |
|---|---|---|---|---|---|---|---|---|
| 1.013 | -0.013 | 0.005 | 1.014 | -0.009 | 0 | 1.013 | -0.008 | 0 |
| 1.013 | -0.009 | 0.005 | 1.015 | -0.009 | 0 | 1.012 | -0.008 | 0 |
| 1.012 | -0.006 | 0.003 | 1.015 | -0.01 | 0 | 1.012 | -0.009 | 0 |
| 1.013 | -0.006 | 0.002 | 1.013 | -0.01 | 0 | 1.012 | -0.009 | 0 |
| 1.013 | -0.003 | 0 | 1.013 | -0.01 | 0 | 1.012 | -0.009 | -0.001 |
| 1.014 | -0.006 | 0 | 1.012 | -0.01 | 0 | 1.013 | -0.009 | -0.001 |
| 1.013 | -0.009 | 0 | 1.012 | -0.009 | 0 | 1.013 | -0.008 | 0 |
| 1.012 | -0.01 | 0 | 1.011 | -0.009 | 0 | 1.012 | -0.009 | 0 |
| 1.012 | -0.011 | 0 | 1.011 | -0.008 | 0 | 1.011 | -0.009 | 0 |
| 1.012 | -0.011 | 0.001 | 1.012 | -0.008 | 0 | 1.012 | -0.009 | 0 |
| 1.011 | -0.01 | 0.004 | 1.012 | -0.008 | 0 | 1.012 | -0.009 | 0 |
| 1.012 | -0.009 | 0.002 | 1.012 | -0.008 | 0 | 1.013 | -0.009 | 0 |
| 1.012 | -0.007 | 0.004 | 1.012 | -0.008 | 0 | 1.015 | -0.009 | 0 |
| 1.012 | -0.007 | 0.002 | 1.013 | -0.008 | 0 | 1.015 | -0.008 | 0 |
| 1.012 | -0.007 | 0 | 1.013 | -0.008 | 0 | 1.016 | -0.009 | 0 |
| 1.012 | -0.008 | 0 | 1.013 | -0.009 | 0 | 1.016 | -0.008 | 0 |
| 1.012 | -0.009 | 0 | 1.013 | -0.01 | 0 | 1.013 | -0.009 | 0 |
| 1.012 | -0.009 | 0.001 | 1.012 | -0.009 | 0 | 1.012 | -0.009 | 0 |
| 1.012 | -0.009 | 0.002 | 1.015 | -0.009 | 0 | 1.013 | -0.009 | 0 |
| 1.012 | -0.009 | 0.003 | 1.015 | -0.008 | 0 | 1.012 | -0.009 | 0 |
| 1.012 | -0.008 | 0.001 | 1.015 | -0.009 | 0 | 1.013 | -0.008 | 0 |
| 1.012 | -0.008 | 0.001 | 1.014 | -0.008 | 0 | 1.013 | -0.008 | 0 |
| 1.012 | -0.008 | 0 | 1.012 | -0.009 | 0.001 | 1.012 | -0.008 | 0 |
| 1.013 | -0.008 | 0 | 1.012 | -0.011 | 0.001 | 1.012 | -0.008 | 0 |
| 1.016 | -0.009 | 0.001 | 1.014 | -0.01 | 0.002 | 1.012 | -0.008 | 0 |
| 1.016 | -0.009 | 0.001 | 1.015 | -0.01 | 0.002 | 1.011 | -0.008 | 0 |
| 1.017 | -0.009 | 0.002 | 1.014 | -0.009 | 0 | 1.012 | -0.008 | 0 |
| 1.016 | -0.009 | 0.002 | 1.014 | -0.008 | 0.001 | 1.012 | -0.008 | 0 |
| 1.013 | -0.009 | 0.001 | 1.013 | -0.008 | 0.001 | 1.012 | -0.008 | 0 |
| 1.012 | -0.009 | 0.001 | 1.012 | -0.008 | 0 | 1.012 | -0.009 | 0 |
| 1.011 | -0.009 | 0 | 1.012 | -0.008 | 0.001 | 1.013 | -0.009 | 0 |
| 1.012 | -0.008 | 0.001 | 1.011 | -0.008 | 0 | 1.012 | -0.01 | 0 |
| 1.012 | -0.008 | 0 | 1.012 | -0.008 | 0 | 1.012 | -0.01 | 0 |
| 1.013 | -0.008 | 0 | 1.013 | -0.009 | 0 | 1.012 | -0.011 | 0 |
| 1.014 | -0.009 | 0 | 1.014 | -0.01 | 0 | 1.011 | -0.01 | 0 |
| 1.014 | -0.009 | 0 | 1.016 | -0.01 | 0 | 1.012 | -0.01 | 0 |
| 1.014 | -0.009 | 0 | 1.016 | -0.01 | 0 | 1.012 | -0.009 | 0 |
| 1.014 | -0.009 | 0 | 1.016 | -0.009 | 0 | 1.012 | -0.009 | 0 |
| 1.013 | -0.009 | 0 | 1.016 | -0.008 | 0 | 1.012 | -0.008 | 0 |
| 1.013 | -0.009 | 0 | 1.013 | -0.008 | 0 | 1.012 | -0.008 | 0 |
| 1.015 | -0.009 | 0 | 1.013 | -0.008 | 0 | 1.013 | -0.008 | 0 |

| Acc. X | Acc. Y | Acc. Z | Acc. X | Acc. Y | Acc. Z | Acc. X | Acc. Y | Acc. Z |
|---|---|---|---|---|---|---|---|---|
| 1.012 | -0.008 | 0 | 1.011 | -0.009 | 0.002 | 1.013 | -0.008 | 0.001 |
| 1.012 | -0.009 | 0 | 1.012 | -0.008 | 0.003 | 1.012 | -0.008 | 0 |
| 1.011 | -0.008 | 0 | 1.012 | -0.008 | 0.003 | 1.013 | -0.008 | 0.001 |
| 1.011 | -0.008 | -0.001 | 1.011 | -0.007 | 0.003 | 1.012 | -0.008 | 0.001 |
| 1.012 | -0.008 | 0 | 1.012 | -0.007 | 0.003 | 1.013 | -0.009 | 0 |
| 1.012 | -0.008 | 0 | 1.012 | -0.007 | 0.002 | 1.013 | -0.009 | 0 |
| 1.012 | -0.009 | 0 | 1.012 | -0.008 | 0.002 | 1.013 | -0.009 | -0.001 |
| 1.013 | -0.008 | 0 | 1.012 | -0.008 | 0.002 | 1.013 | -0.009 | 0 |
| 1.012 | -0.008 | 0 | 1.012 | -0.009 | 0.002 | 1.015 | -0.009 | 0 |
| 1.015 | -0.008 | 0 | 1.012 | -0.01 | 0.002 | 1.016 | -0.009 | 0.001 |
| 1.015 | -0.008 | 0 | 1.012 | -0.01 | 0.002 | 1.015 | -0.009 | 0.001 |
| 1.015 | -0.008 | 0 | 1.012 | -0.009 | 0.001 | 1.014 | -0.008 | 0.001 |
| 1.016 | -0.008 | 0.001 | 1.012 | -0.009 | 0 | 1.011 | -0.008 | 0 |
| 1.014 | -0.009 | 0 | 1.012 | -0.009 | 0 | 1.011 | -0.008 | 0 |
| 1.016 | -0.009 | 0 | 1.012 | -0.009 | 0 | 1.012 | -0.008 | 0 |
| 1.015 | -0.01 | 0 | 1.012 | -0.009 | -0.001 | 1.013 | -0.009 | 0 |
| 1.018 | -0.009 | 0 | 1.013 | -0.009 | 0 | 1.014 | -0.01 | 0 |
| 1.017 | -0.008 | 0 | 1.013 | -0.008 | 0 | 1.014 | -0.01 | 0 |
| 1.015 | -0.008 | 0 | 1.013 | -0.009 | 0 | 1.014 | -0.01 | 0 |
| 1.016 | -0.008 | 0 | 1.012 | -0.009 | 0.001 | 1.013 | -0.009 | 0 |
| 1.016 | -0.008 | 0 | 1.012 | -0.009 | 0 | 1.013 | -0.008 | 0 |
| 1.015 | -0.009 | 0 | 1.012 | -0.009 | 0 | 1.013 | -0.007 | 0 |
| 1.015 | -0.009 | 0 | 1.012 | -0.009 | 0 | 1.013 | -0.008 | 0 |
| 1.015 | -0.009 | 0 | 1.012 | -0.01 | 0 | 1.012 | -0.009 | 0 |
| 1.012 | -0.009 | -0.001 | 1.013 | -0.01 | 0 | 1.011 | -0.009 | -0.001 |
| 1.012 | -0.01 | -0.002 | 1.013 | -0.01 | 0 | 1.011 | -0.01 | -0.002 |
| 1.011 | -0.01 | -0.001 | 1.013 | -0.009 | 0 | 1.012 | -0.01 | -0.002 |
| 1.012 | -0.01 | 0 | 1.014 | -0.009 | 0 | 1.012 | -0.01 | -0.001 |
| 1.012 | -0.009 | 0 | 1.013 | -0.009 | 0 | 1.012 | -0.01 | -0.001 |
| 1.011 | -0.008 | 0 | 1.013 | -0.01 | 0 | 1.012 | -0.008 | -0.001 |
| 1.012 | -0.007 | 0.001 | 1.012 | -0.01 | 0.001 | 1.012 | -0.008 | -0.001 |
| 1.011 | -0.007 | 0.001 | 1.015 | -0.011 | 0 | 1.012 | -0.008 | -0.001 |
| 1.013 | -0.007 | 0.002 | 1.015 | -0.01 | 0 | 1.012 | -0.008 | 0 |
| 1.013 | -0.008 | 0.002 | 1.015 | -0.01 | 0 | 1.012 | -0.008 | 0 |
| 1.013 | -0.008 | 0.001 | 1.015 | -0.009 | 0 | 1.011 | -0.007 | 0 |
| 1.013 | -0.008 | 0 | 1.013 | -0.008 | 0 | 1.01 | -0.007 | -0.001 |
| 1.012 | -0.008 | 0 | 1.013 | -0.008 | 0.001 | 1.011 | -0.007 | -0.001 |
| 1.012 | -0.008 | 0.001 | 1.013 | -0.007 | 0.002 | 1.014 | -0.008 | -0.001 |
| 1.011 | -0.007 | 0 | 1.013 | -0.007 | 0.002 | 1.014 | -0.009 | -0.002 |
| 1.011 | -0.008 | 0.001 | 1.013 | -0.007 | 0.002 | 1.015 | -0.009 | -0.002 |
| 1.011 | -0.009 | 0.001 | 1.013 | -0.008 | 0.001 | 1.015 | -0.009 | -0.003 |
| 1.011 | -0.008 | 0.001 | 1.013 | -0.008 | 0 | 1.013 | -0.008 | -0.003 |
| 1.012 | -0.009 | 0.002 | 1.013 | -0.008 | 0 | 1.012 | -0.008 | -0.002 |

## Sample of data set in Position 4 (cable)

| Acc. X | Acc. Y | Acc. Z | Acc. X | Acc. Y | Acc. Z | Acc. X | Acc. Y | Acc. Z |
|---|---|---|---|---|---|---|---|---|
| -0.997 | 0.014 | 0.003 | -0.999 | 0.012 | 0.004 | -0.998 | 0.014 | 0.006 |
| -0.998 | 0.012 | 0.003 | -1 | 0.012 | 0.004 | -0.998 | 0.013 | 0.006 |
| -0.997 | 0.013 | 0.002 | -1 | 0.012 | 0.004 | -0.998 | 0.014 | 0.006 |
| -0.998 | 0.012 | 0.003 | -1 | 0.013 | 0.005 | -0.998 | 0.013 | 0.006 |
| -0.999 | 0.014 | 0.003 | -0.999 | 0.013 | 0.005 | -0.998 | 0.012 | 0.006 |
| -0.998 | 0.015 | 0.003 | -0.998 | 0.014 | 0.005 | -0.999 | 0.012 | 0.006 |
| -0.997 | 0.013 | 0.004 | -0.998 | 0.015 | 0.006 | -0.998 | 0.013 | 0.006 |
| -0.997 | 0.013 | 0.004 | -0.999 | 0.014 | 0.004 | -0.999 | 0.013 | 0.006 |
| -0.998 | 0.012 | 0.004 | -1 | 0.014 | 0.005 | -0.998 | 0.014 | 0.005 |
| -0.998 | 0.014 | 0.005 | -1 | 0.013 | 0.004 | -0.998 | 0.015 | 0.005 |
| -0.999 | 0.014 | 0.006 | -1.001 | 0.011 | 0.004 | -0.999 | 0.015 | 0.006 |
| -0.998 | 0.014 | 0.005 | -1 | 0.011 | 0.005 | -0.999 | 0.014 | 0.005 |
| -0.998 | 0.014 | 0.006 | -1 | 0.012 | 0.005 | -1 | 0.013 | 0.006 |
| -0.997 | 0.012 | 0.005 | -1 | 0.013 | 0.005 | -1 | 0.013 | 0.006 |
| -0.998 | 0.012 | 0.005 | -1 | 0.014 | 0.005 | -1 | 0.011 | 0.005 |
| -0.999 | 0.014 | 0.005 | -1 | 0.014 | 0.004 | -1 | 0.012 | 0.005 |
| -1 | 0.013 | 0.004 | -0.999 | 0.015 | 0.003 | -1 | 0.012 | 0.004 |
| -1 | 0.014 | 0.004 | -0.999 | 0.015 | 0.003 | -1 | 0.012 | 0.004 |
| -1 | 0.013 | 0.002 | -0.999 | 0.015 | 0.003 | -0.999 | 0.012 | 0.005 |
| -0.998 | 0.012 | 0.002 | -0.999 | 0.015 | 0.003 | -0.998 | 0.014 | 0.006 |
| -0.998 | 0.013 | 0.002 | -0.999 | 0.014 | 0.003 | -0.998 | 0.015 | 0.007 |
| -0.998 | 0.012 | 0.004 | -0.999 | 0.013 | 0.003 | -0.998 | 0.015 | 0.006 |
| -0.999 | 0.014 | 0.005 | -0.999 | 0.011 | 0.003 | -0.999 | 0.016 | 0.006 |
| -0.999 | 0.014 | 0.005 | -0.998 | 0.011 | 0.004 | -0.999 | 0.014 | 0.007 |
| -0.999 | 0.013 | 0.006 | -0.998 | 0.011 | 0.004 | -0.998 | 0.015 | 0.006 |
| -0.999 | 0.015 | 0.005 | -0.998 | 0.012 | 0.004 | -0.998 | 0.014 | 0.007 |
| -0.998 | 0.014 | 0.005 | -0.998 | 0.013 | 0.004 | -0.998 | 0.012 | 0.006 |
| -0.998 | 0.016 | 0.004 | -0.999 | 0.013 | 0.004 | -0.999 | 0.013 | 0.007 |
| -0.999 | 0.015 | 0.004 | -1 | 0.017 | 0.004 | -0.999 | 0.012 | 0.006 |
| -0.998 | 0.014 | 0.004 | -1 | 0.016 | 0.004 | -0.999 | 0.015 | 0.005 |
| -0.999 | 0.014 | 0.005 | -1 | 0.016 | 0.005 | -1 | 0.016 | 0.006 |
| -0.998 | 0.011 | 0.006 | -1 | 0.015 | 0.005 | -0.999 | 0.015 | 0.004 |
| -0.997 | 0.013 | 0.005 | -0.996 | 0.011 | 0.006 | -0.998 | 0.016 | 0.004 |
| -0.998 | 0.012 | 0.005 | -0.995 | 0.011 | 0.006 | -0.998 | 0.014 | 0.003 |
| -0.998 | 0.013 | 0.005 | -0.995 | 0.01 | 0.007 | -0.998 | 0.014 | 0.004 |
| -1 | 0.014 | 0.004 | -0.995 | 0.011 | 0.006 | -0.999 | 0.014 | 0.005 |
| -1 | 0.013 | 0.004 | -0.998 | 0.012 | 0.005 | -0.999 | 0.012 | 0.005 |
| -0.999 | 0.014 | 0.004 | -0.999 | 0.013 | 0.006 | -0.999 | 0.013 | 0.005 |
| -0.998 | 0.013 | 0.003 | -0.998 | 0.014 | 0.005 | -0.998 | 0.013 | 0.004 |
| -0.997 | 0.014 | 0.004 | -0.998 | 0.013 | 0.005 | -0.999 | 0.014 | 0.004 |
| -0.997 | 0.012 | 0.004 | -0.997 | 0.015 | 0.006 | -0.999 | 0.015 | 0.005 |

| Acc. X | Acc. Y | Acc. Z | Acc. X | Acc. Y | Acc. Z | Acc. X | Acc. Y | Acc. Z |
|---|---|---|---|---|---|---|---|---|
| -1 | 0.015 | 0.006 | -1 | 0.015 | 0.005 | -0.999 | 0.014 | 0.005 |
| -1 | 0.016 | 0.006 | -1 | 0.017 | 0.005 | -0.999 | 0.013 | 0.005 |
| -0.999 | 0.015 | 0.006 | -1 | 0.015 | 0.006 | -0.998 | 0.013 | 0.004 |
| -0.999 | 0.016 | 0.006 | -0.999 | 0.014 | 0.006 | -0.998 | 0.013 | 0.004 |
| -0.998 | 0.015 | 0.006 | -0.999 | 0.013 | 0.005 | -0.999 | 0.011 | 0.003 |
| -0.999 | 0.013 | 0.006 | -0.999 | 0.013 | 0.006 | -0.998 | 0.011 | 0.004 |
| -0.999 | 0.013 | 0.005 | -0.999 | 0.013 | 0.005 | -0.998 | 0.011 | 0.004 |
| -0.999 | 0.011 | 0.006 | -0.999 | 0.013 | 0.005 | -0.998 | 0.011 | 0.004 |
| -0.999 | 0.013 | 0.006 | -0.999 | 0.013 | 0.005 | -0.998 | 0.012 | 0.005 |
| -0.999 | 0.014 | 0.005 | -0.999 | 0.012 | 0.005 | -0.999 | 0.013 | 0.004 |
| -0.999 | 0.015 | 0.006 | -0.998 | 0.012 | 0.006 | -0.999 | 0.015 | 0.005 |
| -0.998 | 0.016 | 0.005 | -0.999 | 0.014 | 0.007 | -0.999 | 0.015 | 0.005 |
| -0.997 | 0.015 | 0.004 | -0.998 | 0.014 | 0.006 | -1 | 0.015 | 0.004 |
| -0.997 | 0.014 | 0.004 | -0.998 | 0.015 | 0.006 | -0.999 | 0.014 | 0.004 |
| -0.998 | 0.013 | 0.004 | -0.998 | 0.014 | 0.005 | -1 | 0.012 | 0.003 |
| -0.998 | 0.012 | 0.004 | -0.998 | 0.013 | 0.005 | -0.999 | 0.012 | 0.003 |
| -0.999 | 0.013 | 0.005 | -0.998 | 0.013 | 0.005 | -0.998 | 0.01 | 0.004 |
| -0.997 | 0.012 | 0.005 | -0.998 | 0.011 | 0.006 | -0.998 | 0.011 | 0.003 |
| -0.998 | 0.013 | 0.006 | -0.998 | 0.013 | 0.006 | -0.998 | 0.013 | 0.004 |
| -0.997 | 0.014 | 0.006 | -0.998 | 0.013 | 0.006 | -0.999 | 0.013 | 0.003 |
| -0.998 | 0.014 | 0.005 | -0.999 | 0.014 | 0.006 | -0.999 | 0.016 | 0.003 |
| -0.999 | 0.015 | 0.005 | -0.998 | 0.014 | 0.006 | -0.999 | 0.015 | 0.003 |
| -0.998 | 0.014 | 0.004 | -0.998 | 0.014 | 0.007 | -0.999 | 0.015 | 0.003 |
| -0.998 | 0.014 | 0.004 | -0.998 | 0.015 | 0.007 | -0.999 | 0.013 | 0.004 |
| -0.998 | 0.013 | 0.004 | -0.998 | 0.014 | 0.006 | -0.999 | 0.012 | 0.005 |
| -0.997 | 0.012 | 0.004 | -0.998 | 0.014 | 0.006 | -1 | 0.013 | 0.006 |
| -0.998 | 0.012 | 0.004 | -0.997 | 0.013 | 0.005 | -1 | 0.012 | 0.007 |
| -0.999 | 0.011 | 0.003 | -0.998 | 0.012 | 0.005 | -0.999 | 0.012 | 0.006 |
| -0.999 | 0.013 | 0.003 | -0.997 | 0.012 | 0.006 | -0.999 | 0.012 | 0.006 |
| -1 | 0.014 | 0.003 | -0.998 | 0.011 | 0.005 | -0.999 | 0.012 | 0.006 |
| -0.999 | 0.014 | 0.004 | -0.998 | 0.013 | 0.006 | -0.998 | 0.012 | 0.005 |
| -0.998 | 0.015 | 0.005 | -0.998 | 0.012 | 0.005 | -0.998 | 0.012 | 0.005 |
| -0.997 | 0.014 | 0.005 | -0.999 | 0.014 | 0.005 | -0.997 | 0.013 | 0.004 |
| -0.997 | 0.014 | 0.006 | -0.999 | 0.015 | 0.005 | -0.997 | 0.012 | 0.005 |
| -0.997 | 0.014 | 0.005 | -0.999 | 0.013 | 0.005 | -0.998 | 0.012 | 0.006 |
| -0.998 | 0.014 | 0.006 | -0.998 | 0.014 | 0.005 | -0.998 | 0.014 | 0.005 |
| -0.998 | 0.014 | 0.006 | -0.998 | 0.011 | 0.005 | -1 | 0.012 | 0.006 |
| -0.997 | 0.013 | 0.005 | -0.998 | 0.011 | 0.004 | -0.999 | 0.013 | 0.006 |
| -0.998 | 0.012 | 0.006 | -0.997 | 0.012 | 0.004 | -0.999 | 0.013 | 0.005 |
| -0.998 | 0.011 | 0.005 | -0.998 | 0.012 | 0.003 | -0.999 | 0.012 | 0.005 |
| -0.999 | 0.011 | 0.004 | -0.998 | 0.014 | 0.003 | -0.998 | 0.014 | 0.004 |
| -0.999 | 0.013 | 0.004 | -0.999 | 0.012 | 0.004 | -0.998 | 0.013 | 0.004 |
| -0.999 | 0.014 | 0.004 | -1 | 0.013 | 0.004 | -0.999 | 0.014 | 0.003 |

## Sample of data set in Position 5 (cable)

| Acc. X | Acc. Y | Acc. Z | Acc. X | Acc. Y | Acc. Z | Acc. X | Acc. Y | Acc. Z |
|---|---|---|---|---|---|---|---|---|
| 0.015 | 1.029 | 0 | 0.014 | 1.027 | 0 | 0.015 | 1.027 | 0 |
| 0.015 | 1.027 | 0 | 0.014 | 1.028 | -0.001 | 0.015 | 1.026 | 0 |
| 0.015 | 1.026 | 0 | 0.014 | 1.028 | 0 | 0.015 | 1.026 | 0 |
| 0.015 | 1.027 | 0 | 0.015 | 1.029 | 0 | 0.015 | 1.027 | 0 |
| 0.015 | 1.026 | -0.002 | 0.015 | 1.03 | 0 | 0.015 | 1.027 | 0 |
| 0.015 | 1.028 | -0.002 | 0.015 | 1.03 | 0 | 0.015 | 1.028 | 0 |
| 0.016 | 1.029 | -0.001 | 0.015 | 1.029 | 0 | 0.015 | 1.028 | 0 |
| 0.015 | 1.028 | -0.001 | 0.015 | 1.029 | 0 | 0.015 | 1.028 | -0.001 |
| 0.015 | 1.029 | 0 | 0.014 | 1.028 | 0 | 0.016 | 1.027 | -0.001 |
| 0.015 | 1.029 | -0.001 | 0.014 | 1.028 | 0 | 0.016 | 1.027 | -0.001 |
| 0.014 | 1.029 | -0.002 | 0.015 | 1.028 | 0 | 0.016 | 1.026 | -0.002 |
| 0.014 | 1.029 | -0.002 | 0.014 | 1.028 | 0.001 | 0.016 | 1.026 | -0.001 |
| 0.014 | 1.025 | -0.003 | 0.014 | 1.028 | 0.001 | 0.015 | 1.027 | -0.002 |
| 0.014 | 1.024 | -0.002 | 0.012 | 1.028 | 0.001 | 0.015 | 1.026 | -0.001 |
| 0.015 | 1.022 | -0.002 | 0.013 | 1.027 | 0.001 | 0.015 | 1.027 | -0.001 |
| 0.015 | 1.022 | -0.002 | 0.014 | 1.028 | 0 | 0.015 | 1.028 | -0.002 |
| 0.015 | 1.026 | -0.002 | 0.016 | 1.027 | 0 | 0.015 | 1.028 | -0.002 |
| 0.014 | 1.026 | -0.002 | 0.017 | 1.027 | 0 | 0.014 | 1.029 | -0.003 |
| 0.013 | 1.028 | -0.002 | 0.016 | 1.028 | 0 | 0.014 | 1.03 | -0.002 |
| 0.013 | 1.028 | -0.002 | 0.016 | 1.027 | 0 | 0.014 | 1.028 | -0.002 |
| 0.013 | 1.028 | -0.002 | 0.013 | 1.028 | 0.001 | 0.015 | 1.027 | -0.001 |
| 0.014 | 1.028 | -0.001 | 0.013 | 1.028 | 0.001 | 0.015 | 1.026 | -0.001 |
| 0.014 | 1.029 | -0.002 | 0.013 | 1.028 | 0.002 | 0.014 | 1.026 | 0 |
| 0.014 | 1.029 | -0.003 | 0.013 | 1.029 | 0.001 | 0.014 | 1.026 | 0 |
| 0.015 | 1.028 | -0.002 | 0.014 | 1.029 | 0.001 | 0.014 | 1.027 | -0.001 |
| 0.014 | 1.028 | -0.002 | 0.015 | 1.029 | 0.001 | 0.014 | 1.027 | -0.001 |
| 0.014 | 1.026 | -0.001 | 0.016 | 1.029 | 0 | 0.014 | 1.027 | -0.001 |
| 0.014 | 1.026 | -0.001 | 0.016 | 1.028 | 0.001 | 0.014 | 1.027 | -0.001 |
| 0.014 | 1.027 | -0.002 | 0.016 | 1.027 | 0.001 | 0.014 | 1.028 | -0.001 |
| 0.014 | 1.028 | -0.002 | 0.017 | 1.027 | 0.001 | 0.014 | 1.029 | -0.001 |
| 0.015 | 1.028 | -0.002 | 0.016 | 1.027 | 0.002 | 0.015 | 1.029 | -0.001 |
| 0.015 | 1.028 | 0 | 0.016 | 1.026 | 0.001 | 0.015 | 1.028 | 0 |
| 0.015 | 1.027 | 0 | 0.016 | 1.026 | 0.001 | 0.014 | 1.028 | 0 |
| 0.015 | 1.026 | 0 | 0.015 | 1.026 | 0.001 | 0.015 | 1.027 | 0 |
| 0.015 | 1.026 | 0 | 0.015 | 1.027 | 0 | 0.014 | 1.027 | 0 |
| 0.016 | 1.027 | 0 | 0.015 | 1.027 | 0.001 | 0.015 | 1.027 | 0 |
| 0.016 | 1.027 | 0 | 0.014 | 1.027 | 0.001 | 0.015 | 1.027 | 0 |
| 0.016 | 1.027 | 0 | 0.015 | 1.027 | 0 | 0.015 | 1.028 | -0.001 |
| 0.016 | 1.027 | 0 | 0.014 | 1.027 | 0 | 0.015 | 1.028 | -0.001 |
| 0.015 | 1.027 | 0 | 0.014 | 1.027 | 0.001 | 0.015 | 1.029 | 0 |
| 0.014 | 1.027 | 0 | 0.015 | 1.027 | 0 | 0.016 | 1.03 | 0 |

| Acc. X | Acc. Y | Acc. Z | Acc. X | Acc. Y | Acc. Z | Acc. X | Acc. Y | Acc. Z |
|---|---|---|---|---|---|---|---|---|
| 0.017 | 1.029 | 0 | 0.015 | 1.028 | 0 | 0.014 | 1.028 | -0.001 |
| 0.016 | 1.03 | 0 | 0.015 | 1.028 | 0 | 0.015 | 1.028 | 0 |
| 0.016 | 1.029 | 0 | 0.015 | 1.028 | 0 | 0.015 | 1.028 | 0 |
| 0.015 | 1.028 | 0 | 0.014 | 1.028 | 0 | 0.015 | 1.028 | 0 |
| 0.014 | 1.027 | 0 | 0.013 | 1.028 | 0 | 0.015 | 1.028 | 0 |
| 0.014 | 1.026 | 0.001 | 0.013 | 1.028 | 0 | 0.014 | 1.028 | 0 |
| 0.013 | 1.026 | 0 | 0.013 | 1.028 | 0 | 0.014 | 1.027 | 0 |
| 0.014 | 1.026 | 0 | 0.013 | 1.027 | 0 | 0.014 | 1.027 | 0 |
| 0.014 | 1.027 | 0 | 0.014 | 1.027 | 0 | 0.013 | 1.027 | 0 |
| 0.014 | 1.027 | -0.001 | 0.014 | 1.027 | 0 | 0.014 | 1.027 | 0 |
| 0.014 | 1.027 | 0 | 0.014 | 1.027 | 0 | 0.014 | 1.028 | 0 |
| 0.014 | 1.028 | 0 | 0.015 | 1.028 | 0 | 0.014 | 1.028 | 0 |
| 0.015 | 1.029 | 0 | 0.014 | 1.029 | 0 | 0.015 | 1.028 | 0 |
| 0.015 | 1.028 | -0.001 | 0.015 | 1.029 | 0 | 0.015 | 1.028 | 0 |
| 0.016 | 1.028 | 0 | 0.015 | 1.028 | 0 | 0.015 | 1.028 | 0 |
| 0.015 | 1.028 | -0.001 | 0.014 | 1.028 | 0 | 0.015 | 1.028 | 0 |
| 0.014 | 1.027 | -0.001 | 0.014 | 1.027 | 0 | 0.015 | 1.028 | 0 |
| 0.013 | 1.028 | -0.001 | 0.013 | 1.027 | 0 | 0.015 | 1.028 | 0 |
| 0.013 | 1.028 | -0.002 | 0.013 | 1.028 | 0 | 0.015 | 1.028 | 0 |
| 0.014 | 1.028 | -0.001 | 0.014 | 1.028 | -0.001 | 0.014 | 1.028 | 0 |
| 0.015 | 1.029 | -0.001 | 0.014 | 1.028 | -0.001 | 0.014 | 1.028 | 0 |
| 0.014 | 1.029 | 0 | 0.014 | 1.028 | -0.001 | 0.015 | 1.027 | 0 |
| 0.015 | 1.029 | 0 | 0.014 | 1.028 | -0.001 | 0.015 | 1.026 | 0 |
| 0.015 | 1.028 | 0 | 0.014 | 1.028 | 0 | 0.015 | 1.026 | 0 |
| 0.014 | 1.028 | 0 | 0.014 | 1.028 | 0 | 0.015 | 1.027 | 0.001 |
| 0.015 | 1.027 | 0 | 0.015 | 1.028 | -0.001 | 0.013 | 1.027 | 0.001 |
| 0.014 | 1.027 | 0 | 0.015 | 1.028 | 0 | 0.013 | 1.028 | 0 |
| 0.014 | 1.028 | 0 | 0.015 | 1.028 | 0 | 0.013 | 1.029 | 0 |
| 0.014 | 1.027 | -0.001 | 0.015 | 1.028 | 0 | 0.014 | 1.03 | 0 |
| 0.015 | 1.028 | -0.001 | 0.016 | 1.028 | 0 | 0.015 | 1.03 | 0 |
| 0.015 | 1.028 | -0.002 | 0.016 | 1.028 | 0 | 0.014 | 1.029 | 0 |
| 0.015 | 1.028 | -0.002 | 0.016 | 1.027 | 0.001 | 0.014 | 1.028 | 0 |
| 0.015 | 1.027 | -0.001 | 0.016 | 1.028 | 0.001 | 0.014 | 1.028 | 0 |
| 0.015 | 1.027 | -0.002 | 0.015 | 1.028 | 0 | 0.014 | 1.028 | 0 |
| 0.014 | 1.027 | -0.002 | 0.015 | 1.027 | 0 | 0.014 | 1.027 | 0.001 |
| 0.014 | 1.027 | -0.001 | 0.014 | 1.028 | 0 | 0.014 | 1.027 | 0.001 |
| 0.014 | 1.029 | -0.001 | 0.014 | 1.028 | 0 | 0.015 | 1.028 | 0 |
| 0.014 | 1.029 | 0 | 0.014 | 1.028 | 0 | 0.014 | 1.028 | 0.001 |
| 0.014 | 1.028 | 0 | 0.014 | 1.029 | 0 | 0.014 | 1.028 | 0 |
| 0.015 | 1.028 | 0 | 0.015 | 1.029 | 0 | 0.015 | 1.028 | 0 |
| 0.016 | 1.027 | 0 | 0.015 | 1.029 | 0 | 0.015 | 1.028 | 0 |
| 0.015 | 1.027 | 0 | 0.015 | 1.028 | 0 | 0.015 | 1.028 | 0 |
| 0.015 | 1.028 | 0 | 0.014 | 1.028 | 0 | 0.015 | 1.028 | 0 |

## Sample of data set in Position 6 (cable)

| Acc. X | Acc. Y | Acc. Z | Acc. X | Acc. Y | Acc. Z | Acc. X | Acc. Y | Acc. Z |
|---|---|---|---|---|---|---|---|---|
| -0.011 | -1.019 | 0.01 | -0.01 | -1.018 | 0.008 | -0.012 | -1.018 | 0.008 |
| -0.009 | -1.02 | 0.01 | -0.009 | -1.019 | 0.008 | -0.011 | -1.017 | 0.007 |
| -0.01 | -1.019 | 0.009 | -0.01 | -1.018 | 0.008 | -0.012 | -1.017 | 0.008 |
| -0.01 | -1.019 | 0.008 | -0.01 | -1.017 | 0.008 | -0.011 | -1.018 | 0.008 |
| -0.01 | -1.019 | 0.007 | -0.011 | -1.018 | 0.008 | -0.011 | -1.018 | 0.008 |
| -0.011 | -1.018 | 0.007 | -0.011 | -1.018 | 0.008 | -0.01 | -1.018 | 0.009 |
| -0.012 | -1.017 | 0.008 | -0.011 | -1.02 | 0.009 | -0.01 | -1.018 | 0.008 |
| -0.011 | -1.016 | 0.008 | -0.012 | -1.02 | 0.009 | -0.011 | -1.018 | 0.009 |
| -0.012 | -1.016 | 0.008 | -0.011 | -1.021 | 0.009 | -0.011 | -1.018 | 0.008 |
| -0.012 | -1.016 | 0.008 | -0.01 | -1.021 | 0.008 | -0.012 | -1.018 | 0.008 |
| -0.012 | -1.018 | 0.008 | -0.011 | -1.02 | 0.008 | -0.012 | -1.018 | 0.009 |
| -0.013 | -1.02 | 0.007 | -0.01 | -1.02 | 0.009 | -0.012 | -1.018 | 0.009 |
| -0.011 | -1.02 | 0.009 | -0.01 | -1.019 | 0.009 | -0.011 | -1.018 | 0.009 |
| -0.011 | -1.02 | 0.008 | -0.01 | -1.019 | 0.01 | -0.01 | -1.017 | 0.008 |
| -0.011 | -1.019 | 0.008 | -0.009 | -1.019 | 0.009 | -0.011 | -1.017 | 0.008 |
| -0.01 | -1.017 | 0.009 | -0.009 | -1.019 | 0.008 | -0.01 | -1.018 | 0.008 |
| -0.012 | -1.018 | 0.008 | -0.011 | -1.019 | 0.007 | -0.01 | -1.019 | 0.008 |
| -0.013 | -1.018 | 0.008 | -0.011 | -1.019 | 0.006 | -0.01 | -1.019 | 0.008 |
| -0.013 | -1.018 | 0.008 | -0.012 | -1.021 | 0.006 | -0.01 | -1.019 | 0.009 |
| -0.013 | -1.018 | 0.008 | -0.013 | -1.019 | 0.006 | -0.01 | -1.019 | 0.009 |
| -0.012 | -1.019 | 0.009 | -0.011 | -1.019 | 0.007 | -0.01 | -1.018 | 0.009 |
| -0.012 | -1.019 | 0.01 | -0.012 | -1.019 | 0.007 | -0.011 | -1.019 | 0.008 |
| -0.012 | -1.019 | 0.01 | -0.01 | -1.018 | 0.008 | -0.011 | -1.018 | 0.008 |
| -0.012 | -1.02 | 0.011 | -0.01 | -1.019 | 0.008 | -0.012 | -1.019 | 0.009 |
| -0.012 | -1.018 | 0.01 | -0.011 | -1.019 | 0.008 | -0.013 | -1.019 | 0.008 |
| -0.012 | -1.018 | 0.009 | -0.01 | -1.018 | 0.008 | -0.012 | -1.019 | 0.009 |
| -0.01 | -1.017 | 0.009 | -0.012 | -1.018 | 0.008 | -0.012 | -1.019 | 0.008 |
| -0.01 | -1.017 | 0.008 | -0.012 | -1.018 | 0.008 | -0.011 | -1.018 | 0.007 |
| -0.01 | -1.018 | 0.009 | -0.012 | -1.018 | 0.009 | -0.011 | -1.019 | 0.009 |
| -0.01 | -1.018 | 0.01 | -0.012 | -1.018 | 0.009 | -0.01 | -1.018 | 0.008 |
| -0.011 | -1.019 | 0.009 | -0.011 | -1.019 | 0.009 | -0.01 | -1.019 | 0.009 |
| -0.011 | -1.019 | 0.009 | -0.01 | -1.018 | 0.01 | -0.011 | -1.018 | 0.01 |
| -0.011 | -1.019 | 0.008 | -0.009 | -1.018 | 0.009 | -0.011 | -1.019 | 0.009 |
| -0.012 | -1.019 | 0.007 | -0.01 | -1.018 | 0.011 | -0.012 | -1.019 | 0.008 |
| -0.011 | -1.019 | 0.008 | -0.01 | -1.017 | 0.011 | -0.012 | -1.018 | 0.008 |
| -0.011 | -1.019 | 0.007 | -0.01 | -1.019 | 0.011 | -0.012 | -1.019 | 0.008 |
| -0.01 | -1.02 | 0.008 | -0.01 | -1.018 | 0.01 | -0.012 | -1.019 | 0.008 |
| -0.01 | -1.02 | 0.008 | -0.009 | -1.019 | 0.008 | -0.012 | -1.019 | 0.009 |
| -0.01 | -1.02 | 0.008 | -0.011 | -1.02 | 0.009 | -0.012 | -1.02 | 0.009 |
| -0.01 | -1.019 | 0.008 | -0.012 | -1.02 | 0.009 | -0.011 | -1.019 | 0.008 |
| -0.01 | -1.019 | 0.008 | -0.012 | -1.019 | 0.008 | -0.011 | -1.018 | 0.008 |

| Acc. X | Acc. Y | Acc. Z | Acc. X | Acc. Y | Acc. Z | Acc. X | Acc. Y | Acc. Z |
|---|---|---|---|---|---|---|---|---|
| -0.011 | -1.018 | 0.008 | -0.012 | -1.018 | 0.008 | -0.013 | -1.018 | 0.008 |
| -0.011 | -1.018 | 0.007 | -0.013 | -1.018 | 0.008 | -0.013 | -1.018 | 0.008 |
| -0.012 | -1.018 | 0.008 | -0.011 | -1.019 | 0.009 | -0.013 | -1.018 | 0.009 |
| -0.012 | -1.019 | 0.008 | -0.012 | -1.019 | 0.009 | -0.013 | -1.018 | 0.009 |
| -0.011 | -1.019 | 0.008 | -0.011 | -1.018 | 0.009 | -0.013 | -1.018 | 0.008 |
| -0.011 | -1.018 | 0.008 | -0.01 | -1.018 | 0.01 | -0.013 | -1.018 | 0.009 |
| -0.011 | -1.019 | 0.008 | -0.011 | -1.018 | 0.009 | -0.012 | -1.019 | 0.008 |
| -0.012 | -1.018 | 0.007 | -0.01 | -1.018 | 0.008 | -0.011 | -1.019 | 0.009 |
| -0.012 | -1.018 | 0.007 | -0.011 | -1.018 | 0.008 | -0.011 | -1.02 | 0.009 |
| -0.013 | -1.018 | 0.007 | -0.011 | -1.018 | 0.007 | -0.011 | -1.019 | 0.009 |
| -0.013 | -1.018 | 0.007 | -0.012 | -1.017 | 0.007 | -0.011 | -1.019 | 0.009 |
| -0.011 | -1.018 | 0.007 | -0.012 | -1.018 | 0.007 | -0.011 | -1.02 | 0.009 |
| -0.012 | -1.018 | 0.007 | -0.012 | -1.019 | 0.007 | -0.012 | -1.02 | 0.009 |
| -0.011 | -1.019 | 0.007 | -0.013 | -1.019 | 0.007 | -0.011 | -1.02 | 0.01 |
| -0.011 | -1.019 | 0.007 | -0.012 | -1.021 | 0.006 | -0.012 | -1.02 | 0.009 |
| -0.012 | -1.019 | 0.008 | -0.012 | -1.02 | 0.006 | -0.012 | -1.02 | 0.008 |
| -0.012 | -1.019 | 0.008 | -0.01 | -1.018 | 0.006 | -0.011 | -1.02 | 0.009 |
| -0.013 | -1.019 | 0.008 | -0.009 | -1.019 | 0.007 | -0.01 | -1.021 | 0.009 |
| -0.012 | -1.019 | 0.008 | -0.008 | -1.018 | 0.008 | -0.009 | -1.02 | 0.009 |
| -0.012 | -1.019 | 0.007 | -0.01 | -1.019 | 0.008 | -0.009 | -1.019 | 0.009 |
| -0.013 | -1.018 | 0.006 | -0.01 | -1.02 | 0.008 | -0.009 | -1.019 | 0.007 |
| -0.012 | -1.017 | 0.007 | -0.011 | -1.019 | 0.008 | -0.009 | -1.019 | 0.007 |
| -0.012 | -1.017 | 0.007 | -0.011 | -1.019 | 0.008 | -0.011 | -1.019 | 0.007 |
| -0.011 | -1.019 | 0.008 | -0.011 | -1.018 | 0.007 | -0.011 | -1.019 | 0.007 |
| -0.011 | -1.019 | 0.008 | -0.011 | -1.017 | 0.007 | -0.011 | -1.019 | 0.008 |
| -0.01 | -1.02 | 0.009 | -0.011 | -1.017 | 0.008 | -0.011 | -1.018 | 0.007 |
| -0.01 | -1.02 | 0.009 | -0.012 | -1.017 | 0.007 | -0.011 | -1.018 | 0.008 |
| -0.011 | -1.018 | 0.01 | -0.01 | -1.019 | 0.008 | -0.011 | -1.019 | 0.008 |
| -0.011 | -1.018 | 0.01 | -0.011 | -1.019 | 0.008 | -0.011 | -1.018 | 0.008 |
| -0.012 | -1.018 | 0.01 | -0.011 | -1.02 | 0.008 | -0.011 | -1.018 | 0.009 |
| -0.012 | -1.017 | 0.009 | -0.011 | -1.019 | 0.008 | -0.011 | -1.018 | 0.008 |
| -0.011 | -1.017 | 0.009 | -0.012 | -1.018 | 0.009 | -0.01 | -1.017 | 0.009 |
| -0.012 | -1.018 | 0.008 | -0.012 | -1.018 | 0.01 | -0.011 | -1.017 | 0.009 |
| -0.011 | -1.018 | 0.007 | -0.013 | -1.018 | 0.01 | -0.01 | -1.018 | 0.009 |
| -0.011 | -1.017 | 0.007 | -0.012 | -1.019 | 0.01 | -0.011 | -1.018 | 0.009 |
| -0.01 | -1.018 | 0.007 | -0.013 | -1.02 | 0.008 | -0.012 | -1.019 | 0.009 |
| -0.01 | -1.017 | 0.007 | -0.012 | -1.02 | 0.008 | -0.012 | -1.019 | 0.007 |
| -0.01 | -1.017 | 0.007 | -0.011 | -1.02 | 0.007 | -0.013 | -1.019 | 0.007 |
| -0.009 | -1.018 | 0.008 | -0.011 | -1.021 | 0.008 | -0.012 | -1.02 | 0.007 |
| -0.011 | -1.018 | 0.008 | -0.009 | -1.019 | 0.008 | -0.011 | -1.018 | 0.007 |
| -0.01 | -1.018 | 0.008 | -0.01 | -1.019 | 0.007 | -0.01 | -1.018 | 0.009 |
| -0.011 | -1.018 | 0.008 | -0.011 | -1.019 | 0.007 | -0.01 | -1.018 | 0.01 |
| -0.012 | -1.018 | 0.008 | -0.012 | -1.017 | 0.007 | -0.011 | -1.018 | 0.01 |

## Sample of data set in Position 1 (wireless)

| Acc. X | Acc. Y | Acc. Z | Acc. X | Acc. Y | Acc. Z | Acc. X | Acc. Y | Acc. Z |
|---|---|---|---|---|---|---|---|---|
| 0.003 | 0.004 | 1.029 | 0.003 | 0.006 | 1.029 | 0.003 | 0.007 | 1.031 |
| 0.003 | 0.004 | 1.03 | 0.002 | 0.006 | 1.029 | 0.003 | 0.007 | 1.031 |
| 0.002 | 0.005 | 1.029 | 0.003 | 0.006 | 1.031 | 0.002 | 0.006 | 1.032 |
| 0.003 | 0.004 | 1.029 | 0.002 | 0.006 | 1.03 | 0.004 | 0.006 | 1.031 |
| 0.003 | 0.004 | 1.03 | 0.002 | 0.006 | 1.031 | 0.003 | 0.005 | 1.03 |
| 0.003 | 0.005 | 1.03 | 0.002 | 0.005 | 1.031 | 0.003 | 0.005 | 1.029 |
| 0.003 | 0.005 | 1.03 | 0.002 | 0.005 | 1.029 | 0.004 | 0.005 | 1.027 |
| 0.002 | 0.006 | 1.032 | 0.002 | 0.005 | 1.03 | 0.002 | 0.004 | 1.027 |
| 0.002 | 0.007 | 1.032 | 0.002 | 0.006 | 1.03 | 0.002 | 0.004 | 1.027 |
| 0.002 | 0.007 | 1.032 | 0.002 | 0.007 | 1.03 | 0.002 | 0.004 | 1.026 |
| 0.002 | 0.005 | 1.03 | 0.002 | 0.007 | 1.031 | 0.002 | 0.004 | 1.027 |
| 0.003 | 0.005 | 1.028 | 0.003 | 0.007 | 1.03 | 0.002 | 0.006 | 1.027 |
| 0.004 | 0.004 | 1.027 | 0.003 | 0.007 | 1.03 | 0.002 | 0.006 | 1.026 |
| 0.004 | 0.003 | 1.027 | 0.003 | 0.007 | 1.029 | 0.002 | 0.007 | 1.026 |
| 0.003 | 0.004 | 1.028 | 0.002 | 0.006 | 1.029 | 0.002 | 0.008 | 1.026 |
| 0.002 | 0.005 | 1.029 | 0.002 | 0.006 | 1.029 | 0.002 | 0.007 | 1.026 |
| 0.001 | 0.005 | 1.029 | 0.002 | 0.005 | 1.031 | 0.002 | 0.007 | 1.027 |
| 0.001 | 0.006 | 1.029 | 0.001 | 0.006 | 1.031 | 0.002 | 0.006 | 1.028 |
| 0.001 | 0.006 | 1.029 | 0.001 | 0.006 | 1.031 | 0.002 | 0.005 | 1.029 |
| 0.002 | 0.006 | 1.028 | 0.001 | 0.005 | 1.031 | 0.001 | 0.005 | 1.028 |
| 0.002 | 0.005 | 1.028 | 0.001 | 0.005 | 1.03 | 0.001 | 0.005 | 1.028 |
| 0.002 | 0.005 | 1.028 | 0.002 | 0.005 | 1.03 | 0.002 | 0.004 | 1.028 |
| 0.002 | 0.005 | 1.028 | 0.002 | 0.005 | 1.03 | 0.002 | 0.004 | 1.027 |
| 0.002 | 0.005 | 1.028 | 0.003 | 0.007 | 1.031 | 0.003 | 0.004 | 1.027 |
| 0.002 | 0.005 | 1.028 | 0.003 | 0.006 | 1.03 | 0.003 | 0.003 | 1.028 |
| 0.003 | 0.006 | 1.029 | 0.003 | 0.006 | 1.031 | 0.002 | 0.004 | 1.028 |
| 0.003 | 0.005 | 1.029 | 0.002 | 0.007 | 1.029 | 0.003 | 0.005 | 1.028 |
| 0.003 | 0.006 | 1.029 | 0.002 | 0.006 | 1.029 | 0.002 | 0.005 | 1.027 |
| 0.002 | 0.006 | 1.029 | 0.002 | 0.006 | 1.03 | 0.003 | 0.006 | 1.025 |
| 0.003 | 0.005 | 1.029 | 0.003 | 0.007 | 1.029 | 0.003 | 0.006 | 1.025 |
| 0.001 | 0.007 | 1.028 | 0.002 | 0.007 | 1.029 | 0.002 | 0.007 | 1.025 |
| 0.002 | 0.006 | 1.028 | 0.002 | 0.008 | 1.03 | 0.001 | 0.007 | 1.026 |
| 0.002 | 0.006 | 1.028 | 0.002 | 0.008 | 1.03 | 0 | 0.007 | 1.027 |
| 0.001 | 0.006 | 1.028 | 0.001 | 0.007 | 1.032 | 0 | 0.006 | 1.027 |
| 0.003 | 0.006 | 1.028 | 0.002 | 0.006 | 1.032 | 0.002 | 0.006 | 1.027 |
| 0.002 | 0.006 | 1.028 | 0.002 | 0.006 | 1.032 | 0.003 | 0.006 | 1.027 |
| 0.003 | 0.006 | 1.028 | 0.002 | 0.005 | 1.032 | 0.003 | 0.007 | 1.027 |
| 0.003 | 0.006 | 1.028 | 0.003 | 0.006 | 1.032 | 0.002 | 0.007 | 1.027 |
| 0.003 | 0.005 | 1.028 | 0.003 | 0.005 | 1.032 | 0.001 | 0.006 | 1.027 |
| 0.003 | 0.005 | 1.028 | 0.003 | 0.006 | 1.032 | 0.001 | 0.006 | 1.027 |
| 0.002 | 0.006 | 1.029 | 0.003 | 0.007 | 1.032 | 0.001 | 0.006 | 1.026 |

| Acc. X | Acc. Y | Acc. Z | Acc. X | Acc. Y | Acc. Z | Acc. X | Acc. Y | Acc. Z |
|---|---|---|---|---|---|---|---|---|
| 0.003 | 0.006 | 1.026 | 0.003 | 0.005 | 1.026 | 0.003 | 0.006 | 1.026 |
| 0.003 | 0.006 | 1.026 | 0.004 | 0.005 | 1.027 | 0.002 | 0.005 | 1.027 |
| 0.003 | 0.007 | 1.027 | 0.003 | 0.005 | 1.026 | 0.002 | 0.005 | 1.027 |
| 0.004 | 0.006 | 1.027 | 0.003 | 0.005 | 1.025 | 0.003 | 0.005 | 1.027 |
| 0.003 | 0.005 | 1.027 | 0.002 | 0.005 | 1.025 | 0.002 | 0.005 | 1.027 |
| 0.002 | 0.005 | 1.028 | 0.001 | 0.005 | 1.025 | 0.002 | 0.005 | 1.027 |
| 0.002 | 0.005 | 1.027 | 0.003 | 0.005 | 1.026 | 0.002 | 0.005 | 1.028 |
| 0.002 | 0.006 | 1.027 | 0.002 | 0.006 | 1.026 | 0.001 | 0.006 | 1.027 |
| 0.001 | 0.006 | 1.027 | 0.003 | 0.005 | 1.026 | 0.002 | 0.006 | 1.028 |
| 0.002 | 0.006 | 1.027 | 0.003 | 0.006 | 1.027 | 0.002 | 0.006 | 1.027 |
| 0.002 | 0.006 | 1.027 | 0.003 | 0.006 | 1.026 | 0.003 | 0.006 | 1.026 |
| 0.003 | 0.005 | 1.027 | 0.002 | 0.006 | 1.026 | 0.003 | 0.006 | 1.026 |
| 0.003 | 0.005 | 1.028 | 0.002 | 0.007 | 1.026 | 0.003 | 0.007 | 1.025 |
| 0.002 | 0.005 | 1.029 | 0 | 0.006 | 1.025 | 0.003 | 0.006 | 1.024 |
| 0.003 | 0.006 | 1.03 | 0 | 0.006 | 1.024 | 0.002 | 0.006 | 1.024 |
| 0.002 | 0.006 | 1.03 | 0.001 | 0.006 | 1.024 | 0.002 | 0.005 | 1.024 |
| 0.002 | 0.006 | 1.029 | 0.002 | 0.005 | 1.024 | 0.001 | 0.005 | 1.025 |
| 0.003 | 0.006 | 1.029 | 0.003 | 0.005 | 1.025 | 0.002 | 0.006 | 1.025 |
| 0.002 | 0.006 | 1.028 | 0.003 | 0.005 | 1.026 | 0.002 | 0.006 | 1.026 |
| 0.003 | 0.007 | 1.029 | 0.003 | 0.005 | 1.026 | 0.003 | 0.006 | 1.026 |
| 0.003 | 0.007 | 1.028 | 0.003 | 0.005 | 1.027 | 0.002 | 0.006 | 1.026 |
| 0.002 | 0.007 | 1.027 | 0.002 | 0.005 | 1.026 | 0.002 | 0.005 | 1.026 |
| 0.003 | 0.006 | 1.027 | 0.002 | 0.006 | 1.026 | 0.001 | 0.005 | 1.026 |
| 0.002 | 0.005 | 1.027 | 0.001 | 0.006 | 1.026 | 0.001 | 0.005 | 1.027 |
| 0.002 | 0.005 | 1.026 | 0.001 | 0.007 | 1.025 | 0.002 | 0.006 | 1.028 |
| 0.002 | 0.004 | 1.025 | 0.002 | 0.006 | 1.025 | 0.002 | 0.007 | 1.028 |
| 0.002 | 0.005 | 1.025 | 0.002 | 0.006 | 1.026 | 0.003 | 0.007 | 1.027 |
| 0.002 | 0.005 | 1.025 | 0.002 | 0.006 | 1.026 | 0.003 | 0.008 | 1.027 |
| 0.003 | 0.004 | 1.026 | 0.002 | 0.006 | 1.026 | 0.003 | 0.007 | 1.025 |
| 0.004 | 0.005 | 1.026 | 0.002 | 0.006 | 1.025 | 0.003 | 0.006 | 1.025 |
| 0.004 | 0.006 | 1.027 | 0.002 | 0.005 | 1.024 | 0.004 | 0.005 | 1.025 |
| 0.004 | 0.006 | 1.026 | 0.003 | 0.005 | 1.024 | 0.003 | 0.005 | 1.025 |
| 0.003 | 0.006 | 1.026 | 0.003 | 0.005 | 1.023 | 0.003 | 0.005 | 1.025 |
| 0.003 | 0.005 | 1.025 | 0.004 | 0.005 | 1.024 | 0.003 | 0.004 | 1.026 |
| 0.003 | 0.005 | 1.024 | 0.004 | 0.005 | 1.024 | 0.002 | 0.005 | 1.027 |
| 0.003 | 0.005 | 1.025 | 0.004 | 0.005 | 1.022 | 0.003 | 0.005 | 1.027 |
| 0.003 | 0.006 | 1.025 | 0.003 | 0.005 | 1.024 | 0.002 | 0.005 | 1.028 |
| 0.003 | 0.006 | 1.026 | 0.003 | 0.005 | 1.024 | 0.003 | 0.005 | 1.027 |
| 0.003 | 0.006 | 1.028 | 0.003 | 0.005 | 1.023 | 0.003 | 0.005 | 1.027 |
| 0.002 | 0.005 | 1.026 | 0.002 | 0.005 | 1.023 | 0.002 | 0.005 | 1.026 |
| 0.003 | 0.005 | 1.025 | 0.003 | 0.005 | 1.023 | 0.002 | 0.005 | 1.026 |
| 0.002 | 0.004 | 1.025 | 0.003 | 0.006 | 1.024 | 0.001 | 0.006 | 1.025 |
| 0.003 | 0.004 | 1.025 | 0.002 | 0.005 | 1.026 | 0.001 | 0.006 | 1.026 |

## Sample of data set in Position 2 (wireless)

| Acc. X | Acc. Y | Acc. Z | Acc. X | Acc. Y | Acc. Z | Acc. X | Acc. Y | Acc. Z |
|---|---|---|---|---|---|---|---|---|
| 0.001 | 0.007 | -1.023 | 0 | 0.007 | -1.021 | 0 | 0.007 | -1.021 |
| 0.001 | 0.007 | -1.023 | 0 | 0.007 | -1.022 | 0 | 0.008 | -1.023 |
| 0 | 0.007 | -1.023 | 0 | 0.008 | -1.022 | 0 | 0.008 | -1.022 |
| 0 | 0.007 | -1.023 | 0 | 0.007 | -1.021 | 0 | 0.008 | -1.022 |
| 0 | 0.008 | -1.021 | 0 | 0.008 | -1.021 | 0 | 0.007 | -1.023 |
| 0 | 0.007 | -1.022 | 0 | 0.008 | -1.021 | 0 | 0.008 | -1.023 |
| 0 | 0.007 | -1.021 | 0 | 0.008 | -1.021 | 0 | 0.009 | -1.023 |
| 0.001 | 0.008 | -1.021 | 0 | 0.008 | -1.022 | 0 | 0.009 | -1.024 |
| 0 | 0.007 | -1.024 | 0 | 0.008 | -1.022 | 0 | 0.01 | -1.023 |
| 0 | 0.008 | -1.023 | 0 | 0.008 | -1.022 | 0 | 0.009 | -1.022 |
| 0 | 0.008 | -1.023 | 0 | 0.008 | -1.023 | 0 | 0.008 | -1.023 |
| 0 | 0.008 | -1.024 | 0 | 0.008 | -1.022 | 0.001 | 0.008 | -1.022 |
| 0 | 0.008 | -1.024 | 0 | 0.008 | -1.021 | 0 | 0.007 | -1.021 |
| 0 | 0.008 | -1.024 | 0 | 0.008 | -1.023 | 0 | 0.007 | -1.021 |
| -0.001 | 0.007 | -1.023 | 0 | 0.008 | -1.023 | 0 | 0.007 | -1.021 |
| 0 | 0.007 | -1.024 | 0 | 0.008 | -1.023 | 0 | 0.007 | -1.021 |
| 0 | 0.008 | -1.024 | 0 | 0.009 | -1.023 | 0 | 0.008 | -1.021 |
| 0 | 0.008 | -1.023 | 0 | 0.01 | -1.022 | 0 | 0.007 | -1.021 |
| 0 | 0.008 | -1.023 | 0 | 0.01 | -1.022 | 0 | 0.008 | -1.021 |
| 0 | 0.008 | -1.022 | 0 | 0.009 | -1.023 | 0 | 0.007 | -1.022 |
| 0 | 0.007 | -1.022 | 0 | 0.009 | -1.022 | 0 | 0.007 | -1.022 |
| 0 | 0.007 | -1.023 | 0 | 0.008 | -1.022 | 0 | 0.006 | -1.024 |
| 0 | 0.008 | -1.022 | 0 | 0.008 | -1.022 | 0 | 0.007 | -1.023 |
| 0 | 0.009 | -1.022 | 0 | 0.008 | -1.021 | 0 | 0.008 | -1.022 |
| 0 | 0.01 | -1.023 | 0 | 0.008 | -1.022 | 0 | 0.007 | -1.022 |
| 0 | 0.009 | -1.023 | 0 | 0.007 | -1.021 | 0 | 0.008 | -1.021 |
| 0 | 0.008 | -1.023 | 0.001 | 0.008 | -1.022 | -0.001 | 0.007 | -1.021 |
| 0 | 0.008 | -1.023 | 0 | 0.008 | -1.022 | -0.001 | 0.007 | -1.022 |
| 0 | 0.008 | -1.022 | 0.001 | 0.007 | -1.022 | -0.001 | 0.007 | -1.021 |
| 0 | 0.007 | -1.021 | 0 | 0.007 | -1.022 | 0 | 0.007 | -1.021 |
| 0 | 0.007 | -1.023 | 0 | 0.007 | -1.021 | 0 | 0.008 | -1.022 |
| 0 | 0.007 | -1.023 | 0 | 0.007 | -1.022 | 0 | 0.007 | -1.021 |
| 0 | 0.008 | -1.022 | 0 | 0.008 | -1.021 | -0.001 | 0.008 | -1.022 |
| 0 | 0.008 | -1.023 | 0 | 0.008 | -1.021 | -0.001 | 0.008 | -1.022 |
| 0 | 0.009 | -1.022 | 0 | 0.008 | -1.021 | -0.001 | 0.008 | -1.021 |
| 0 | 0.009 | -1.022 | 0 | 0.008 | -1.021 | 0 | 0.008 | -1.022 |
| 0 | 0.009 | -1.022 | 0 | 0.007 | -1.022 | 0 | 0.008 | -1.022 |
| 0 | 0.008 | -1.022 | 0 | 0.008 | -1.022 | 0 | 0.008 | -1.021 |
| 0 | 0.007 | -1.021 | 0 | 0.007 | -1.022 | 0 | 0.008 | -1.022 |
| 0 | 0.007 | -1.021 | 0 | 0.007 | -1.022 | 0 | 0.007 | -1.022 |
| 0 | 0.006 | -1.021 | 0 | 0.007 | -1.022 | 0 | 0.007 | -1.022 |

| Acc. X | Acc. Y | Acc. Z | Acc. X | Acc. Y | Acc. Z | Acc. X | Acc. Y | Acc. Z |
|---|---|---|---|---|---|---|---|---|
| 0 | 0.007 | -1.022 | 0 | 0.006 | -1.022 | -0.001 | 0.008 | -1.022 |
| 0.001 | 0.007 | -1.022 | 0 | 0.006 | -1.023 | 0 | 0.008 | -1.022 |
| 0 | 0.007 | -1.022 | 0 | 0.006 | -1.022 | 0 | 0.009 | -1.022 |
| 0 | 0.007 | -1.021 | 0.001 | 0.007 | -1.022 | 0 | 0.008 | -1.022 |
| 0 | 0.008 | -1.021 | 0 | 0.007 | -1.021 | 0 | 0.008 | -1.021 |
| -0.001 | 0.008 | -1.021 | 0.001 | 0.008 | -1.021 | 0 | 0.008 | -1.021 |
| 0 | 0.008 | -1.021 | 0 | 0.008 | -1.021 | 0 | 0.007 | -1.02 |
| 0 | 0.008 | -1.021 | 0 | 0.009 | -1.021 | 0 | 0.007 | -1.02 |
| 0 | 0.008 | -1.021 | 0 | 0.009 | -1.021 | 0 | 0.007 | -1.021 |
| 0.001 | 0.008 | -1.021 | 0 | 0.008 | -1.021 | -0.001 | 0.008 | -1.021 |
| 0 | 0.008 | -1.021 | 0 | 0.008 | -1.021 | 0 | 0.007 | -1.022 |
| 0 | 0.009 | -1.021 | 0 | 0.008 | -1.021 | 0 | 0.008 | -1.022 |
| 0 | 0.009 | -1.02 | 0 | 0.008 | -1.021 | -0.001 | 0.008 | -1.021 |
| 0 | 0.009 | -1.021 | 0 | 0.008 | -1.021 | 0 | 0.007 | -1.022 |
| 0 | 0.009 | -1.02 | 0 | 0.008 | -1.021 | 0 | 0.008 | -1.021 |
| 0 | 0.008 | -1.021 | -0.001 | 0.007 | -1.02 | 0 | 0.007 | -1.022 |
| 0 | 0.008 | -1.021 | -0.001 | 0.007 | -1.02 | 0 | 0.007 | -1.022 |
| 0 | 0.008 | -1.021 | 0 | 0.008 | -1.02 | 0 | 0.007 | -1.022 |
| 0 | 0.008 | -1.021 | 0 | 0.007 | -1.02 | 0 | 0.008 | -1.021 |
| 0 | 0.008 | -1.021 | 0 | 0.007 | -1.02 | 0 | 0.008 | -1.021 |
| 0 | 0.008 | -1.021 | 0 | 0.008 | -1.02 | 0 | 0.009 | -1.021 |
| 0 | 0.008 | -1.02 | 0 | 0.007 | -1.02 | 0 | 0.009 | -1.021 |
| 0 | 0.008 | -1.02 | 0 | 0.007 | -1.02 | 0 | 0.008 | -1.021 |
| 0 | 0.008 | -1.021 | 0 | 0.007 | -1.02 | 0 | 0.008 | -1.021 |
| -0.001 | 0.009 | -1.023 | 0 | 0.007 | -1.021 | 0 | 0.008 | -1.021 |
| -0.001 | 0.009 | -1.023 | 0 | 0.007 | -1.022 | 0 | 0.007 | -1.021 |
| -0.001 | 0.008 | -1.024 | 0 | 0.007 | -1.022 | 0 | 0.007 | -1.022 |
| 0 | 0.008 | -1.024 | -0.001 | 0.007 | -1.022 | 0 | 0.007 | -1.022 |
| 0 | 0.007 | -1.023 | -0.001 | 0.006 | -1.022 | 0 | 0.007 | -1.023 |
| 0 | 0.008 | -1.023 | -0.001 | 0.007 | -1.021 | -0.001 | 0.007 | -1.024 |
| 0 | 0.008 | -1.022 | -0.001 | 0.007 | -1.021 | -0.001 | 0.007 | -1.023 |
| 0 | 0.008 | -1.022 | 0 | 0.008 | -1.02 | -0.001 | 0.007 | -1.023 |
| 0 | 0.008 | -1.02 | 0 | 0.008 | -1.02 | -0.001 | 0.008 | -1.023 |
| -0.001 | 0.007 | -1.022 | 0 | 0.008 | -1.021 | 0 | 0.008 | -1.023 |
| 0 | 0.008 | -1.022 | 0 | 0.008 | -1.021 | 0 | 0.009 | -1.025 |
| 0 | 0.008 | -1.022 | 0 | 0.008 | -1.021 | 0 | 0.009 | -1.025 |
| 0 | 0.008 | -1.023 | 0 | 0.008 | -1.021 | 0 | 0.008 | -1.025 |
| 0 | 0.008 | -1.022 | 0 | 0.008 | -1.022 | 0 | 0.009 | -1.023 |
| 0 | 0.007 | -1.022 | 0 | 0.009 | -1.022 | 0 | 0.008 | -1.022 |
| 0 | 0.007 | -1.021 | 0 | 0.009 | -1.023 | 0 | 0.009 | -1.022 |
| -0.001 | 0.007 | -1.021 | 0 | 0.009 | -1.023 | 0 | 0.008 | -1.022 |
| -0.001 | 0.007 | -1.021 | 0 | 0.009 | -1.022 | 0 | 0.008 | -1.023 |
| 0 | 0.006 | -1.022 | -0.001 | 0.009 | -1.022 | 0.001 | 0.008 | -1.023 |

## Sample of data set in Position 3 (wireless)

| Acc. X | Acc. Y | Acc. Z | Acc. X | Acc. Y | Acc. Z | Acc. X | Acc. Y | Acc. Z |
|---|---|---|---|---|---|---|---|---|
| 1.031 | 0.015 | -0.001 | 1.031 | 0.015 | 0 | 1.031 | 0.014 | 0 |
| 1.032 | 0.019 | -0.001 | 1.031 | 0.014 | 0 | 1.031 | 0.014 | 0 |
| 1.032 | 0.019 | -0.001 | 1.031 | 0.014 | 0 | 1.031 | 0.015 | 0 |
| 1.031 | 0.018 | -0.001 | 1.031 | 0.013 | -0.001 | 1.031 | 0.015 | 0 |
| 1.03 | 0.016 | -0.001 | 1.03 | 0.014 | -0.002 | 1.032 | 0.015 | 0 |
| 1.03 | 0.015 | -0.001 | 1.031 | 0.014 | -0.002 | 1.032 | 0.015 | -0.001 |
| 1.031 | 0.014 | -0.001 | 1.031 | 0.014 | -0.002 | 1.032 | 0.015 | -0.001 |
| 1.031 | 0.015 | -0.001 | 1.03 | 0.014 | -0.002 | 1.031 | 0.015 | -0.001 |
| 1.031 | 0.014 | 0 | 1.03 | 0.014 | -0.001 | 1.03 | 0.015 | -0.001 |
| 1.031 | 0.014 | 0 | 1.03 | 0.015 | -0.002 | 1.03 | 0.015 | -0.001 |
| 1.031 | 0.014 | 0 | 1.03 | 0.014 | -0.004 | 1.03 | 0.015 | -0.001 |
| 1.03 | 0.014 | 0 | 1.03 | 0.014 | -0.002 | 1.031 | 0.014 | -0.001 |
| 1.031 | 0.014 | 0 | 1.031 | 0.014 | -0.002 | 1.031 | 0.014 | 0 |
| 1.031 | 0.014 | 0 | 1.03 | 0.015 | -0.001 | 1.031 | 0.014 | -0.001 |
| 1.03 | 0.014 | 0 | 1.03 | 0.015 | -0.001 | 1.031 | 0.014 | 0 |
| 1.031 | 0.014 | 0 | 1.031 | 0.015 | -0.001 | 1.031 | 0.014 | 0 |
| 1.031 | 0.015 | 0 | 1.031 | 0.015 | -0.001 | 1.031 | 0.014 | 0 |
| 1.03 | 0.015 | 0 | 1.033 | 0.014 | -0.001 | 1.031 | 0.015 | 0 |
| 1.031 | 0.015 | 0.001 | 1.033 | 0.013 | 0 | 1.03 | 0.015 | 0 |
| 1.031 | 0.015 | 0.001 | 1.033 | 0.014 | 0 | 1.03 | 0.015 | 0 |
| 1.032 | 0.014 | 0.001 | 1.031 | 0.015 | 0 | 1.029 | 0.015 | 0 |
| 1.032 | 0.014 | 0.002 | 1.03 | 0.015 | 0 | 1.03 | 0.014 | 0 |
| 1.031 | 0.014 | 0.001 | 1.03 | 0.015 | 0 | 1.031 | 0.014 | 0 |
| 1.031 | 0.014 | 0 | 1.03 | 0.015 | 0 | 1.032 | 0.013 | 0 |
| 1.031 | 0.014 | 0.001 | 1.029 | 0.014 | 0 | 1.032 | 0.014 | 0 |
| 1.033 | 0.013 | 0 | 1.03 | 0.014 | 0 | 1.032 | 0.013 | 0 |
| 1.033 | 0.013 | 0 | 1.032 | 0.014 | 0 | 1.032 | 0.013 | 0 |
| 1.032 | 0.014 | 0 | 1.032 | 0.014 | 0 | 1.031 | 0.013 | 0 |
| 1.032 | 0.015 | 0 | 1.033 | 0.015 | 0 | 1.031 | 0.013 | 0 |
| 1.031 | 0.015 | 0 | 1.032 | 0.015 | 0 | 1.03 | 0.013 | 0 |
| 1.03 | 0.015 | 0 | 1.031 | 0.015 | 0 | 1.03 | 0.013 | 0 |
| 1.03 | 0.015 | 0 | 1.031 | 0.015 | 0 | 1.03 | 0.014 | 0 |
| 1.031 | 0.015 | 0 | 1.031 | 0.015 | 0 | 1.029 | 0.015 | 0 |
| 1.03 | 0.015 | 0 | 1.031 | 0.015 | 0 | 1.03 | 0.016 | 0 |
| 1.029 | 0.015 | 0 | 1.031 | 0.015 | 0 | 1.031 | 0.016 | 0 |
| 1.029 | 0.015 | 0 | 1.031 | 0.016 | 0 | 1.031 | 0.016 | 0 |
| 1.029 | 0.014 | 0 | 1.031 | 0.015 | 0 | 1.031 | 0.014 | -0.002 |
| 1.03 | 0.015 | 0 | 1.031 | 0.015 | 0 | 1.032 | 0.014 | -0.002 |
| 1.03 | 0.015 | 0 | 1.031 | 0.014 | 0 | 1.031 | 0.013 | -0.003 |
| 1.03 | 0.015 | 0.001 | 1.031 | 0.013 | 0 | 1.031 | 0.014 | -0.002 |
| 1.031 | 0.016 | 0.001 | 1.03 | 0.014 | 0 | 1.032 | 0.014 | -0.001 |

| Acc. X | Acc. Y | Acc. Z | Acc. X | Acc. Y | Acc. Z | Acc. X | Acc. Y | Acc. Z |
|---|---|---|---|---|---|---|---|---|
| 1.03 | 0.014 | -0.001 | 1.032 | 0.015 | 0 | 1.03 | 0.015 | 0 |
| 1.03 | 0.014 | 0 | 1.032 | 0.015 | 0 | 1.031 | 0.015 | 0 |
| 1.031 | 0.015 | 0 | 1.031 | 0.014 | -0.001 | 1.032 | 0.014 | 0 |
| 1.03 | 0.015 | 0 | 1.029 | 0.014 | -0.002 | 1.032 | 0.014 | 0 |
| 1.03 | 0.015 | 0 | 1.029 | 0.015 | -0.002 | 1.032 | 0.015 | 0 |
| 1.03 | 0.015 | -0.001 | 1.029 | 0.016 | -0.002 | 1.032 | 0.014 | 0 |
| 1.029 | 0.014 | -0.001 | 1.03 | 0.017 | 0 | 1.032 | 0.014 | 0 |
| 1.029 | 0.014 | -0.001 | 1.031 | 0.016 | 0 | 1.031 | 0.015 | 0 |
| 1.029 | 0.015 | -0.001 | 1.031 | 0.016 | 0 | 1.031 | 0.015 | 0 |
| 1.03 | 0.015 | -0.001 | 1.032 | 0.016 | 0 | 1.03 | 0.015 | 0 |
| 1.03 | 0.015 | -0.001 | 1.033 | 0.015 | 0 | 1.03 | 0.015 | 0 |
| 1.03 | 0.014 | 0 | 1.033 | 0.015 | 0 | 1.03 | 0.015 | 0 |
| 1.03 | 0.014 | 0 | 1.032 | 0.014 | 0 | 1.031 | 0.015 | 0 |
| 1.031 | 0.014 | 0 | 1.032 | 0.014 | 0 | 1.031 | 0.014 | 0 |
| 1.031 | 0.014 | 0 | 1.031 | 0.015 | 0 | 1.031 | 0.014 | 0 |
| 1.031 | 0.014 | 0 | 1.03 | 0.015 | 0 | 1.032 | 0.014 | 0 |
| 1.032 | 0.014 | 0 | 1.031 | 0.016 | 0 | 1.031 | 0.014 | 0 |
| 1.032 | 0.014 | 0 | 1.032 | 0.016 | 0 | 1.031 | 0.014 | 0 |
| 1.031 | 0.014 | 0 | 1.032 | 0.015 | 0 | 1.03 | 0.015 | 0 |
| 1.031 | 0.014 | 0 | 1.032 | 0.015 | 0 | 1.03 | 0.016 | 0 |
| 1.032 | 0.014 | 0 | 1.031 | 0.015 | 0 | 1.03 | 0.016 | 0 |
| 1.032 | 0.014 | 0 | 1.03 | 0.015 | 0 | 1.029 | 0.017 | 0 |
| 1.032 | 0.014 | -0.002 | 1.03 | 0.015 | 0 | 1.03 | 0.017 | 0 |
| 1.031 | 0.013 | -0.001 | 1.03 | 0.015 | 0 | 1.031 | 0.016 | 0 |
| 1.031 | 0.013 | -0.001 | 1.03 | 0.015 | 0 | 1.031 | 0.015 | 0 |
| 1.031 | 0.014 | -0.001 | 1.03 | 0.015 | 0 | 1.032 | 0.015 | 0 |
| 1.031 | 0.014 | -0.002 | 1.031 | 0.015 | 0 | 1.032 | 0.015 | 0 |
| 1.031 | 0.014 | -0.001 | 1.031 | 0.015 | 0 | 1.031 | 0.015 | 0 |
| 1.03 | 0.014 | -0.001 | 1.032 | 0.014 | 0 | 1.032 | 0.015 | 0 |
| 1.031 | 0.014 | -0.001 | 1.032 | 0.015 | 0 | 1.032 | 0.015 | 0 |
| 1.03 | 0.014 | 0 | 1.031 | 0.015 | 0 | 1.032 | 0.014 | 0 |
| 1.03 | 0.014 | 0 | 1.031 | 0.014 | 0 | 1.032 | 0.014 | 0 |
| 1.031 | 0.015 | 0 | 1.031 | 0.014 | 0 | 1.031 | 0.014 | 0 |
| 1.031 | 0.015 | 0 | 1.031 | 0.013 | 0 | 1.031 | 0.015 | 0 |
| 1.032 | 0.015 | 0 | 1.031 | 0.014 | 0 | 1.03 | 0.015 | 0 |
| 1.032 | 0.015 | 0 | 1.031 | 0.014 | 0 | 1.03 | 0.015 | 0 |
| 1.032 | 0.014 | 0 | 1.032 | 0.014 | 0 | 1.029 | 0.015 | 0 |
| 1.031 | 0.014 | -0.001 | 1.032 | 0.015 | 0 | 1.029 | 0.015 | 0 |
| 1.03 | 0.014 | 0 | 1.031 | 0.015 | 0 | 1.028 | 0.016 | 0 |
| 1.03 | 0.014 | 0 | 1.031 | 0.015 | 0 | 1.029 | 0.016 | 0 |
| 1.03 | 0.015 | 0 | 1.031 | 0.015 | 0 | 1.029 | 0.017 | 0 |
| 1.031 | 0.014 | 0 | 1.03 | 0.016 | 0 | 1.031 | 0.016 | 0 |
| 1.032 | 0.015 | 0 | 1.031 | 0.015 | 0 | 1.031 | 0.016 | 0 |

## Sample of data set in Position 4 (wireless)

| Acc. X | Acc. Y | Acc. Z | Acc. X | Acc. Y | Acc. Z | Acc. X | Acc. Y | Acc. Z |
|---|---|---|---|---|---|---|---|---|
| -1.017 | -0.01 | 0.009 | -1.015 | -0.012 | 0.008 | -1.017 | -0.012 | 0.01 |
| -1.017 | -0.011 | 0.009 | -1.015 | -0.012 | 0.008 | -1.017 | -0.012 | 0.01 |
| -1.016 | -0.011 | 0.01 | -1.015 | -0.011 | 0.008 | -1.017 | -0.012 | 0.009 |
| -1.015 | -0.011 | 0.01 | -1.016 | -0.011 | 0.008 | -1.019 | -0.012 | 0.009 |
| -1.014 | -0.012 | 0.01 | -1.017 | -0.011 | 0.007 | -1.018 | -0.012 | 0.009 |
| -1.014 | -0.011 | 0.01 | -1.017 | -0.012 | 0.007 | -1.016 | -0.011 | 0.01 |
| -1.014 | -0.011 | 0.009 | -1.017 | -0.011 | 0.007 | -1.016 | -0.01 | 0.01 |
| -1.014 | -0.011 | 0.008 | -1.016 | -0.011 | 0.008 | -1.015 | -0.009 | 0.01 |
| -1.014 | -0.009 | 0.008 | -1.014 | -0.012 | 0.009 | -1.014 | -0.01 | 0.01 |
| -1.015 | -0.01 | 0.009 | -1.014 | -0.011 | 0.009 | -1.016 | -0.011 | 0.011 |
| -1.016 | -0.011 | 0.009 | -1.016 | -0.011 | 0.009 | -1.016 | -0.011 | 0.011 |
| -1.016 | -0.011 | 0.009 | -1.016 | -0.01 | 0.008 | -1.015 | -0.011 | 0.012 |
| -1.018 | -0.012 | 0.01 | -1.018 | -0.01 | 0.008 | -1.015 | -0.011 | 0.012 |
| -1.018 | -0.012 | 0.01 | -1.019 | -0.011 | 0.009 | -1.015 | -0.011 | 0.011 |
| -1.019 | -0.012 | 0.01 | -1.019 | -0.011 | 0.009 | -1.015 | -0.011 | 0.011 |
| -1.02 | -0.011 | 0.01 | -1.02 | -0.011 | 0.009 | -1.017 | -0.012 | 0.01 |
| -1.019 | -0.011 | 0.01 | -1.021 | -0.012 | 0.008 | -1.017 | -0.011 | 0.01 |
| -1.018 | -0.01 | 0.009 | -1.019 | -0.011 | 0.008 | -1.016 | -0.012 | 0.01 |
| -1.016 | -0.01 | 0.009 | -1.019 | -0.011 | 0.008 | -1.017 | -0.011 | 0.01 |
| -1.014 | -0.011 | 0.01 | -1.018 | -0.011 | 0.008 | -1.017 | -0.011 | 0.01 |
| -1.016 | -0.011 | 0.01 | -1.017 | -0.01 | 0.009 | -1.018 | -0.011 | 0.011 |
| -1.017 | -0.011 | 0.01 | -1.019 | -0.01 | 0.009 | -1.018 | -0.011 | 0.011 |
| -1.019 | -0.012 | 0.01 | -1.017 | -0.012 | 0.009 | -1.018 | -0.011 | 0.011 |
| -1.019 | -0.012 | 0.01 | -1.019 | -0.013 | 0.01 | -1.016 | -0.012 | 0.012 |
| -1.017 | -0.012 | 0.01 | -1.019 | -0.013 | 0.01 | -1.016 | -0.012 | 0.011 |
| -1.017 | -0.01 | 0.011 | -1.018 | -0.012 | 0.009 | -1.018 | -0.012 | 0.011 |
| -1.017 | -0.009 | 0.011 | -1.018 | -0.011 | 0.009 | -1.016 | -0.012 | 0.011 |
| -1.017 | -0.01 | 0.012 | -1.017 | -0.011 | 0.009 | -1.018 | -0.011 | 0.01 |
| -1.018 | -0.012 | 0.011 | -1.015 | -0.012 | 0.009 | -1.017 | -0.012 | 0.01 |
| -1.017 | -0.013 | 0.01 | -1.015 | -0.011 | 0.009 | -1.017 | -0.013 | 0.011 |
| -1.018 | -0.013 | 0.011 | -1.014 | -0.011 | 0.01 | -1.018 | -0.013 | 0.01 |
| -1.018 | -0.012 | 0.01 | -1.014 | -0.012 | 0.011 | -1.017 | -0.013 | 0.01 |
| -1.018 | -0.012 | 0.01 | -1.014 | -0.011 | 0.011 | -1.017 | -0.014 | 0.01 |
| -1.017 | -0.012 | 0.009 | -1.015 | -0.011 | 0.011 | -1.016 | -0.013 | 0.01 |
| -1.014 | -0.01 | 0.008 | -1.016 | -0.012 | 0.01 | -1.016 | -0.014 | 0.01 |
| -1.014 | -0.011 | 0.007 | -1.016 | -0.011 | 0.01 | -1.016 | -0.014 | 0.01 |
| -1.014 | -0.011 | 0.007 | -1.018 | -0.01 | 0.01 | -1.015 | -0.012 | 0.009 |
| -1.015 | -0.011 | 0.008 | -1.017 | -0.01 | 0.011 | -1.015 | -0.011 | 0.009 |
| -1.016 | -0.011 | 0.009 | -1.017 | -0.009 | 0.011 | -1.014 | -0.011 | 0.01 |
| -1.016 | -0.011 | 0.01 | -1.017 | -0.01 | 0.011 | -1.014 | -0.01 | 0.01 |
| -1.017 | -0.012 | 0.009 | -1.016 | -0.012 | 0.01 | -1.015 | -0.01 | 0.011 |

| Acc. X | Acc. Y | Acc. Z | Acc. X | Acc. Y | Acc. Z | Acc. X | Acc. Y | Acc. Z |
|---|---|---|---|---|---|---|---|---|
| -1.014 | -0.011 | 0.011 | -1.017 | -0.012 | 0.009 | -1.017 | -0.011 | 0.009 |
| -1.014 | -0.011 | 0.012 | -1.017 | -0.012 | 0.01 | -1.016 | -0.013 | 0.009 |
| -1.015 | -0.011 | 0.011 | -1.016 | -0.012 | 0.01 | -1.017 | -0.012 | 0.009 |
| -1.014 | -0.012 | 0.01 | -1.016 | -0.011 | 0.01 | -1.016 | -0.012 | 0.009 |
| -1.015 | -0.011 | 0.009 | -1.017 | -0.012 | 0.01 | -1.016 | -0.013 | 0.008 |
| -1.015 | -0.011 | 0.01 | -1.015 | -0.011 | 0.01 | -1.014 | -0.011 | 0.008 |
| -1.015 | -0.012 | 0.011 | -1.015 | -0.011 | 0.01 | -1.013 | -0.011 | 0.009 |
| -1.015 | -0.011 | 0.011 | -1.015 | -0.011 | 0.01 | -1.014 | -0.011 | 0.01 |
| -1.015 | -0.012 | 0.01 | -1.015 | -0.01 | 0.009 | -1.014 | -0.011 | 0.01 |
| -1.016 | -0.011 | 0.009 | -1.015 | -0.01 | 0.009 | -1.014 | -0.011 | 0.011 |
| -1.015 | -0.011 | 0.009 | -1.015 | -0.01 | 0.01 | -1.017 | -0.011 | 0.011 |
| -1.017 | -0.011 | 0.009 | -1.016 | -0.011 | 0.01 | -1.016 | -0.012 | 0.01 |
| -1.017 | -0.012 | 0.01 | -1.017 | -0.01 | 0.01 | -1.016 | -0.011 | 0.01 |
| -1.015 | -0.011 | 0.01 | -1.017 | -0.011 | 0.01 | -1.017 | -0.011 | 0.01 |
| -1.016 | -0.011 | 0.009 | -1.017 | -0.012 | 0.009 | -1.016 | -0.009 | 0.009 |
| -1.017 | -0.012 | 0.01 | -1.016 | -0.011 | 0.01 | -1.015 | -0.008 | 0.01 |
| -1.018 | -0.011 | 0.01 | -1.015 | -0.01 | 0.01 | -1.017 | -0.01 | 0.01 |
| -1.019 | -0.012 | 0.011 | -1.016 | -0.01 | 0.011 | -1.015 | -0.01 | 0.011 |
| -1.018 | -0.012 | 0.011 | -1.015 | -0.01 | 0.011 | -1.017 | -0.009 | 0.012 |
| -1.016 | -0.011 | 0.011 | -1.017 | -0.01 | 0.01 | -1.017 | -0.011 | 0.012 |
| -1.017 | -0.011 | 0.011 | -1.017 | -0.011 | 0.01 | -1.017 | -0.01 | 0.013 |
| -1.015 | -0.012 | 0.011 | -1.016 | -0.01 | 0.01 | -1.018 | -0.011 | 0.012 |
| -1.015 | -0.011 | 0.011 | -1.017 | -0.011 | 0.01 | -1.017 | -0.012 | 0.012 |
| -1.015 | -0.011 | 0.01 | -1.015 | -0.011 | 0.01 | -1.017 | -0.011 | 0.011 |
| -1.013 | -0.011 | 0.01 | -1.014 | -0.011 | 0.01 | -1.016 | -0.012 | 0.012 |
| -1.014 | -0.01 | 0.011 | -1.014 | -0.011 | 0.01 | -1.016 | -0.012 | 0.013 |
| -1.014 | -0.01 | 0.01 | -1.015 | -0.011 | 0.011 | -1.015 | -0.012 | 0.012 |
| -1.014 | -0.012 | 0.01 | -1.017 | -0.011 | 0.011 | -1.016 | -0.012 | 0.012 |
| -1.016 | -0.011 | 0.01 | -1.017 | -0.011 | 0.012 | -1.018 | -0.011 | 0.011 |
| -1.016 | -0.012 | 0.01 | -1.016 | -0.011 | 0.012 | -1.017 | -0.012 | 0.011 |
| -1.015 | -0.014 | 0.01 | -1.015 | -0.009 | 0.011 | -1.018 | -0.012 | 0.011 |
| -1.014 | -0.011 | 0.011 | -1.015 | -0.01 | 0.01 | -1.016 | -0.012 | 0.012 |
| -1.015 | -0.012 | 0.01 | -1.017 | -0.01 | 0.01 | -1.015 | -0.011 | 0.011 |
| -1.015 | -0.012 | 0.01 | -1.019 | -0.01 | 0.01 | -1.016 | -0.011 | 0.011 |
| -1.016 | -0.012 | 0.011 | -1.02 | -0.01 | 0.011 | -1.016 | -0.012 | 0.011 |
| -1.018 | -0.012 | 0.011 | -1.019 | -0.011 | 0.011 | -1.016 | -0.011 | 0.011 |
| -1.017 | -0.012 | 0.011 | -1.018 | -0.011 | 0.012 | -1.016 | -0.012 | 0.012 |
| -1.016 | -0.011 | 0.011 | -1.016 | -0.012 | 0.011 | -1.016 | -0.011 | 0.011 |
| -1.016 | -0.012 | 0.01 | -1.015 | -0.012 | 0.012 | -1.017 | -0.012 | 0.011 |
| -1.014 | -0.013 | 0.01 | -1.014 | -0.011 | 0.011 | -1.017 | -0.011 | 0.012 |
| -1.015 | -0.012 | 0.01 | -1.016 | -0.011 | 0.01 | -1.018 | -0.011 | 0.012 |
| -1.017 | -0.013 | 0.009 | -1.016 | -0.011 | 0.009 | -1.017 | -0.01 | 0.011 |
| -1.017 | -0.013 | 0.009 | -1.017 | -0.011 | 0.009 | -1.017 | -0.009 | 0.011 |

## Sample of data set in Position 5 (wireless)

| Acc. X | Acc. Y | Acc. Z | Acc. X | Acc. Y | Acc. Z | Acc. X | Acc. Y | Acc. Z |
|---|---|---|---|---|---|---|---|---|
| -0.012 | 0.992 | -0.003 | -0.011 | 0.99 | -0.001 | -0.011 | 0.992 | -0.002 |
| -0.011 | 0.992 | -0.003 | -0.01 | 0.99 | 0 | -0.011 | 0.992 | -0.002 |
| -0.01 | 0.992 | -0.004 | -0.01 | 0.99 | 0 | -0.011 | 0.993 | -0.003 |
| -0.009 | 0.993 | -0.004 | -0.011 | 0.991 | 0 | -0.01 | 0.992 | -0.003 |
| -0.009 | 0.991 | -0.003 | -0.01 | 0.991 | 0 | -0.01 | 0.992 | -0.003 |
| -0.011 | 0.99 | -0.002 | -0.011 | 0.991 | 0 | -0.01 | 0.991 | -0.002 |
| -0.011 | 0.99 | -0.002 | -0.011 | 0.991 | 0 | -0.01 | 0.991 | -0.002 |
| -0.011 | 0.99 | -0.002 | -0.011 | 0.991 | 0 | -0.011 | 0.991 | -0.002 |
| -0.012 | 0.99 | -0.002 | -0.011 | 0.991 | 0 | -0.01 | 0.99 | -0.003 |
| -0.011 | 0.99 | -0.002 | -0.011 | 0.991 | 0 | -0.01 | 0.991 | -0.002 |
| -0.011 | 0.989 | -0.003 | -0.011 | 0.991 | 0 | -0.011 | 0.99 | -0.002 |
| -0.011 | 0.989 | -0.002 | -0.011 | 0.991 | 0 | -0.011 | 0.991 | -0.002 |
| -0.011 | 0.99 | -0.004 | -0.011 | 0.991 | 0 | -0.011 | 0.991 | -0.001 |
| -0.011 | 0.99 | -0.003 | -0.011 | 0.991 | 0 | -0.011 | 0.991 | -0.002 |
| -0.012 | 0.99 | -0.003 | -0.01 | 0.991 | 0.001 | -0.011 | 0.992 | -0.001 |
| -0.012 | 0.99 | -0.003 | -0.01 | 0.991 | 0.001 | -0.011 | 0.992 | -0.002 |
| -0.012 | 0.989 | -0.002 | -0.011 | 0.992 | 0 | -0.011 | 0.992 | -0.002 |
| -0.012 | 0.991 | -0.002 | -0.01 | 0.992 | 0 | -0.011 | 0.992 | -0.003 |
| -0.012 | 0.991 | -0.003 | -0.011 | 0.992 | 0 | -0.011 | 0.991 | -0.003 |
| -0.012 | 0.991 | -0.003 | -0.01 | 0.991 | 0 | -0.01 | 0.99 | -0.002 |
| -0.012 | 0.992 | -0.002 | -0.01 | 0.99 | 0 | -0.01 | 0.99 | -0.003 |
| -0.012 | 0.991 | -0.002 | -0.011 | 0.99 | -0.001 | -0.01 | 0.989 | -0.001 |
| -0.012 | 0.991 | -0.001 | -0.011 | 0.99 | 0 | -0.01 | 0.99 | 0 |
| -0.012 | 0.992 | 0 | -0.011 | 0.991 | -0.001 | -0.01 | 0.99 | -0.002 |
| -0.011 | 0.992 | 0 | -0.011 | 0.991 | -0.001 | -0.009 | 0.991 | -0.001 |
| -0.01 | 0.992 | 0 | -0.01 | 0.991 | 0 | -0.01 | 0.992 | 0 |
| -0.01 | 0.991 | 0 | -0.01 | 0.991 | -0.002 | -0.01 | 0.993 | -0.002 |
| -0.01 | 0.991 | 0 | -0.012 | 0.991 | -0.001 | -0.01 | 0.992 | -0.001 |
| -0.009 | 0.991 | 0 | -0.012 | 0.991 | 0 | -0.01 | 0.991 | 0 |
| -0.01 | 0.99 | 0 | -0.011 | 0.992 | 0 | -0.01 | 0.991 | -0.001 |
| -0.009 | 0.991 | 0 | -0.012 | 0.991 | 0 | -0.01 | 0.99 | 0 |
| -0.009 | 0.991 | 0 | -0.011 | 0.992 | 0 | -0.01 | 0.991 | 0 |
| -0.009 | 0.991 | 0 | -0.011 | 0.992 | -0.001 | -0.01 | 0.99 | -0.001 |
| -0.008 | 0.991 | 0 | -0.011 | 0.992 | -0.002 | -0.011 | 0.99 | 0 |
| -0.009 | 0.99 | 0 | -0.011 | 0.992 | -0.001 | -0.01 | 0.991 | 0 |
| -0.009 | 0.991 | 0 | -0.011 | 0.99 | -0.002 | -0.01 | 0.991 | 0 |
| -0.009 | 0.99 | 0 | -0.012 | 0.99 | -0.002 | -0.01 | 0.992 | 0 |
| -0.01 | 0.99 | 0 | -0.011 | 0.99 | -0.002 | -0.009 | 0.992 | 0 |
| -0.01 | 0.99 | -0.001 | -0.01 | 0.99 | -0.003 | -0.009 | 0.992 | 0 |
| -0.01 | 0.99 | -0.001 | -0.011 | 0.991 | -0.002 | -0.009 | 0.991 | 0 |
| -0.01 | 0.99 | -0.001 | -0.01 | 0.992 | -0.001 | -0.009 | 0.991 | 0 |

| Acc. X | Acc. Y | Acc. Z | Acc. X | Acc. Y | Acc. Z | Acc. X | Acc. Y | Acc. Z |
|---|---|---|---|---|---|---|---|---|
| -0.009 | 0.991 | 0 | -0.012 | 0.991 | 0 | -0.009 | 0.991 | 0 |
| -0.01 | 0.991 | 0 | -0.011 | 0.991 | 0 | -0.01 | 0.991 | 0 |
| -0.011 | 0.991 | -0.001 | -0.01 | 0.992 | 0.001 | -0.01 | 0.99 | 0 |
| -0.011 | 0.99 | -0.002 | -0.01 | 0.992 | 0.001 | -0.01 | 0.991 | 0 |
| -0.012 | 0.99 | -0.003 | -0.009 | 0.992 | 0 | -0.011 | 0.991 | 0 |
| -0.011 | 0.99 | -0.003 | -0.01 | 0.992 | 0 | -0.011 | 0.991 | 0 |
| -0.01 | 0.99 | -0.002 | -0.011 | 0.991 | 0 | -0.011 | 0.99 | 0 |
| -0.01 | 0.991 | -0.001 | -0.01 | 0.991 | 0 | -0.011 | 0.99 | 0 |
| -0.011 | 0.991 | 0 | -0.011 | 0.991 | 0 | -0.011 | 0.99 | 0 |
| -0.011 | 0.991 | 0 | -0.01 | 0.991 | 0 | -0.011 | 0.99 | 0 |
| -0.011 | 0.992 | 0 | -0.01 | 0.992 | 0 | -0.011 | 0.991 | 0 |
| -0.01 | 0.993 | 0 | -0.012 | 0.991 | 0 | -0.012 | 0.991 | 0 |
| -0.01 | 0.992 | 0 | -0.012 | 0.991 | 0 | -0.011 | 0.991 | 0 |
| -0.01 | 0.992 | 0 | -0.012 | 0.991 | 0 | -0.011 | 0.991 | 0 |
| -0.01 | 0.993 | -0.001 | -0.013 | 0.991 | 0 | -0.01 | 0.992 | 0 |
| -0.011 | 0.992 | -0.001 | -0.012 | 0.992 | 0 | -0.01 | 0.993 | 0 |
| -0.011 | 0.993 | -0.001 | -0.011 | 0.992 | 0 | -0.01 | 0.993 | 0 |
| -0.011 | 0.993 | -0.001 | -0.011 | 0.992 | 0 | -0.01 | 0.993 | 0 |
| -0.01 | 0.992 | 0 | -0.011 | 0.991 | 0 | -0.01 | 0.991 | 0 |
| -0.01 | 0.992 | 0 | -0.01 | 0.991 | 0 | -0.01 | 0.99 | 0 |
| -0.009 | 0.991 | 0 | -0.011 | 0.991 | 0 | -0.011 | 0.99 | 0 |
| -0.009 | 0.992 | -0.001 | -0.011 | 0.99 | 0 | -0.011 | 0.991 | 0.001 |
| -0.01 | 0.991 | -0.001 | -0.01 | 0.991 | 0 | -0.011 | 0.992 | 0.001 |
| -0.01 | 0.992 | -0.001 | -0.01 | 0.99 | 0 | -0.011 | 0.992 | 0.001 |
| -0.011 | 0.993 | -0.001 | -0.009 | 0.99 | 0 | -0.011 | 0.992 | 0.001 |
| -0.011 | 0.991 | -0.001 | -0.01 | 0.99 | 0 | -0.01 | 0.992 | 0 |
| -0.011 | 0.992 | 0 | -0.011 | 0.991 | 0 | -0.01 | 0.992 | 0 |
| -0.011 | 0.992 | 0 | -0.011 | 0.991 | 0 | -0.01 | 0.991 | 0 |
| -0.01 | 0.991 | 0 | -0.011 | 0.992 | 0 | -0.01 | 0.991 | 0 |
| -0.009 | 0.991 | 0 | -0.01 | 0.991 | 0 | -0.012 | 0.991 | 0.001 |
| -0.009 | 0.991 | 0 | -0.01 | 0.991 | 0 | -0.011 | 0.99 | 0.001 |
| -0.01 | 0.991 | 0 | -0.009 | 0.991 | 0 | -0.011 | 0.991 | 0.002 |
| -0.01 | 0.992 | 0 | -0.011 | 0.99 | 0 | -0.011 | 0.991 | 0 |
| -0.01 | 0.991 | 0 | -0.01 | 0.991 | 0 | -0.011 | 0.992 | 0 |
| -0.011 | 0.991 | 0 | -0.01 | 0.991 | 0 | -0.011 | 0.992 | 0 |
| -0.011 | 0.992 | 0.001 | -0.01 | 0.991 | 0 | -0.011 | 0.993 | 0 |
| -0.011 | 0.991 | 0.001 | -0.009 | 0.991 | 0 | -0.011 | 0.993 | 0 |
| -0.011 | 0.991 | 0.001 | -0.01 | 0.991 | 0 | -0.01 | 0.992 | 0 |
| -0.01 | 0.992 | 0 | -0.01 | 0.992 | 0 | -0.011 | 0.992 | 0 |
| -0.011 | 0.992 | 0 | -0.01 | 0.992 | 0 | -0.011 | 0.992 | 0 |
| -0.011 | 0.992 | 0 | -0.01 | 0.992 | 0 | -0.011 | 0.991 | 0 |
| -0.012 | 0.992 | 0 | -0.009 | 0.992 | 0 | -0.01 | 0.992 | 0 |
| -0.012 | 0.992 | 0 | -0.01 | 0.991 | 0 | -0.01 | 0.992 | 0 |

## Sample of data set in Position 6 (wireless)

| Acc. X | Acc. Y | Acc. Z | Acc. X | Acc. Y | Acc. Z | Acc. X | Acc. Y | Acc. Z |
|---|---|---|---|---|---|---|---|---|
| 0.012 | -0.976 | 0.008 | 0.011 | -0.977 | 0.007 | 0.012 | -0.976 | 0.007 |
| 0.012 | -0.977 | 0.008 | 0.012 | -0.975 | 0.007 | 0.013 | -0.976 | 0.007 |
| 0.012 | -0.976 | 0.009 | 0.013 | -0.975 | 0.007 | 0.013 | -0.975 | 0.008 |
| 0.013 | -0.976 | 0.008 | 0.013 | -0.975 | 0.008 | 0.012 | -0.975 | 0.007 |
| 0.013 | -0.974 | 0.009 | 0.013 | -0.975 | 0.007 | 0.013 | -0.975 | 0.007 |
| 0.013 | -0.975 | 0.008 | 0.014 | -0.975 | 0.007 | 0.012 | -0.974 | 0.007 |
| 0.014 | -0.975 | 0.01 | 0.014 | -0.976 | 0.007 | 0.014 | -0.974 | 0.007 |
| 0.014 | -0.976 | 0.009 | 0.015 | -0.974 | 0.007 | 0.014 | -0.974 | 0.007 |
| 0.014 | -0.977 | 0.01 | 0.015 | -0.975 | 0.007 | 0.014 | -0.975 | 0.007 |
| 0.013 | -0.976 | 0.01 | 0.014 | -0.976 | 0.007 | 0.014 | -0.975 | 0.007 |
| 0.013 | -0.975 | 0.009 | 0.014 | -0.976 | 0.008 | 0.013 | -0.975 | 0.007 |
| 0.013 | -0.974 | 0.009 | 0.015 | -0.976 | 0.009 | 0.013 | -0.976 | 0.007 |
| 0.013 | -0.975 | 0.008 | 0.014 | -0.975 | 0.009 | 0.013 | -0.975 | 0.007 |
| 0.013 | -0.976 | 0.009 | 0.015 | -0.975 | 0.009 | 0.013 | -0.975 | 0.007 |
| 0.013 | -0.977 | 0.009 | 0.016 | -0.975 | 0.009 | 0.013 | -0.975 | 0.007 |
| 0.012 | -0.978 | 0.009 | 0.014 | -0.975 | 0.008 | 0.014 | -0.975 | 0.007 |
| 0.013 | -0.977 | 0.009 | 0.014 | -0.976 | 0.009 | 0.013 | -0.975 | 0.007 |
| 0.013 | -0.976 | 0.009 | 0.014 | -0.976 | 0.009 | 0.013 | -0.975 | 0.007 |
| 0.014 | -0.975 | 0.009 | 0.013 | -0.976 | 0.01 | 0.013 | -0.975 | 0.008 |
| 0.014 | -0.975 | 0.009 | 0.013 | -0.976 | 0.01 | 0.013 | -0.974 | 0.008 |
| 0.014 | -0.974 | 0.008 | 0.013 | -0.975 | 0.009 | 0.014 | -0.974 | 0.007 |
| 0.014 | -0.975 | 0.007 | 0.013 | -0.976 | 0.01 | 0.015 | -0.974 | 0.008 |
| 0.013 | -0.975 | 0.007 | 0.014 | -0.976 | 0.009 | 0.015 | -0.974 | 0.008 |
| 0.013 | -0.974 | 0.007 | 0.014 | -0.975 | 0.008 | 0.014 | -0.975 | 0.008 |
| 0.012 | -0.974 | 0.007 | 0.014 | -0.975 | 0.01 | 0.014 | -0.976 | 0.009 |
| 0.012 | -0.974 | 0.007 | 0.014 | -0.974 | 0.01 | 0.012 | -0.976 | 0.01 |
| 0.011 | -0.974 | 0.007 | 0.013 | -0.973 | 0.011 | 0.012 | -0.975 | 0.008 |
| 0.012 | -0.974 | 0.008 | 0.013 | -0.974 | 0.011 | 0.013 | -0.974 | 0.008 |
| 0.013 | -0.975 | 0.008 | 0.013 | -0.975 | 0.01 | 0.014 | -0.974 | 0.008 |
| 0.014 | -0.976 | 0.009 | 0.012 | -0.976 | 0.01 | 0.014 | -0.974 | 0.007 |
| 0.015 | -0.976 | 0.009 | 0.014 | -0.976 | 0.009 | 0.014 | -0.975 | 0.007 |
| 0.013 | -0.977 | 0.01 | 0.014 | -0.976 | 0.009 | 0.014 | -0.975 | 0.007 |
| 0.013 | -0.976 | 0.01 | 0.014 | -0.976 | 0.009 | 0.013 | -0.975 | 0.007 |
| 0.012 | -0.976 | 0.01 | 0.013 | -0.975 | 0.009 | 0.013 | -0.976 | 0.008 |
| 0.012 | -0.976 | 0.009 | 0.012 | -0.975 | 0.009 | 0.013 | -0.975 | 0.007 |
| 0.014 | -0.975 | 0.009 | 0.011 | -0.975 | 0.01 | 0.013 | -0.976 | 0.007 |
| 0.013 | -0.976 | 0.008 | 0.011 | -0.975 | 0.009 | 0.014 | -0.975 | 0.007 |
| 0.013 | -0.976 | 0.007 | 0.012 | -0.975 | 0.008 | 0.014 | -0.974 | 0.006 |
| 0.013 | -0.977 | 0.007 | 0.012 | -0.976 | 0.009 | 0.013 | -0.975 | 0.007 |
| 0.011 | -0.977 | 0.008 | 0.013 | -0.977 | 0.007 | 0.013 | -0.975 | 0.008 |
| 0.011 | -0.976 | 0.007 | 0.014 | -0.977 | 0.008 | 0.013 | -0.976 | 0.008 |

| Acc. X | Acc. Y | Acc. Z | Acc. X | Acc. Y | Acc. Z | Acc. X | Acc. Y | Acc. Z |
|---|---|---|---|---|---|---|---|---|
| 0.012 | -0.976 | 0.009 | 0.014 | -0.974 | 0.007 | 0.012 | -0.975 | 0.007 |
| 0.012 | -0.976 | 0.008 | 0.013 | -0.974 | 0.007 | 0.012 | -0.975 | 0.007 |
| 0.012 | -0.976 | 0.008 | 0.014 | -0.975 | 0.007 | 0.013 | -0.974 | 0.007 |
| 0.012 | -0.975 | 0.008 | 0.015 | -0.974 | 0.007 | 0.014 | -0.974 | 0.007 |
| 0.014 | -0.975 | 0.008 | 0.014 | -0.974 | 0.007 | 0.014 | -0.974 | 0.007 |
| 0.014 | -0.975 | 0.008 | 0.015 | -0.975 | 0.007 | 0.014 | -0.973 | 0.007 |
| 0.014 | -0.975 | 0.008 | 0.014 | -0.974 | 0.007 | 0.015 | -0.974 | 0.006 |
| 0.014 | -0.974 | 0.008 | 0.014 | -0.974 | 0.008 | 0.014 | -0.974 | 0.006 |
| 0.012 | -0.975 | 0.008 | 0.015 | -0.975 | 0.007 | 0.014 | -0.975 | 0.006 |
| 0.012 | -0.976 | 0.008 | 0.014 | -0.975 | 0.007 | 0.014 | -0.975 | 0.006 |
| 0.012 | -0.976 | 0.008 | 0.013 | -0.976 | 0.007 | 0.013 | -0.975 | 0.007 |
| 0.012 | -0.975 | 0.008 | 0.014 | -0.975 | 0.007 | 0.013 | -0.975 | 0.007 |
| 0.013 | -0.975 | 0.007 | 0.013 | -0.975 | 0.007 | 0.014 | -0.975 | 0.007 |
| 0.013 | -0.975 | 0.007 | 0.013 | -0.975 | 0.006 | 0.014 | -0.974 | 0.007 |
| 0.014 | -0.975 | 0.007 | 0.013 | -0.975 | 0.007 | 0.014 | -0.975 | 0.007 |
| 0.014 | -0.975 | 0.007 | 0.013 | -0.975 | 0.007 | 0.014 | -0.975 | 0.007 |
| 0.013 | -0.976 | 0.007 | 0.014 | -0.975 | 0.006 | 0.014 | -0.975 | 0.007 |
| 0.014 | -0.974 | 0.007 | 0.014 | -0.975 | 0.007 | 0.014 | -0.975 | 0.008 |
| 0.012 | -0.974 | 0.008 | 0.014 | -0.974 | 0.008 | 0.015 | -0.975 | 0.007 |
| 0.012 | -0.974 | 0.008 | 0.014 | -0.975 | 0.008 | 0.014 | -0.975 | 0.007 |
| 0.012 | -0.974 | 0.009 | 0.015 | -0.974 | 0.009 | 0.014 | -0.975 | 0.008 |
| 0.013 | -0.974 | 0.008 | 0.015 | -0.974 | 0.008 | 0.014 | -0.975 | 0.008 |
| 0.012 | -0.974 | 0.007 | 0.015 | -0.975 | 0.008 | 0.015 | -0.975 | 0.008 |
| 0.012 | -0.974 | 0.007 | 0.014 | -0.975 | 0.008 | 0.016 | -0.974 | 0.008 |
| 0.011 | -0.975 | 0.005 | 0.013 | -0.975 | 0.007 | 0.015 | -0.974 | 0.007 |
| 0.01 | -0.975 | 0.005 | 0.014 | -0.976 | 0.007 | 0.014 | -0.975 | 0.007 |
| 0.011 | -0.976 | 0.007 | 0.013 | -0.975 | 0.007 | 0.012 | -0.974 | 0.008 |
| 0.01 | -0.975 | 0.007 | 0.013 | -0.975 | 0.006 | 0.012 | -0.974 | 0.008 |
| 0.012 | -0.974 | 0.008 | 0.013 | -0.976 | 0.007 | 0.013 | -0.974 | 0.009 |
| 0.013 | -0.974 | 0.008 | 0.013 | -0.974 | 0.007 | 0.014 | -0.973 | 0.009 |
| 0.013 | -0.974 | 0.006 | 0.013 | -0.975 | 0.007 | 0.016 | -0.974 | 0.01 |
| 0.013 | -0.974 | 0.008 | 0.013 | -0.975 | 0.007 | 0.015 | -0.973 | 0.009 |
| 0.012 | -0.974 | 0.009 | 0.014 | -0.974 | 0.008 | 0.015 | -0.974 | 0.009 |
| 0.011 | -0.974 | 0.009 | 0.013 | -0.974 | 0.008 | 0.014 | -0.975 | 0.009 |
| 0.011 | -0.974 | 0.01 | 0.014 | -0.975 | 0.008 | 0.012 | -0.974 | 0.009 |
| 0.013 | -0.975 | 0.008 | 0.014 | -0.974 | 0.008 | 0.013 | -0.975 | 0.009 |
| 0.014 | -0.975 | 0.007 | 0.014 | -0.975 | 0.007 | 0.014 | -0.974 | 0.01 |
| 0.015 | -0.975 | 0.007 | 0.014 | -0.975 | 0.006 | 0.015 | -0.974 | 0.009 |
| 0.015 | -0.974 | 0.005 | 0.014 | -0.975 | 0.006 | 0.014 | -0.974 | 0.007 |
| 0.014 | -0.974 | 0.005 | 0.013 | -0.975 | 0.006 | 0.014 | -0.974 | 0.008 |
| 0.013 | -0.973 | 0.005 | 0.013 | -0.975 | 0.007 | 0.014 | -0.975 | 0.007 |
| 0.014 | -0.973 | 0.004 | 0.013 | -0.976 | 0.007 | 0.015 | -0.974 | 0.008 |
| 0.014 | -0.974 | 0.006 | 0.013 | -0.975 | 0.007 | 0.014 | -0.975 | 0.009 |